

Die configuration effects on electrical conductivity of polypropylene reinforced milled carbon fiber

Nabilah Afifah Mohd Radzuan ^{1*}, Abu Bakar Sulong², Mahendra Rao Somalu¹, Hendra Suherman³

¹Fuel Cell Institute, Universiti Kebangsaan Malaysia, 43600 UKM Bangi, Malaysia.

²Department of Mechanical and Material Engineering,
Faculty of Engineering and Built Environment, Universiti Kebangsaan Malaysia,
43600 Bangi, Selangor, Malaysia.

³Department of Mechanical Engineering, Universitas Bung Hatta, 25137 Padang, West Sumatera, Indonesia

*Corresponding e-mail: afiqahmradzuan@gmail.com

Keywords: Milled carbon fiber, Electrical conductivity, Die configuration, Mechanical testing, Extrusion.

ABSTRACT – Extrusion is one of the pre-mixing process that able in producing a high conductive polymer composite (CPCs) material when applying an appropriate die geometry. Suitable dies geometry enhances the electrical conductivity by developing larger conductivity networks when fillers are dispersing evenly in polymer matrix. Electrical conductivity can be predicted easily using a common conductivity model. However, development of conductivity model is still in preliminary stage as current model used unable to predict electrical conductivity accurately. Thus, studies using MCF/PP composite are conducted using different types of dies which are rod and sheet dies to measure the electrical conductivity. Results indicated that MCF/PP composite produced using rod die have highest electrical conductivity. Filler orientation aligns better in converging die which enhance the electrical conductivity of composite materials.

1. INTRODUCTION

Manufacturing process such as injection molding and compression molding process are the main process in producing highly conductive polymer composite materials (Antunes et al., 2011). However, by only applying these manufacturing processes the composite materials, performances still relatively low specially in order to balance between the mechanical properties and the electrical conductivity of the composite materials (Planes et al., 2012). Therefore, pre-mixing process seems to be an alternative which aid in enhancing both mechanical properties and electrical conductivity of the composite materials (Jimenez and Jana, 2007). Studies reported that researchers usually used mechanical mixer in order to disperse fillers randomly in polymer matrix before materials undergo the manufacturing process (Suherman et al., 2013a, Suherman et al., 2013b, Zakaria et al., 2015). However, no details studies were conducted to explain the consequence of pre-mixing process of electrical conductivity of composite materials. The extrusion process is a pre-mixing process which allowed the fillers to disperse and distribute randomly in the polymer matrix. Thus, melt mixing process using the twin screw extruder is a good alternative in developing highly conductive polymer composite materials due to fact that this twin screw extruder is able to undergo several processes including blending, premixed and

melting continuously (Mejía et al., 2014, Nakayama et al., 2011, Zhang et al., 2012). Besides, pre-mixing by twin screw extruder is an effective way to induce the filler orientations aligned in the extrusion direction which later enhance the electrical conductivity of polymer composite materials (Wang et al., 2011). There are a few methods in order to induce the filler orientations such as shear rate, extrusion geometry and filler aspect ratio (Kim et al., 2006, Wang et al., 2011, Ausias et al., 1996, Kuriger et al., 2002, Taipalus et al., 2001).

2. METHODOLOGY

The MCF/PP composites were physically pre-mixed at 1200rpm for 60 seconds using a mechanical mixer, model RM 20-KIKA-WERK in a small container at room temperature before being melted compounded in a Thermo Haake TSE twin screw extruder. During the extrusion process, the twin screw extruder was set at a temperature of 230°C and a rotational speed at 50rpm for 30 minutes of extrusion time. Three different dies geometries including sheet dies with thicknesses of 3mm and 5mm, and a rod die with diameter of 5mm were used in this study. The in-plane electrical conductivity was measured by the four-point probe technique using a Jandel four-point probe and an RM3 test unit [1-3]. Besides that, the morphological structure of the composite material was observed using a Zeiss Scanning Electron Microscope (SEM).

3. RESULTS AND DISCUSSION

The electrical conductivity of extruded composite MCF/PP using three different dies, which are rod dies and sheet dies were investigated. The highest electrical conductivity obtained was used rod dies with 3.7S/cm due to the fact that filler tends to orientate better in converging dies compare to sheet dies [4, 5]. Converging dies offer better filler orientation compare to diverging dies, which improve the electrical conductivity of the composite materials. Besides, lowest shear rate experience by the rod dies aid to minimise the fillers rapture and improve the fillers orientations [6]. However, previous studies reported that higher shear rate not only aid in orientate the filler to desire direction, but also maximize the rapture of fillers thus deteriorates the electrical conductivity and mechanical properties of

composite materials [7, 8].

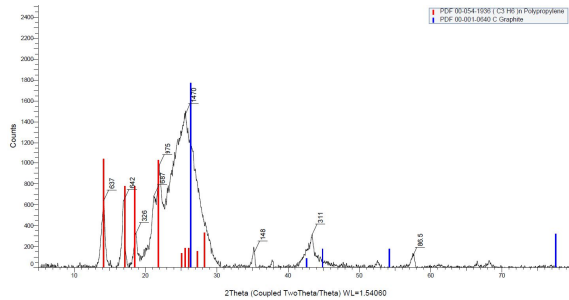


Figure 1 XRD analysis of extruded MCF/PP composites

Meanwhile, Figure 1 shows the XRD pattern of extruded MCF/PP composite materials which mainly composed of graphite particles and polypropylene structures. Thus, this verified that the extruded MCF/PP compositions were pure composites without being contaminated by others conductive elements. Besides, it can clearly observe that between the degree of 23° to 30° the compositions of MCF were wider and having higher intensity compared to polypropylene at 16° to 19° . These reflected with the electrical conductivity produced using the extrusion process which was considered higher compared to G/PP composite produced using the compression molding process [1]. Moreover, the MCF/PP composites were significant with the electrical conductivity produced since materials need to undergo the manufacturing process in order to maximize the electrical conductivity produces [9, 10].

4. CONCLUSIONS

The electrical conductivity of extruded MCF/PP composite using rod dies geometry with 5mm diameter have the highest electrical conductivity compared to the sheet dies geometry with 3mm and 5mm thickness due to better filler orientation occurred in converging dies.

5. REFERENCES

- [1] R. Dweiri, J. Sahari, "Electrical properties of carbon-based polypropylene composites for bipolar plates in polymer electrolyte membrane fuel cell (PEMFC)," *Journal of Power Sources*, vol. 171(2), pp. 424-432, 2007.
- [2] H. Suherman, A.B. Sulong, J. Sahari, "Effect of the compression molding parameters on the in-plane and through-plane conductivity of carbon nanotubes/graphite/epoxy nanocomposites as bipolar plate material for a polymer electrolyte membrane fuel cell," *Ceramics International*, vol. 39(2), pp. 1277-1284, 2013.
- [3] M.Y. Zakaria, A.B. Sulong, J. Sahari, H. Suherman, "Effect of the addition of milled carbon fiber as a secondary filler on the electrical conductivity of graphite/epoxy composites for electrical conductive material," *Composites Part B: Engineering*, vol. 83, pp. 75-80, 2015.
- [4] P.J. Hine, N. Davidson, R.A. Duckett, I.M. Ward,

"Measuring the fibre orientation and modelling the elastic properties of injection-moulded long-glass-fibre-reinforced nylon," *Composites Science and Technology* vol. 53(2), pp. 125-131, 1995.

- [5] T. Köpplmayr, I. Milosavljevic, M. Aigner, R. Hasslacher, B. Plank, D. Salaberger, J. Miethlinger, "Influence of fiber orientation and length distribution on the rheological characterization of glass-fiber-filled polypropylene," *Polymer Testing*, vol. 32(3), pp. 535-544, 2013.
- [6] A. Unverfehrt, H. Rehage, "Deformation, Orientation and Bursting of Microcapsules in Simple Shear Flow: Wrinkling Processes, Tumbling and Swinging Motions," *Procedia IUTAM*, vol. 16, pp. 12-21, 2015.
- [7] R. Taipalus, T. Harmia, M.Q. Zhang, K. Friedrich, "The electrical conductivity of carbon-fibre-reinforced polypropylene/polyaniline complex-blends: experimental characterisation and modelling," *Composites Science and Technology*, vol. 61(6), pp. 801-814, 2001.
- [8] G.A. Jimenez, S.C. Jana, "Electrically conductive polymer nanocomposites of polymethylmethacrylate and carbon nanofibers prepared by chaotic mixing," *Composites Part A: Applied Science and Manufacturing*, vol. 38(3), pp. 983-993, 2007.
- [9] H. Suherman, J. Sahari, A.B. Sulong, "Effect of small-sized conductive filler on the properties of an epoxy composite for a bipolar plate in a PEMFC," *Ceramics International*, vol. 39(6), pp. 7159-7166, 2013.
- [10] R.A. Antunes, M.C.L. de Oliveira, G. Ett, V. Ett, "Carbon materials in composite bipolar plates for polymer electrolyte membrane fuel cells: A review of the main challenges to improve electrical performance," *Journal of Power Sources*, vol. 196(6), pp. 2945-2961, 2011.

Optimization of injection molding parameters for Kenaf/PP composite using Taguchi method

Mohd Khairul Fadzly Md Radzi¹, Abu Bakar Sulong^{1*}, Norhamidi Muhamad¹, Zakaria Razak¹

¹Department of Mechanical and Material Engineering,
Faculty of Engineering and Built Environment, Universiti Kebangsaan Malaysia,
43600 Bangi, Selangor, Malaysia.

*Corresponding e-mail: abubakar@ukm.edu.my

Keywords: Injection molding; Optimization; Taguchi method; Kenaf reinforced composite

ABSTRACT- Injection molding has become the most probably important method of processing in order to fabricate excellent surface finish of complex geometric components with good dimensional and specification properties. However, molded polymers composites possibility being effected by machine parameters and other process condition that may cause poor quality of composites product. Thus in this study, composite of thermoplastic polypropylene (PP) reinforced with kenaf filler were prepared using a sigma blade mixer, followed by an injection molding process. To determine the optimal processing of injection parameters, Taguchi method with L_{27} orthogonal array was used on statistical analysis of tensile and flexural properties of kenaf/PP composites. The results obtained that optimum parameters are: injection temperature 190°C, injection pressure 1300bar, holding pressure 1900bar and flow rate 20cm³/s. From the analysis of variance (ANOVA), both injection temperature and flow rate give highest contribution factor to the strength properties of the composites.

1. INTRODUCTION

Generally, plastics injection molding is probably the most widely used cyclic process for manufacturing derived from thermoplastics materials. This processing technologies is possible to fabricate excellent surface finish of complex geometric components with good dimensional and specification properties[1]. Injection molding has been used for automotive components, especially for exteriors and interiors parts where made from polymer-matrix composites. Through this method, melts polymer is injected into the mold cavity. The process takes the fluids material under high pressure and temperature, then were cooled to form the products. In other way, injection molding covered four stage process included plasticization, injection, packing and cooling. However, Akbarzadeh et al. [2] explained that molded polymers composites are being effected by machine parameters and other process condition, may cause poor quality of surface roughness and dimensional precision, warpage, time consuming and high cost waste. Therefore, the optimization of injection molding parameters is required in order to achieve the desirable components that meet the specification rules in various industries.

Taguchi method has been explored successfully in several industrial applications, such as mechanical component design, manufacturing processes, and process optimization. From previous studies, most of researchers used this method to characterize and optimize the injection molding parameter. Ibrahim et al. claimed that changes in the injection parameter setting give difference tensile strength of HDPE/kenaf composite. Optimization technique using Taguchi method has been implement in their study and defined that melt temperature was the most significant parameter[3]. Tuo et al. approached the optimum parameters on mechanical properties of kenaf fiber-reinforced composites using Taguchi method of experimental design. The results shows influences and contributions of barrel temperature and injection pressure towards quality of composites strength properties[4]. Lin et al. investigated the comparison between two different approaches, which are the Taguchi method and the design of experiments (DOE) to determination an optimal injection molding parameter setting, in mission to predict the highest stresses and lowest wear properties of polypropylene composites[5].

Thus in this study, composite of thermoplastic polypropylene (PP) reinforced with kenaf filler were prepared using a sigma blade mixer, followed by an injection molding process. To determine the optimal processing of injection parameters, Taguchi method with L_{27} orthogonal array was used on statistical analysis of tensile and flexural properties of kenaf/PP composites. The results obtained that optimum parameters are: injection temperature 190°C, injection pressure 1300bar, holding pressure 1900bar and flow rate 20cm³/s. From the analysis of variance (ANOVA), both injection temperature and injection rate give highest contribution factor to the strength properties of the kenaf/PP composites.

2. METHODOLOGY

During the process, Taguchi orthogonal arrays L_{27} experiments of three levels were applied, and four processing parameters were used in the analysis. Table 3 show the list of processing parameters and levels. Based on the simulation observation, the significant results will be analysed and discussed further.

Table 3 Parameters and levels of process

| Factors | Description (unit) | Levels | | |
|---------|--------------------------------|--------|------|------|
| | | 1 | 2 | 3 |
| A | Injection Temperature (°C) | 190 | 200 | 210 |
| B | Injection Pressure (Bar) | 1200 | 1300 | 1400 |
| C | Holding Pressure (Bar) | 1800 | 1900 | 2000 |
| D | Flow Rate (cm ³ /s) | 18 | 19 | 20 |

The Taguchi signal-to-noise (S/N) analysis of *bigger-is-better* was chosen to obtain the optimum parameters for each response: tensile strength, Young's modulus, flexural strength and flexural modulus. Moreover, ANOVA was also used to investigate the collected data to obtain which significant factors would affect all responses. The S/N ratio can be calculated by equation below:

$$\frac{S}{N} = -10 \log \frac{1}{n} \sum_{i=1}^n \frac{1}{y_i^2} \quad (1)$$

where y_i is the measurement of experimental results and n represent the number of the samples in each mechanical test.

3. RESULTS AND DISCUSSION

Figure 1 show the mean of tensile strength and Young's modulus value which determined by Taguchi S/N ratio of *larger the better*. The highest tensile strength at 19.864MPa and highest Young's modulus strength at 2285.51MPa were achieved when applied the optimum injection parameters at injection temperature (190°C), injection pressure (1300bar), holding pressure (1900bar), and flow rate (20cm³/s).

Based on ANOVA analysis, found that injection temperature and flow rate was the most important parameter that influenced the tensile and flexural properties of the kenaf/PP composites. This was proven by the ANOVA analysis results, where the highest values of F-ratio for tensile strength and Young's modulus influenced by flow rate were 41.94 and 74.01 respectively. Meanwhile the contribution from injection temperature give the highest of F-ratio for flexural strength and flexural modulus which were 45.94 and 1.69 respectively.

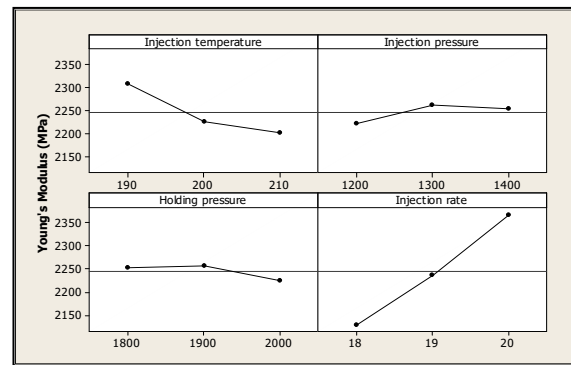
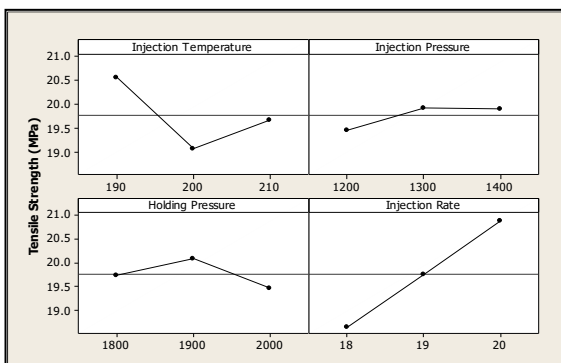


Figure 1 Mean for tensile strength and Young's modulus at various level of injection parameters

4. CONCLUSIONS

In conclusion, the optimisation of injection moulding parameters was required in order to investigate the effects of optimum parameters (injection temperature, injection pressure, holding pressure and flow rate) regarding the mechanical properties (tensile strength, Young's modulus, flexural strength and flexural modulus) of mouldability. The ANOVA analysis ascertained that injection temperature and flow rate were the most significant parameter for enhancement of mechanical properties of kenaf/PP composites.

5. ACKNOWLEDGEMENTS

The authors expresses their sincere thanks and appreciation to the Ministry of High Education Malaysia for their financial support under grant LRGS/TD/2012/USM-UKM/P1/05.

6. REFERENCES

- [1] Chen, D., et al., "Warpage of injection-molded automotive B pillar trim fabricated with ramie fiber-reinforced polypropylene composites," *Journal of Reinforced Plastics and Composites*, 2015.
- [2] Akbarzadeh Tootoonchi, A.R., "Parameter study in plastic injection molding process using statistical methods and IWO algorithm," *International Journal of Modeling and Optimization*, 2011.
- [3] Ibrahim, M.H.I., "Optimisation of Processing Condition Using Taguchi Method on Strength of HDPE-Natural Fibres Micro Composite," *Applied Mechanics and Materials*, 2014.
- [4] Tuo, X., T. Kawai, and S.-I. Kuroda, "Optimal Injection-Molding Conditions for Mechanical Properties of Kenaf Fiber Composite Materials by Taguchi Method," *Advanced Science Letters*, 2013.
- [5] Lin, Y.-H., "Optimization of injection molding process for tensile and wear properties of polypropylene components via Taguchi and design of experiments method," *Polymer-Plastics Technology and Engineering*, 2007.

Development of New Dynamic-Assisted Tool Milling using NPD and TRIZ to Fabricate Dimple Structures

Sharudin Hassan^{1,2}, Jaharah A. Ghani^{2*}, Che Hassan Che Haron², Mohd Nor Azam Mohd Dali^{1,2}

¹)Politeknik Ungku Omar, Jalan Raja Musa Mahadi,
31400 Ipoh, Perak, Malaysia.

²)Department of Mechanical and Material Engineering,
Faculty of Engineering and Built Environment, Universiti Kebangsaan Malaysia,
43600 Bangi, Selangor, Malaysia.

*Corresponding e-mail: jaharahghani@ukm.edu.my

Keywords: Vibration-assisted machining; dimple structure; new product development

ABSTRACT – In the development of new products, the techniques and methods used will affect the manufacturing process. New product development (NPD) and the Theory of Inventive Problem Solving (TRIZ) were used to design and develop a dynamic-assisted tool milling (DATM) to generate dimple structures on a flat surface. This method was chosen as it saves time and reduces the cost of fabrication.

INTRODUCTION

Nowadays, the technology concerning the manufacture of products is changing very rapidly. Manufacturers must be able to react to this factor to meet demands and to survive in the global market. In the manufacturing industry, the demand from customers will have a direct effect on the rate of production of a product. Without the discovery of new technologies and the latest production methods, the production rate will be drastically affected.

To fulfil the demands of customers, a new and effective approach needs to be used in the making of a new product. NPD is an approach that is applied in global industries when developing a product or redeveloping an old product. NPD involves the use of certain data collection methods, followed by the production of a new product that meets the objectives [1].

Studies have shown that NPD will affect the performance of an industry in terms of financial, corporate and brand identity [2][3]. This method has been used by Ford Motor Company, General Motors, Motorola, and Digital Equipment Corp. to fulfil market demands and to produce good quality products within a short period [4]. This method was chosen because the development of the product can be completed in a short time, is cheap and is of good quality.

Besides the NPD method, the TRIZ has also been used extensively in developing a product. This theory was developed in Russia in 1946 by Genrich Altshuller, and it has been applied widely to solve product or system design problems, etc. [5]. TRIZ is a method of identifying a problem and solving it in the early stages of the process right up to the development of the end product. TRIZ provides a systematic and innovative approach to solving design problems compared to existing conventional methods [6]. This method received a lot of attention from researchers when it was able to successfully achieve a targeted production rate in

the manufacturing process. For example, in the development of environmentally friendly gloves from the recycling of bottles by Chen et al., TRIZ and the Analytic Hierarchy Process (AHP) were combined to produce environmentally friendly products from recycled materials [7]

In the automotive industry, friction and wear on engine components have a significant impact on fuel consumption, engine performance and the environment. To solve this problem, surface texturing, such as dimple structures, will be fabricated on the surfaces of engine components to reduce friction and wear. Previous research has shown that a dimple structure can reduce friction by about 30-50% in engine components [8]. The quality of the dimple structure is translated via its ability to increase the tribological attributes on the sliding surfaces. A dimple structure has two functions; it acts as a reservoir, and it traps debris in lubricants. In previous studies, it was discovered that a dimple structure (profile: $\varnothing 400 \mu\text{m}$, depth $30 \mu\text{m}$ and density 15%) is able to improve the tribological performance of components compared to a non-textured surface [9].

1. METHODOLOGY

The DATM was developed in order to fabricate a dimple structure on a flat surface. To design the DATM, the conceptual design (CD) of new product development (NPD) was applied to help in the production of the DATM within a short time, as shown in Figure 1.

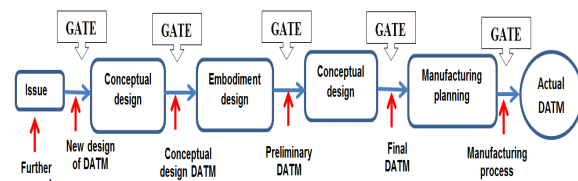


Figure 1 Conceptual design flow for DATM

All aspects of this conceptual design were refined by means of the theory of inventive problem solving (TRIZ) in order to obtain the best solution for the DATM design, as shown in Figure 2. This model was developed to discover any weaknesses that existed during the DATM development process.

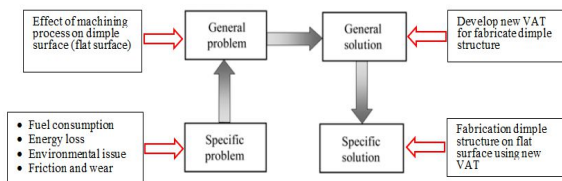


Figure 2 General model from TRIZ to develop a new DATM

The DATM prototype that was developed was tested in order to produce the dimple structure, as shown in Figure 3.

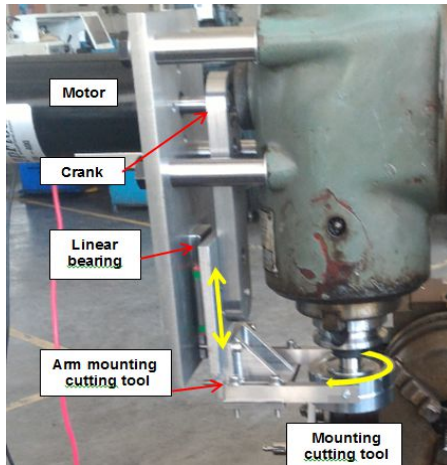


Figure 3 Dynamic-assisted tool milling on milling machine

The machining parameter that was related to the dimple structure was tested during the pilot test. This was essential in order to observe the ability of the DATM that was currently being developed for the production of a dimple structure.

2. RESULTS AND DISCUSSION

In conclusion, a DATM has currently been developed for the fabrication of a dimple structure as required on a flat surface. The array of the dimples generated by this assisted tooling depends on the feed rate, cutting speed (machine), type of cutting tool, frequency and the amplitude generated by the motor, as shown in Figure 4.

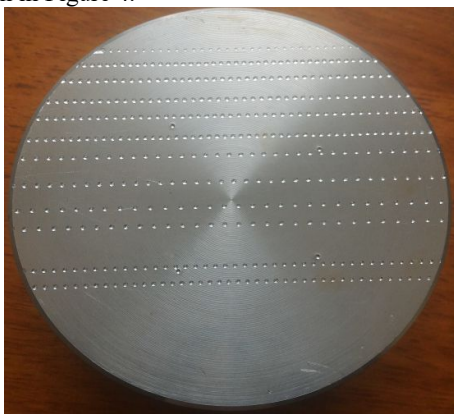


Figure 4 Dimple structure produced by using DATM

This assisted tool is able to produce multiple dimple

structures by means of the inclination of the spindle head (conventional) and the working table of the CNC machine. The depth of the dimple structure formed depends on the maximum distance generated by the crank shift. The depth of the dimple structure can also be varied according to the requirements of the study.

3. CONCLUSIONS

The new product development method can produce a dynamic-assisted tool milling (DATM) within a short time. This newly-developed DATM can be integrated with a conventional milling machine or CNC milling machine to fabricate a dimple structure on a flat surface.

4. REFERENCES

- [1] Carlos, V., Juan, C. A., "An approach to conceptual and embodiment design within a new product development lifecycle framework," *International Journal of Production Research*, 2015
- [2] Beverland, M.B., "Managing the design innovation-brand marketing interface: resolving the tension between artistic creation and commercial imperatives". *Journal of Production Innovation Management*, vol. 22, pp. 193–207, 2005
- [3] Raves, D., Stygian, I., "Product design: a review and research agenda for management studies," *International Journal of Management Reviews*, vol. 14, pp. 464–488. 2012
- [4] Boothroyd, G. "Product design for manufacture and assembly," *Computer Aided Design*, vol. 26, July 1994.
- [5] Feng, Y., Tai-yong, W., Hui-juan, N., "Function and principle innovative design of mechanical products based on TRIZ/FA," *Higher Education Press and Springer-Verlag*, pp. 350-355, 2006.
- [6] Mansor, M. R., Sapuan, S. M., Zainudin, E. S., Nuraini, A.A., Hambali, A. "Conceptual design of kenaf fibre polymer composite automotive parking brake lever using integrated TRIZ–Morphological Chart–Analytic Hierarchy Process method," *Material and Design*, vol. 54, pp. 473 - 482, 2014.
- [7] Chen H.S., Tu J. C., Guan S. S., "Applying the theory of problem-solving and AHP to develop eco-innovative design," *Springer Science and Business Media*, pp. 489–94, 2012.
- [8] Roy T., Choudhury D., Ghosh S., Bin Mamat A., and Pingguan-Murphy B., "Improved friction and wear performance of micro dimpled ceramic-on-ceramic interface for hip joint arthroplasty," *Ceramic International*, pp. 681–690, 2015
- [9] Nakano M., Korenaga A., Korenaga A., Miyake K., Murakami T., Ando Y., Usami H., Sasaki S., "Applying Micro-Texture to Cast Iron Surfaces to Reduce the Friction Coefficient Under Lubricated Conditions," *Tribology Letter*, pp. 131 – 137, 2007.

Characterizations of compression moulded polymer composite reinforced with kenaf fiber

Nur Farhani Ismail^{1,*}, Abu Bakar Sulong¹, Norhamidi Muhamad¹, Che Hassan Che Haron¹, Dulina Tholibon¹, Izdihar Tharazi¹, Mohd Khairul Fadzly Md. Radzi¹

1) Department of Mechanical and Material Engineering,
Faculty of Engineering and Built Environment, Universiti Kebangsaan Malaysia,
43600 Bangi, Selangor, Malaysia.

*Corresponding e-mail: nurfarhaniismail@yahoo.com

Keywords: Kenaf thermoset composite; Material processing; Flexural strength; Tensile strength; Microstructure.

ABSTRACT – Kenaf composites have been widely used for the engineering and industrial applications such as air cleaner, dashboard, insulation mats, fibreboard and etc. Due to considerable attentions, kenaf fibers are reinforced in polymers for the fabrication of polymer composites. This work deals with the fabrication and characterizations of untreated and treated temafa kenaf fibers. The microstructure (SEM), flexural properties and tensile properties of the prepared kenaf polymer composites were discussed in this study. The kenaf fibers were treated with 6 wt% sodium hydroxide, NaOH solution for 24 hours soaking time. The epoxy thermoset reinforced with randomly oriented temafa kenaf was fabricated using compression molding technique. The composite samples of kenaf were prepared with different kenaf fiber loadings; 20%, 30%, 40%, 50% and 60% in weight. It was found that the properties of kenaf composites mainly depend on the compositions of kenaf fibers. It has also been investigated that the treatment influences the properties of kenaf itself. Overall, the results revealed that the treated kenaf composites have better mechanical properties such as flexural strength as compared to the untreated kenaf composites. However, it is observed that the flexural strength also increases with the increment percentage of kenaf fibers. Finally, these prepared kenaf composites with better mechanical properties may be used for automotive applications.

1. INTRODUCTION

The interest of using renewable and biodegradable natural fibers as reinforcement materials in polymer composites had been increased in industries and in academic field as well [1,2]. The increment of using natural fibers is to replace the conventional synthetic or manmade fibers; Kevlar, glass, carbon and etc. This is due to the natural fibers are environmental friendly; for economic purpose and it's beneficial to the health concern. As compared to synthetic fiber, the natural fiber has many advantages such as low density, low cost, and easily available. Furthermore, they offer less abrasive to tooling processing, less irritating for the human in respiratory system and good thermal properties. These advantages are utilized to form lightweight composite especially in automotive and aerospace industries in order to reduce the weight and therefore fuel saving.

Although kenaf fiber has many advantages as mentioned, researchers encountered a main problem of difficultie in mixing between kenaf fiber and polymer.

This is because kenaf has a strong polar character (hydrophilic) which can lead to incompatibility with the most polymer matrices (hydrophobic) [3]. Therefore, the chemical treatment is required for the kenaf fiber in order to increase the wetting of the fiber with the polymer matrix [4-6]. It is well known that, chemical treatment has successfully improve the fiber strength and adhesion between matrices and fiber. Basically, chemical treatment remove lignin, hemicellulose, and wax and oils covering the surface of the fiber which can leads to the better adhesion between fiber and polymer

2. METHODOLOGY

Polymer composites materials were prepared using epoxy resin and temafa kenaf fibers. Epoxy (D.E.RTM 331TM) resin as matrix and curing agent was provided by the Dow Chemical Company. This epoxy come together with the hardener (JOINTMINETM 925-3STM) for the fast curing process. The discontinuous long fibers, temafa kenaf were supplied by *Lembaga Kenaf & Tembakau Negara* (LKTN), Malaysia.

Compression moulding process was used for the fabrication of epoxy reinforced with temafa kenaf fiber. The composites with size 100 mm x 100 mm and thickness ± 3 mm were fabricated with different percentage of untreated and treated NaOH temafa kenaf. Six different percentages of kenaf were 0%, 20%, 30%, 40%, 50% and 60% in weight were produced from the hardened steel mould. The treated kenaf (UT) were treated with 6 wt% sodium hydroxide (NaOH) solution for 24 hours soaking time. Firstly, the untreated (UT) and treated (T) fibers need to be pressed at 8 MPa for 5 minutes compression machine for making the randomly mat shape. Then, epoxy and hardener with ratio 2:1 were mixed using mechanical stirrer at lowest speed rate; 2 rpm for 5 minutes before casting into the mould. These parameters were used in order to avoid bubble and resin become jelly. The mould was placed under compression moulding environment for 15 minutes for the curing process. Then the mould was pressed at 8 MPa of compression moulding for 25 minutes.

3. RESULTS AND DISCUSSION

From the histogram in Figure 1(a), it is obvious that addition of kenaf fiber either treated or not, resulted in superior flexural strength for the composite. Similar trend in Figure 1(b) is shown for the flexural modulus of composite after reinforced with kenaf fiber. The flexural strength and modulus increase with increasing of kenaf

loading for both types of kenaf; untreated and treated. In this research, the weight percentage of fiber loading is increased up to 50 wt%.

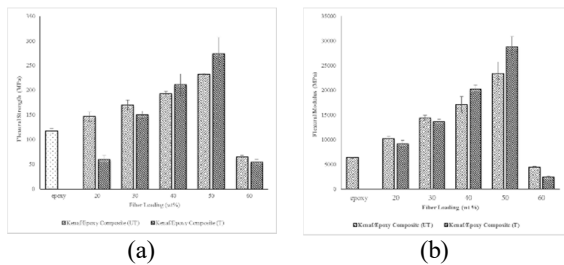


Figure 1 (a) Flexural strength and (b) flexural modulus for the kenaf/epoxy composite

Figure 2 (a) and (b) show the tensile properties of the epoxy composite reinforced with untreated and treated kenaf fiber. All the composite reinforced with the untreated kenaf show higher tensile properties than the treated kenaf fiber. Generally, reinforcement of the fiber increase the tensile strength and modulus due to the fiber has higher strength and stiffness compare to the matrix [7]. However, slight difference is shown in this work with reinforcement of 20 wt% of untreated and treated produced lower tensile strength. From the results, clearly shown that addition of 40 wt % of untreated and treated kenaf loading has produced higher tensile strength and tensile modulus.

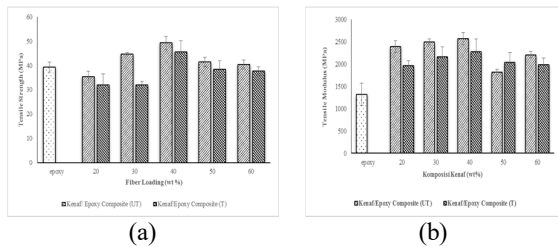


Figure 2 (a) Tensile strength and (b) tensile modulus for the kenaf/epoxy composite

The distribution and the bonding of the untreated and treated kenaf fiber were observed and analyzed after running the flexural analysis. Figure 3 shows the SEM image; a comparison of the untreated and treated kenaf shows different distribution of fiber. This obviously shows that epoxy resin was not able to penetrate the untreated kenaf fiber.

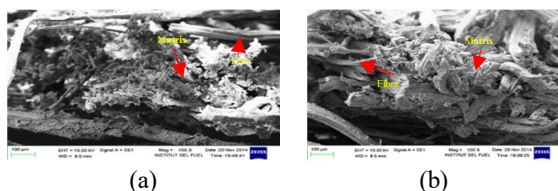


Figure 3 (a) Observation of Bonding between Kenaf Fiber and Epoxy Resin

4. CONCLUSIONS

The results indicate that alkali treatment and fiber loading of the natural fiber highly influence the mechanical properties of the epoxy composite reinforced with kenaf fiber. From the SEM image, the epoxy composite reinforced with treated kenaf has a better microstructure because the epoxy can penetrate the kenaf.

5. ACKNOWLEDGEMENT

The authors would like to thanks to the Universiti Kebangsaan Malaysia & Kementerian Pengajian Tinggi Malaysia for financial support; MyPhD & Long Term Research Grant (LRGS/TD/2012/USM-UKM/PT/05).

6. REFERENCES

- [1] Nguong, C. W., Lee, S. N. B., & Sujana, D., "A Review on Natural Fibre Reinforced Polymer Composites," pp. 1123–1130, 2013.
- [2] Mohanty, A.K., Misra, M., & Drzal, L., "Natural Fiber, Biopolymer & Biocomposite." Taylor & Francis Group, 2005.
- [3] Mahjoub, R., Mohamad, J., Rahman, A., Sam, M., & Hamid, S., "Tensile Properties Of Kenaf Fiber Due to Various Conditions Of Chemical Fiber Surface Modifications," *Construction and Building Materials*, vol. 55, pp. 103–113, 2014.
- [4] Abdan, K., "Effect of Fiber Treatment on Mechanical Properties of Kenaf Fiber-Ecoflex Composites," *Journal of Reinforced Plastics and Composites*, vol. 29, no. 14, pp. 2192–2198, 2009.
- [5] Meon, M. S., Othman, M. F., Husain, H., Remeli, M. F., & Syawal, M. S. M., "Improving Tensile Properties of Kenaf Fibers Treated with Sodium Hydroxide," *Procedia Engineering*, vol. 41 (Iris), pp. 1587–1592, 2012.
- [6] Edeerozey, A. M. M., Akil, H. M., Azhar, A. B., & Ariffin, M. I. Z., "Chemical modification of kenaf fibers.," *Materials Letters*, vol. 61, no. 10, pp. 2023–2025, 2007
- [7] Sumaila, M., Amber, I., & Bawa, M., "Effect of fiber length on the physical and mechanical properties of random oriented, nonwoven short banana (musa balbisiana) fibre / epoxy composite," *Asian Journal of Natural and Applied Sciences*, vol. 2, no. 1, pp. 39–49, 2013.

Evaluation on the Process Parameters Influencing the Surface Texture using Open-Source 3D Printing

Nor Aiman Bin Sukindar^{1,2*}, Mohd Khairol Anuar Bin Mohd Ariffin², B.T. Hang Tuah Bin Baharudin²,
Che Nor Aiza Binti Jaafar², Mohd Idris Shah Bin Ismail²

¹)Mechanical Department of Politeknik Kuching Sarawak, KM 22 Jalan Matang,
93050 Kuching, Sarawak, Malaysia.

²)Department of Mechanical and Manufacturing, Universiti Putra Malaysia,
43400 Serdang, Selangor, Malaysia.

*Corresponding e-mail: noraimansukindar@yahoo.com.my

Keywords: Surface texture; Open source 3D Printing; Process parameter.

ABSTRACT – Fused deposition modeling (FDM) or three-dimensional (3D) printing is becoming ubiquitous today because it allows the fabrication of 3D products directly from computer-aided design software. The quality of 3D parts is influenced by several parameters that need to be carefully tuned to obtain a high-quality final product. The surface finish of the finished parts is one of the major factors to consider because it affects both the dimensional accuracy and the functionality of the piece. Thus, the present study focuses on improving the surface finish of parts produced by FDM by manipulating different parameters such as layer height, raster angle, extruder temperature, printing speed, and percent infill. Polylactic acid was used in this study, which is a material present in filament form, and was extruded using a newly developed 3D printer; the design-of-experiment method was used to design the experiment. The results indicate that raster angle and extruder temperature are the most influential process parameters. The results show that raster angle and extruder temperature exert the strongest influence on the surface quality of the final product.

1. INTRODUCTION

Fused deposition modeling (FDM), also known as additive manufacturing (AM), has significantly improved since it was patented by Crump [1] in 1992. The idea of FDM is quite simple: a three-dimensional (3D) object is constructed from a melted material that is deposited layer by layer and allowed to solidify [2]. Acrylonitrile butadiene styrene and polylactic acid (PLA) are the most common materials used in FDM. Since the original patent expired a few years ago, a variety of software and hardware designs for FDM have become available on the market.

Because of its low cost, the demand for FDM technology is increasing. In 1996, Stratasys introduced the Genisys machine, which uses the inkjet printing mechanism. In the same year, Z Corp. also launched its Z402 3D printer. Other companies commercializing this technology include Beijing Yinhua Laser Rapid Prototypes Making & Mould Technology Co., Ltd. and BPM Technology [3]. However, Stratasys dominates the FDM market with a 41.5% share of all systems in 2010, making it the biggest manufacturer of AM technology [4].

The development of low-cost 3D printing began in 2004 with an open-source 3D printing project called RepRap (replicating rapid prototyping). Since then,

several 3D printers have become available on the market for as little as \$5000 [5]. However, the performance of such low-cost 3D printers remains questionable; much research and development have been done to improve this situation. For example, Melenka [6] evaluated the dimensional accuracy of parts made with the MakerbotBot Replicator 2 desktop 3D printer; the results demonstrated that settings need to be carefully monitored if a consistent geometry is required. In addition, research on how process parameters affect parts made from PLA materials shows that different process parameters (e.g., infill orientation or the number of shells) significantly impact the mechanical performance of the material [7].

Surface finish is a vital quality of the finished part because it directly affects the dimensional accuracy and, therefore, the functionality of finished parts. The present research investigates the surface finish of parts made of PLA materials by varying the process parameters of layer height, raster angle, extruder temperature, printing speed, and percent infill. All process parameters are analyzed to find which are the most influential for optimizing the printing process.

2. METHODOLOGY

2.1 Sample preparation

The experiment was conducted by using a newly developed three-axis 3D printer. The open-source software Repetier-Host, which is freely available online, was used in this work. A sample was designed by using Autodesk Inventor (Autodesk, USA) and comprised a $20 \times 20 \times 5$ mm³ rectangular cuboid converted into standard triangular language (STL) format. Various process parameters were fixed throughout the experiment such as nozzle diameter, shell thickness and also bead temperature.

2.2 Materials and Method

White PLA with a diameter of 1.75 mm was used. The specimen was fabricated with all parameter combinations considered by using Taguchi's 3⁵ design-of-experiment method implemented in Minitab 16.0 software (Minitab, USA), which gave a total of 27 experiments. The parameters were varied as shown in Table 1.

Table 1 Five parameters varied for measuring surface roughness.

| Layer thickness (mm) | Raster angle (degrees) | Printing speed (mm/s) | Liquefier temperature (°C) | Percentage infill (%) |
|----------------------|------------------------|-----------------------|----------------------------|-----------------------|
| 0.2 | 45 | 60 | 200 | 20 |
| 0.3 | 70 | 80 | 230 | 60 |
| 0.4 | 90 | 90 | 260 | 100 |

2.3 Surface roughness measurements

To measure the surface roughness, we used a Perthometer S2 PGK (Mahr, Germany) surface analyzer. To ensure consistent data, three readings were taken, each at three different spots on the sample surface.

3. RESULTS AND DISCUSSION

Table 2 shows the results of analysis of variance for this experiment. The raster angle was set at 45°, 70°, and 90°. The result of an analysis of variance shows that raster angle is a dominant parameter (p -value = 0.000) for determining surface roughness, which is consistent with previous results [8, 9]. The parameter “liquefier temperature” is also significant for the surface roughness (p -value = 0.001), and a liquefier temperature of 200°C gives the highest Ra . The liquefier temperature must be carefully monitored to determine the optimum temperature for printing.

Table 2 Results of analysis of variance.

| Source | DF | Seq SS | Adj SS | Adj MS | F | p -value |
|----------------------|----|---------|--------|--------|-------|------------|
| Printing Speed | 2 | 27.63 | 48.07 | 24.03 | 0.93 | 0.414 |
| Extruder Temperature | 2 | 453.93 | 602.97 | 301.48 | 11.68 | 0.001 |
| Layer Thickness | 2 | 426.58 | 152.65 | 76.32 | 2.96 | 0.081 |
| Raster Angle | 2 | 668.33 | 668.33 | 334.17 | 12.95 | 0.000 |
| Percentage Infill | 2 | 43.37 | 43.37 | 21.69 | 0.84 | 0.450 |
| Error | 16 | 412.94 | 412.94 | 25.81 | | |
| Total | 26 | 2032.78 | | | | |

The effect of printing temperature was observed by imaging with a scanning electron microscope (Hitachi SU1510, Japan) as shown in Figure 1.

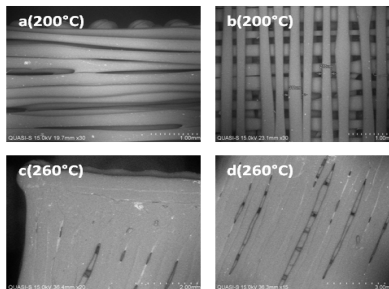


Figure 1 Finished parts made at different temperatures.

If the temperature is too low, the bonding between each layer is affected and the surface finish is rough [cf. Figures 1(a) and 1(b)]. In addition, the road width of

each layer becomes inconsistent if the liquefier does not sufficiently heat the filament. However, if the temperature is much higher than it should be, the road width causes expansion, as shown in Figures 1(c) and 1(d), and this phenomenon affects the accuracy of the final product. Based on this analysis, 230°C is the optimum temperature because it gives the lowest Ra .

4. CONCLUSIONS

All parameters of the 3D printing process were analyzed to obtain optimum results. Based on our analysis, the raster angle and extruder temperature exert the strongest influence on the surface roughness of the final pieces

5. REFERENCES

- [1] Crump, S. S., “Apparatus and method for creating three-dimensional objects,” U.S. Patent 5,121,329, issued June 9, 1992.
- [2] Gibson, I., Rosen, D. W., and Stucker, B., “Additive Manufacturing Technologies,” Springer New York Heidelberg Dordrecht London, 2010.
- [3] Wohlers, T. and Gornet, T., “History of additive manufacturing Introduction of non-SL systems Introduction of low-cost 3D printers,” *Wohlers Rep. 2011*, pp. 1–23, 2011.
- [4] Turner, B. N., Strong, R., and Gold, S. A., “A review of melt extrusion additive manufacturing processes: I. Process design and modeling,” *Rapid Prototyp. Journal*, vol. 20, no. 3, pp. 192–204, 2014.
- [5] Roberson, D. A., Espalin, D., and Wicker, R. B., “3D printer selection: A decision-making evaluation and ranking model,” *Virtual Phys. Prototyp.*, vol. 8, no. 3, pp. 201–212, 2013.
- [6] Melenka, G. W., Schofield, J. S., Dawson, M. R., and Carey, J. P., “Evaluation of dimensional accuracy and material properties of the MakerBot 3D desktop printer,” *Rapid Prototyp. Journal*, vol. 21, no. 5, pp. 618–627, 2015.
- [7] Lanzotti, A., Grasso, M., Staiano, G., and Martorelli, M., “The impact of process parameters on mechanical properties of parts fabricated in PLA with an open-source 3-D printer,” *Rapid Prototyp. Journal*, vol. 21, no. 5, pp. 604–617, 2015.
- [8] Vasudevarao, B., Natarajan, D. P., and Henderson, M., “Sensitivity of R_p Surface Finish To Process,” *Solid Free. Fabr. Proc.*, pp. 251–258, 2000.
- [9] O. Canada and O. Canada, “Evaluation of the Surface Roughness of Additive Manufacturing Parts Based on the Modelling of Cusp Geometry Farzaneh Kaji *, Ahmad Barari **,” *15th IFAC Symp. Inf. Control Manuf.*, vol. 48, no. 3, pp. 692–697, 2015.

Optimization of Tool Geometry Design: The Effects on Surface Roughness

Rosdi Mohammad¹, Mohamad Khairol Anuar Ariffin^{1*}, B. T. Hang Tuah Baharuddin¹, Faizal Mustapha² and Hideki Aoyama³

¹) Department of Mechanical and Manufacturing Engineering, Fac. of Engineering, Univ. Putra Malaysia, 43400 Serdang, Malaysia.

²) Department of Aerospace Engineering, Fac. of Engineering, Univ. Putra Malaysia, 43400 Serdang, Malaysia.

³) Department of Mechanical Engineering, Fac. of Science and Technology, Keio University, Yokohama 223-8522, Japan.

*Corresponding e-mail: khairol@upm.edu.my

Keywords: AISI12L14; Turning; Rake angle; Surface roughness.

ABSTRACT – This paper aims to optimize a new cutter design for turning of AISI12L14 with TiAlN-coated tungsten carbide tool. The interaction of the tool geometry and work-piece on the performance characteristic of surface roughness has been investigated, and Taguchi method is selected as the technique for the optimization. Results showed that gradually altering negative to positive rake angles will give significant influence on part's surface finishing. However, the minor cutting tool edge, $Kr2$ with 3° is found to be the predominant factor in influencing surface roughness, Ry . Taguchi parameter design was found to be a simple, systematic, reliable, and efficient tools for the tool's optimization process in turning of AISI 12L14.

1. INTRODUCTION

All manufacturers are presumed to have higher and higher productivity in their machining processes, continually improving performance and experiencing cost reduction in their machining productivity processes. Therefore, major improvements in the design of cutting tools are needed. Apart from considering the tool life, strict control on the quality of surface finishing during turning is extremely important. The surface roughness significantly depends on the characteristic of work-piece, while the tool life and the chip controllability are often managed by the development of tool technology. Also, the mass production circumstances are some of the important keys to being considered in turning-interrelated factors optimization. Optimization is impossible or otherwise, all the interaction parameters are known. Multiple factors instead of one factor at one time must be considered when conducting the experiment. Numerous optimization techniques have been introduced, and Taguchi method is likely to be the most practical and superior design technique widely chosen by many industrial practices and researchers. According to Taguchi method, all factors can be considered at once, as well as it gives a better graphic visualization via S/N ratio calculation to obtain an accurate optimum machining condition, and eventually capable of saving time and reducing cost [1].

Turning process is the mechanical actions where a single point cutting tool is used to cut the work-piece by the means of mechanical deformation to produce the desired shapes. Turning involves the use of high-speed

rotation of the spindle and/or sub-spindle while doing their jobs. Turning with high feeding allowed the increase of manufacturing volume, but other problems will arise; the cutting forces increment and larger metal removal rate, which decrease the cutting tool life significantly. Cutting speed, depth of cut, feed rate, and other machine regimes control parameters contributed to the formed magnitude of forces, temperature, chip formation, which lead to the tool effectiveness and performance. Other factors, e.g. heat, wear, and chemical resistant, toughness or difficult to break characteristic are some of the most identical aspects intensively focused by the majority of tool/insert manufacturers in designing and fabricating their tool/insert for the optimum performance.

In spite of extensive research on tool geometry design, determining the optimum tool geometry of WC tool for AISI 12L14 free cutting steel (an 'easy-to-machine' material yet has sticky characteristic), in an industrial setting, is still relies on the operators' skill and also trial-and-error methods. On top of that, their effects on the surface finishing of AISI12L14 work-piece in turning are still lacking. Therefore, the aim of this work is to obtain optimized tool geometry of single cutting tool coated with TiAlN on AISI12L14, as the function of surface roughness (Ry) based on Taguchi technique. Experiments were carried out to study the effects of major and minor cutting tool angle, rake angle, and inclination angle on work-piece affecting the performance characteristics of surface roughness.

2. METHODOLOGY

Three levels and four parameters (L9) Taguchi orthogonal array (OA) design was used to determine the relationships of tool geometries on the cutting forces and machined surface roughness. A total of nine experiments were conducted. Table 1 shows the L9 Taguchi orthogonal array was used for the four factors (major tool cutting edge angle, minor tool cutting edge angle, rake angle and inclination angle) considered at three levels, respectively. Three major cutting parameters, cutting speed, Vc : 100m/min, depth of cut, ap : 2.00mm, and feed rate, fr : 0.3mm/rev. was set. The surface roughness Ry was obtained using Mitutoyo Surftest SV-400 using cut-off length and traverse lengths of 0.8 and 4.0mm, respectively.

Table 1. : Taguchi orthogonal array (L9) design

| Test | Major tool cutting edge angle ($Kr1$) $^{\circ}$ | Minor tool cutting edge angle ($Kr2$) $^{\circ}$ | Rake angle (γ) $^{\circ}$ | Inclination angle (λ) $^{\circ}$ |
|------|--|--|------------------------------------|--|
| 1 | 90 | 7 | +10 | +3 |
| 2 | 90 | 5 | 0 | 0 |
| 3 | 90 | 3 | -10 | -3 |
| 4 | 70 | 7 | 0 | -3 |
| 5 | 70 | 5 | -10 | +3 |
| 6 | 70 | 3 | +10 | 0 |
| 7 | 60 | 7 | -10 | 0 |
| 8 | 60 | 5 | +10 | -3 |
| 9 | 60 | 3 | 0 | +3 |

3. RESULTS AND DISCUSSION

Quality characteristic for smaller-the-better was applied to assess the surface roughness, Ry . The smaller values are always preferred and it indicates that the high accuracy parts produced. The experimental results (Table 2) showed the obtained surface roughness (Ry) values were low i.e. between $6.76\mu\text{m}$ to $16.18\mu\text{m}$, and within a desirable range in manufacturing requirements. The optimum turning operation was obtained at T9 test setting with $Kr1$: 60° , $Kr2$: 3° , rake angle: 0° , and inclination angle: $+3^{\circ}$; which provided the smallest surface roughness (Ry) value.

Table 2: Experimental result for Ry using four tool geometry ($Kr1$: major cutting tool edge angle, $Kr2$: minor cutting tool edge, γ : rake angle, and λ : inclination angle) for nine tests (N°).

| N° | $Kr1$ ($^{\circ}$) | $Kr2$ ($^{\circ}$) | γ ($^{\circ}$) | λ ($^{\circ}$) | Ry (μm) |
|-------------|----------------------|----------------------|-------------------------|--------------------------|------------------------|
| T1 | 90 | 7 | +10 | +3 | 12.46 |
| T2 | 90 | 5 | 0 | 0 | 09.19 |
| T3 | 90 | 3 | -10 | -3 | 08.48 |
| T4 | 70 | 7 | 0 | -3 | 15.73 |
| T5 | 70 | 5 | -10 | +3 | 13.31 |
| T6 | 70 | 3 | +10 | 0 | 07.38 |
| T7 | 60 | 7 | -10 | 0 | 16.18 |
| T8 | 60 | 5 | +10 | -3 | 07.70 |
| T9 | 60 | 3 | 0 | +3 | 06.76 |

Furthermore, the analysis of S/N ratio for surface roughness in Table 3 shows that $Kr2$ gave the highest delta value of 5.83, followed by rake angle, $Kr1$, and inclination angle with the respective delta value of 2.74, 1.73, and 0.25. A high delta indicates a strong effect of tool geometry on the resultant surface roughness, Ry . This indicated that $Kr2$ has a major influence on the surface finish of workpiece. The effects of $Kr2$ which is having 3° of the extended surface area are larger than other geometry tools, it's provided as an extended tool cutting edge length engagement between the tool and machined surface compared to other cutting tools, which causes a better surface roughness. As $Kr2$ extended angle increased to 5° and 7° , poor surface quality was obtained. Zhanqiang et. al. [4] also reported the same.

Table 3: Response table for surface roughness S/N ratio.

| Level | $Kr1$ ($^{\circ}$) | $Kr2$ ($^{\circ}$) | γ ($^{\circ}$) | λ ($^{\circ}$) |
|-------|----------------------|----------------------|-------------------------|--------------------------|
| 1 | -19.93 | -23.35 | -19.01 | -20.34 |
| 2 | -21.26 | -19.85 | -19.95 | -20.28 |
| 3 | -19.53 | -17.52 | -21.75 | -20.09 |
| Delta | 1.73 | 5.83 | 2.74 | 0.25 |
| Rank | 3 | 1 | 2 | 4 |

4. CONCLUSIONS

At cutting speed, $Vc = 100\text{m/min}$, depth of cut, $ap = 2.0\text{mm}$ and feed rate, $fr = 0.3\text{mm/rev}$. the optimum tool geometry on Ry was obtained at $Kr2$: 3° , and rake angle at $+10^{\circ}$. In general, $Kr2$ with 3° having an extended contact length between cutting edge and machined surface was found to be the predominant factor in influencing surface roughness, Ry .

5. ACKNOWLEDGEMENTS

The authors wish to thank MPM Precision Sdn. Bhd. for providing the tools, work material and technical support towards the project. They also wish to thank the UN/SEED.NET program for financial assistance under grant no. UPM CRI 1501 vote number 6386000.

6. REFERENCES

- [1] Mohd Sazali M.S., Jaharah A.G., Mohd Shahir K., Siti Haryani T., Che Hassan C.H., "Comparison Between Taguchi Method And Response Surface Methodology (Rsm) In Optimizing Machining Condition," *Proceeding of 1st International Conference on Robust Quality Engineering 2013 Universiti Technology Malaysia*, 2013.
- [2] Hashimura M., Miyanishi K., Mizuno A., "Development Of Low-Carbon Lead-Free Free-Cutting Steel Friendly To Environment," *Nippon Steel Technical Report*, no. 96, 2007.
- [3] Basim A.K., Mohamed B., "Machining Of Nickel Based Alloys Using Different Cemented Carbide Tools," *Journal of Engineering Sciences and Technology*, vol. 5, no. 3, 2010.
- [4] Zhanqiang L., Zhang P., Guo P., Ai X., "Surface Roughness In High Feed Turning With Wiper Insert," *Key Engineering Materials*, pp. 375:376, 2008.

Tensile Properties of Unidirectional Kenaf Fibre Reinforced Poly(lactic-Acid) Composites

Izdihar Tharazi^{1,2*}, Abu Bakar Sulong¹, Norhamidi Muhamad¹, Che Hassan Che Haron¹, Dulina Tholibon^{1,3}, Nur Farhani Ismail¹, Mohd Khairul Fadzly Md Radzi¹, Zakaria Razak¹

¹)Department of Mechanical and Material Engineering,
Faculty of Engineering and Built Environment, Universiti Kebangsaan Malaysia,
43600 Bangi, Selangor, Malaysia.

²) Faculty of Mechanical Engineering, Universiti Teknologi MARA Shah Alam,
40450 Shah Alam, Selangor.

³) Department of Mechanical Engineering, Politeknik Merlimau,
KB 1031, Pejabat Pos Merlimau, Melaka, Malaysia.

*Corresponding e-mail: izdihar.tharazi@gmail.com

Keywords: Natural fibres; Biodegradable Polymer; Mechanical Properties.

ABSTRACT – Recent developments in the field of natural fibre reinforced polymer composite have led to a renewed interest in fully biodegradable composite or called as a green composite. The interest in using green composites is due to environmental awareness concern as well as new rules and stringent government regulations. The study is aimed to investigate the tensile properties of kenaf reinforced biodegradable polymer. In this study, unidirectional long kenaf fibre is used as reinforcement in poly(lactic acid) (PLA) composites. The volume fraction of kenaf used is 10%wt to 50%wt prepared by film stacking method with a hot-press machine. A series of tensile tests were performed to obtain the perfect fibre content of kenaf composites. The unidirectional fibre-reinforced composites showed tensile and modulus of 183 MPa and 15 GPa, respectively. The tensile and modulus of the kenaf fibre-reinforced composites increased linearly up to a fibre content of 40%. This composite should find applications in ranging from non-structural to structural especially in the field of aerospace, automotive, and construction industries.

1. INTRODUCTION

Over the years, the application of natural fibres as reinforcement in polymer composites has increased due to its good specific mechanical properties, lightweight, non-toxic, non-abrasive, low cost and also environmental friendly properties. There are three types of origin of natural fibres such as animals, plants, and minerals. However, plants fibre is the most popular and widely used due to its availability, abundant and cost. In Malaysia, kenaf cultivation has started early in the year 2000 to replace the tobacco plantation. Kenaf has been identified the new potential crop due to its fast grown and low pest attacks compared to other plants [1].

The use of kenaf as reinforcement in synthetic polymer makes the composite semi-biodegradable or not fully biodegraded. Therefore, to achieve fully biodegradable composite or green composite, kenaf or natural fibre must be reinforced with the biodegradable polymer matrix. PLA or poly(lactic acid) or sometimes called as polylactide is an aliphatic polyester and biocompatible thermoplastic, which can be semicrystalline or totally amorphous in nature. PLA is currently a most promising and popular material with the brightest development prospect and considered as

the ‘green’ eco friendly material. The study by Huda et al. [2] demonstrated that a good mechanical properties laminated composite could be successfully developed with surface treated of kenaf fibres reinforced with PLA by using the film-stacking method. In the study, the author used 40 wt% of kenaf fibre in average of 18-24 mm long. Romhany et al. [3] determined that unidirectional flax fibre reinforced starch composites strongly improves both stiffness and strength compared to the pure matrix at a fibre content of 40%. The main objective of this paper is to determine the perfect kenaf fibre content in unidirectional orientation for fabrication of green composites. The effects of fibre content on tensile properties of the composites were discussed.

2. METHODOLOGY

Continuous long fibre of kenaf (LKF) from bast undergone bio-retting process was supplied locally by Innovative Pultrusion Sdn. Bhd. PLA powders and pellets from Shenzun Esun China Ltd were also supplied by Innovative Pultrusion Sdn. Bhd. The properties of the PLA pellets can be found in Table 1.

Table 1 Typical properties of PLA

| Properties | Details |
|----------------------------|------------------------|
| Melt Index at 190°C/2.16kg | 10-12 g/10 min |
| Density | 1.25 g/cm ³ |
| Yield Strength | 55 MPa |
| Elongation at Break (%) | 2 |
| Flexural Strength | 78 MPa |
| Flexural Modulus | 3110 MPa |
| Impact Strength | 4.4 KJ/m ² |

LKF and PLA pellets were dried in an oven at a temperature of 40°C for 48 hours. PLA and LKF (average length 175 mm) composites were produced by hot pressing using film-stacking method at five different fibre contents (10, 20, 30, 40 and 50 wt.%). For this work, 60%wt fibre content can not be done because of an insufficient amount of matrix was observed. Prior to aligning, the LKF were combed to produce long, clean and untangle the strong bonding of individual fibres [4]. PLA films and fibres were weighed prior to composite fabrication to determine the weight percentage of fibres and matrix of the resulting composites. Initially, two films of PLA were prepared and LKF with the sprinkled PLA powder were shaken in the container. After that, followed by sandwiching the LKF with the two layers

of PLA films for composite fabrication. The composites were pressed at 190°C for 5 min keeping a constant pressure of 5 MPa using a hot press machine. The assembly was cooled under a pressure of 5 MPa for 5 min. Composite plates were cut to desired shapes using a shearing machine for the tensile test. Tensile testing was carried out according to the ASTM D 638. Five samples were assessed for each batch of samples by Zwick tensile test machine with 100kN load. The cross-head speed was set to 5 mm/min.

3. RESULTS AND DISCUSSION

The average results of tensile strength and tensile modulus of the unidirectional long fibre kenaf composite as a function of fibre content are shown in Figure 1 and 2. Results show that the tensile properties depend strongly on the LKF which have higher tensile compared to pure PLA. As can be seen, tensile strength and modulus increase linearly with fibre content up to 40%. The tensile strength and modulus were 183 MPa and 15 GPa, respectively, in samples with a fibre content of 40 wt%. However, tensile strength and modulus of composite decreased to 153 MPa and 14 GPa as fibre content increased to 50 wt%. It could be explained that at this high fibre content, the wetting of fibre by PLA became worse resulting in weaker fibre/matrix bonding which caused the reduction of composite tensile strength. According to Ochi [5], the optimum fibre content should be kept less than 60% wt because some voids and an insufficient amount of resin are observed with fibre content at 70wt%. The result obtained in this work was similarly and in agreement with reported tensile properties for the long natural fibre reinforced PLA composites [2][5][6][7].

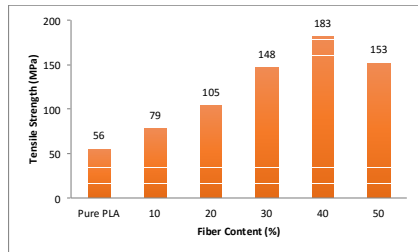


Figure 1 Tensile Strength of Kenaf/PLA as function fibre content

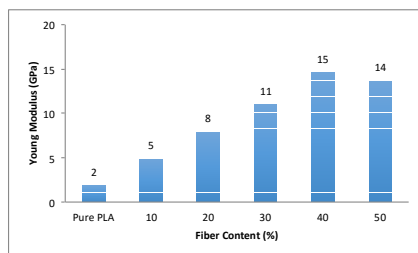


Figure 2 Young Modulus of Kenaf/PLA as function fibre content

4. CONCLUSIONS

PLA could be reinforced with a maximum of 50 wt% fibres using film stacking method but could not be processed at higher fibre content due to the insufficient matrix to cover the composite plates. While the 40 wt% fibres give the maximum tensile properties overall, the 50wt% fibres samples exhibit fibre/matrix delamination after several days. Further processing studies will be done in next future where as a determination for optimum processing parameters on the kenaf composites with 40 wt% fibre content.

5. ACKNOWLEDGEMENT

The authors would like to appreciate the Universiti Kebangsaan Malaysia and Kementerian Pengajian Tinggi Malaysia for the financial support under Long Term Research Grant Scheme (LRGS/TD/2012/USM-UKM/PT/05).

6. REFERENCES

- [1] M. Z. A. Thirmizir, Z. a M. Ishak, R. M. Taib, S. Rahim, and S. M. Jani, "Natural Weathering of Kenaf Bast Fibre-Filled Poly(Butylene Succinate) Composites: Effect of Fibre Loading and Compatibiliser Addition," *J. Polym. Environ.*, vol. 19, no. 1, pp. 263–273, 2011.
- [2] M. S. Huda, L. T. Drzal, A. K. Mohanty, and M. Misra, "Effect of fiber surface-treatments on the properties of laminated biocomposites from poly(lactic acid) (PLA) and kenaf fibers," *Compos. Sci. Technol.*, vol. 68, no. 2, pp. 424–432, Feb. 2008.
- [3] G.Romhany, J. Karger-Kocsis, and T. Czigany, "Tensile fracture and failure behavior of thermoplastic starch with unidirectional and cross-ply flax fiber reinforcements," *Macromol. Mater. Eng.*, vol. 288, no. 9, pp. 699–707, 2003.
- [4] M. Bernard, A. Khalina, A. Ali, R. Janius, M. Faizal, K. S. Hasnah, and A. B. Sanuddin, "The effect of processing parameters on the mechanical properties of kenaf fibre plastic composite," *Mater. Des.*, vol. 32, no. 2, pp. 1039–1043, 2011.
- [5] S. Ochi, "Mechanical properties of kenaf fibers and kenaf/PLA composites," *Mech. Mater.*, vol. 40, no. 4–5, pp. 446–452, 2008.
- [6] K. Oksman, M. Skrifvars, and J.-F. Selin, "Natural fibres as reinforcement in polylactic acid (PLA) composites," *Compos. Sci. Technol.*, vol. 63, no. 9, pp. 1317–1324, 2003.
- [7] T. Nishino, K. Hirao, M. Kotera, K. Nakamae, and H. Inagaki, "Kenaf reinforced biodegradable composite," *Compos. Sci. Technol.*, vol. 63, no. 9, pp. 1281–1286, 2003.

Effect of UV/O₃ modified RH on the Tensile Properties of rHDPE/RH Composite

Nishata Royan Rajendran Royan^{1*}, Abu Bakar Sulong¹, Nor Yuliana Yuhana Mohd¹, Hafizuddin Ab Ghani², Sahrim Ahmad²

¹Faculty of Engineering and Built Environment, Universiti Kebangsaan Malaysia,
43600 Bangi, Selangor, Malaysia.

²Faculty of Science and Technology, Universiti Kebangsaan Malaysia,
43600 Bangi, Selangor, Malaysia

*Corresponding e-mail: ry_nish@yahoo.com

Keywords: Surface Modification; UV/O₃ Treatment; Tensile Properties.

ABSTRACT – Modification of rice husk (RH) surfaces by ultraviolet-ozonolysis (UV/O₃) treatment were carried out in order to study the effects on the tensile strength. The untreated and treated RH was characterized by FTIR and SEM. Recycled HDPE/RH composites were prepared with five different loading of RH fibers (10, 20, 30, 40 and 50 wt %) using the twin screw extrusion method. MAPE was added as a coupling agent. A quantitative improvement in tensile strength was observed in composites filled with UV/O₃-treated RH in comparison with composites filled with untreated RH. UV/O₃ treatment removes lignin, hemicellulose, fats and waxes from RH surfaces thus giving a rougher surface on RH. Therefore, UV/O₃ treatment can be used as an alternative method to modify RH surface in order to improve the adhesion between hydrophilic RH fibre and the hydrophobic rHDPE polymer matrix.

1. INTRODUCTION

There are an increasing number of research studies and developments of the use of natural fibers to reinforce polymers in the WPC technology recently. This is due to their biodegradability, low costs, environmentally friendly, low density, non-hazardous, nonabrasive nature and a wide variety of fiber types. [1].

Rice husk (RH) is one of the agricultural waste materials that acts like a cellulose-based fibre. It is estimated that RH of approximately 20% is obtained from the total rice by the milling process. Generally, rice husk contains 35% cellulose, 25% hemicellulose, 20% lignin and 17% ash (94% silica) by weight depends on the geographic location [2]. Many types of research are currently interested on rice husk reinforced thermoplastic composites.

The main problem of the broad usage of these fibres in thermoplastic polymers is the poor incompatibility between the hydrophilic natural fibres and the hydrophobic thermoplastic matrices. This leads to undesirable properties of the composites. It is therefore necessary to modify the fibre surface by employing chemical modifications to improve the adhesion between fibre and matrix [3]. There are many types of research on the types of surface modifications of RH reported typically the alkali treatment but few reported on the alternative ozone surface modification method.

In the ozonolysis process, the biomass is treated with ozone, which causes degradation of lignin by attacking aromatic rings structures, while hemicellulose and cellulose are not damaged [4]. It can be used to

disrupt the structure of many different lignocellulosic materials, such as wheat straw, bagasse, pine, peanut, cotton straw and poplar sawdust [5].

Therefore, the main objective of this study is to explore an alternative approach to modify the rice husk surface using the ultra-violet/ozone (UV/O₃) treatment. Also, the effect of untreated RH and UV/O₃ treated RH composites on the tensile strength is being reported here.

2. METHODOLOGY

Rice husk (RH) were supplied by DinXings(M) Sdn Bhd with mesh size 212 µm while recycled HDPE is used as a matrix in the biocomposites. Maleic anhydride grafted polyethylene (MAPE) is used as coupling agent.

Rice husk was oven dried at 80°C for 24 h in order to reduce the moisture content and then stored in sealed plastic bag before compounding. For surface modification of UV/O₃-treatment, the RH is exposed to a self-made in-house UV/O₃ system for 30 min exposure time and 10 Lm⁻¹ ozone flowrate.

For the composite processing of raw and surface modified RH, a counter-rotating twin screw extruder (Thermo Prism TSE 16PC) was employed for compounding and hot and cold press process (LP50, LABTECH Engineering Company LTD) was used to make the specimen panels for testing.

The raw and surface modified RH were analysed using FTIR and scanning electron microscope (SEM). Prepared composite specimens were characterized by tensile tests according to ASTM D 638-03 using Materials Testing Machine, model: M350-10CT with the speed of 5 mm/min.

3. RESULTS AND DISCUSSION

Figure 1 shows the FTIR spectra of untreated RH and UV/O₃-treated RH. It can be seen that there are significant changes between untreated RH and UV/O₃-treated RH in the spectrum of 3200–3400 cm⁻¹, which represents the stretching vibration of intermolecular hydrogen-bonded -OH groups in the cellulose fibers. UV/O₃-treated RH shows a broader peak at 3318 cm⁻¹ compared to the peak at 3294 cm⁻¹ from untreated RH which indicates a higher concentration of hydroxyl group which contributed by ozone. Ozone exists as both molecular and atomic oxygen on the surface of the carbon. Atomic oxygen is a powerful oxidizing agent, which oxidizes the carbon surface into acidic functional groups such as carboxylic, ketonic and phenolic on ozone treatment[6].

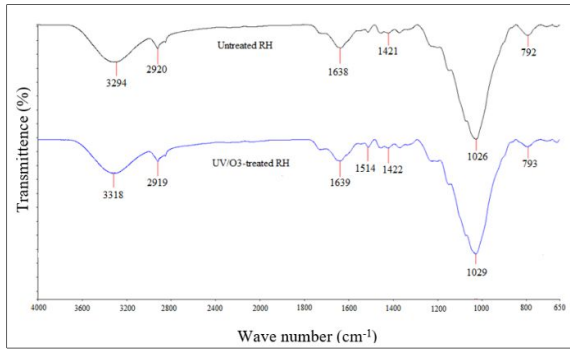


Figure 1 FTIR spectra of untreated and UV/O₃-treated rice husk

Scanning electron (SEM) micrographs of untreated and UV/O₃-treated rice husk are shown in Figure 2. Untreated RH possesses a smooth, flat and cloudy surface due to the presence of lignin, wax, and hemicelluloses [7]. However, UV/O₃-treated RH possess a rougher surface. Rougher surface allow improvement on the compatibility between fibers and matrix [8].

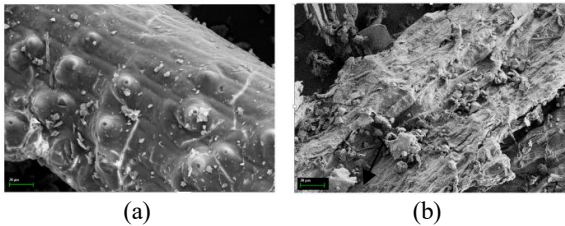


Figure 2 SEM image of (a) untreated and (b) UV/O₃-treated rice husk under 500x magnification

Figure 3 illustrates the results obtained from tensile Young's Modulus for untreated and UV/O₃-treated rice husk reinforced rHDPE composite. Both results show an increase of composite stiffness as the RH filler increases [9]. However, UV/O₃-treated RH reinforced rHDPE composite shows better results compared to the untreated RH composite. This supports that ozone treatment removes lignin, hemicellulose, fats and waxes from RH surfaces thus giving a rougher surface on RH. Therefore, UV/O₃-treated RH improves the compatibility between hydrophobic polymer and hydrophilic rice husk [4,5,6].

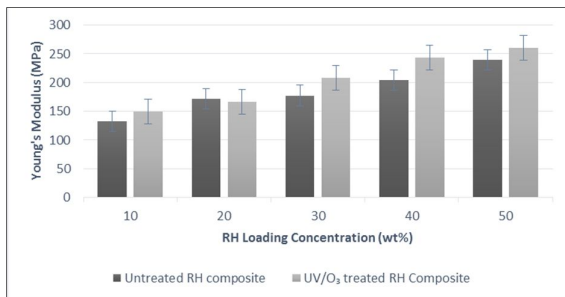


Figure3 Tensile strength of untreated and UV/O₃-treated rice husk composites

4. CONCLUSIONS

The UV/O₃ treatment can be used as an alternative method to modify RH surface in order to improve the adhesion between hydrophilic RH fibre and the hydrophobic rHDPE polymer matrix.

5. ACKNOWLEDGEMENT

The authors would like to acknowledge Kementerian Pengajian Tinggi Malaysia for the financial support under Long Term Research Grant Scheme (LRGS/TD/2012/USM-UKM/PT/05).

6. REFERENCES

- [1] A.Ashori, 2008. Wood-plastic composites as promising green-composites for automotive industries! *Bioresources Technology*, vol. 99, pp. 4661-4667, 2008.
- [2] H. G. B. Premalal, H. Ismail, and A. Baharin, "Comparison of the mechanical properties of rice husk powder filled polypropylene composites with talc filled polypropylene composites," *Polymer Testing*, vol. 21, pp. 833-839, 2002.
- [3] Malkapuram, R, Kumar, V and Yuvraj, S N, Recent Development in Natural Fibre Reinforced Polypropylene Composites," *Journal of Reinforced Plastics and Composites*, vol. 28, pp. 1169-1189, 2008.
- [4] Nakamura Y, Daidai M, Kobayashi F. Ozonolysis mechanism of lignin model compounds and microbial treatment of organic acids produced," *Water Science Technology*, vol. 50, no. 3, pp. 167-172, 2004.
- [5] Sun Y, Cheng J. Hydrolysis of lignocellulosic materials for ethanol production: A review," *Bioresources Technology*, 2002; 83:1-11
- [6] Sugashini S, Begum K.M.S, Performance of ozone treated rice husk carbon (OTRHC) for continuous adsorption of Cr (VI) ions from synthetic effluent," *Journal of Environmental Chemical Engineering*, no. 1, pp. 79-85, 2013.
- [7] Mohanty, A.K., M. Misra, L.T. Drzal, "Natural fibre, biopolymer and biocomposites," New York: *Taylor & Francis Group, LLC*, 2005.
- [8] Syafri, R., I. Ahmad, I. Abdullah, "Effect of rice husk surface modification by LENR the on mechanical properties of NR/HDPE reinforced rice husk composite," *Sains Malaysiana*, vol. 40, no. 7, pp. 749-756, 2011.
- [9] Rahman, M.R., Islam, M.N., Haque, M.M. and Ahmed, A.S., "Effect of Chemical Treatment on Rice Husk (RH) Reinforced Polyethylene (PE) Composites," *Bioresources*, vol. 5, no. 2, pp. 854-892, 2010.

Process Optimization of Unidirectional Kenaf Polypropylene Composites by Full Factorial Design

Dulina Tholibon^{1,2,*}, Abu Bakar Sulong¹, Norhamidi Muhamad¹, Nur Farhani Ismail¹,
Izdihar Tharazi^{1,3} and Mohd Khairul Fadzly Md Radzi¹

¹)Department of Mechanical and Material Engineering,
Faculty of Engineering and Built Environment, Universiti Kebangsaan Malaysia,
43600 Bangi, Selangor, Malaysia.

²)Department of Mechanical Engineering, Politeknik Merlimau. KB 1031,
Pejabat Pos Merlimau, Melaka, Malaysia

³) Faculty of Mechanical Engineering, Universiti Teknologi MARA Shah Alam,
40450 Shah Alam, Selangor.

*Corresponding e-mail: dulinatholib@gmail.com

Keywords: Natural fiber; Unidirectional; Optimization process; Two-level factorial design.

ABSTRACT – In recent years, the use of kenaf fibers as reinforcement in composite has grown rapidly due to an increasing demands in developing sustainable materials. In this research, unidirectional kenaf polypropylene (PP) composites were prepared using the hot pressing method. One of the challenges in the fabrication of unidirectional kenaf/PP composites is the properties of the composite tend to produce a variety of strengths. Therefore, the optimum processing parameter (temperature, pressure, time) and percentage of kenaf fibers on the tensile properties were investigated by conducting a two-level full factorial design. One set of 2⁴ factorial designs with one center point (17 experiments) was tested. The effect of the individual factors and their interaction were observed. From statistical analysis, the main factor of tensile strength and young modulus, the kenaf fibers contribute up to 21.67%. The interaction between kenaf percentage and pressing time also contributes an effect on the tensile properties and modulus with 13.29% contribution. Finally, the result showed that at temperature 190°C, pressure 5MPa, with 5 minutes pressing time and 50% fiber content will give the optimum tensile strength and young modulus at 164.13MPa and 11.9GPa respectively.

1. INTRODUCTION

The great interest in natural fiber polymer composites is growing rapidly due to environment and sustainability issues. Compared to synthetic fibers such as glass, carbon and aramid, natural fibers offer less expensive, renewable, low cost, light weight, high strength and stiffness makes it widely used in the production of lightweight composites [1]. This is supported by Mohanty et al. [2], stated that natural fiber composite delivers the same performance for lower weight and 25-30% stronger for the same weight of glass composite. The potential of natural fibers such as kenaf as a reinforcement agent in the polymer composites has proven when the automobile industry, Toyota RAUM equipped with a spare tire cover made of kenaf fiber composites [3].

However, there are challenges in handling natural fibers in producing composites which will fabricate a large variation in fiber properties due to various types of

plant fiber, plant maturity, plant originality, location in plant and retting process. These challenges will indirectly affect the properties of the composites [4]. While Hashim et al. 2015 [5], in their study suggests that few factors should be considered and improved to acquire the superior mechanical properties such as fiber orientation, fiber length, fiber content and processing parameter. For this purpose, the optimization process using design of experiment is suggested.

Full factorial design is an important engineering tool in improving the process of optimizing the effect of variable factors and minimizing time with reduced total number of experiment in order to achieve the best operating conditions at once together with reduced overall costs of the manufacturing [6]. It also has an extensive application in the development of new processes. According to Sharifi et al. 2014 [7], factorial design gives the main effect of each parameter a change in the level of other parameters and the effects of the interactions for different factors. This research is focused on four factor two-level full factorial design and analyzed using Design Expert version 9.0.3.1 software.

2. METHODOLOGY

The materials used in this study consisted of kenaf bast fibers and polypropylene in the form of pallet and powder. Kenaf bast fibers which have undergone water retting process to produce long fibers were locally purchased from Lembaga Kenaf dan Tembakau Negara, LKTN, Kelantan. While, Polypropylene (TITANPRO PX 617) in the form of pallet and powder (HM20/70P) were supplied by Lotte Chemical Titan (M) Sdn. Bhd., Pasir Gudang, Johor, Malaysia and Goonvean Fibres Ltd., United Kingdom respectively. Samples were prepared using the hot pressing method.

The properties of unidirectional Kenaf/PP composites from the hot pressing method may be affected by a number of processing or material parameters. Four factors (percentage of kenaf fibers, processing temperature, time and pressure) were identified as likely to impact the mechanical properties of the composites. In the present study, two-level factorial design was applied to explore the effect of factors on the response in the region of the investigation. In order to measure the effect of all the

factor combinations which influence the tensile properties, 16 factorial experiments were carried out at two levels with one other being at the center point. The factors and levels for full factorial design listed in Table 1. The low and high levels for the factors were assigned according to some preliminary experiments.

Table 1 Factors and level for full factorial design

| Factors | Level | | |
|----------------------|-------|--------|------|
| | Low | Center | High |
| Temperature (°C) | 190 | 200 | 210 |
| Pressure (MPa) | 5 | 7.5 | 10 |
| Time (minutes) | 5 | 10 | 15 |
| Fiber Percentage (%) | 30 | 40 | 50 |

For each combination of these factors, hot pressing is conducted to produce samples for the testing. Table 2 shows the experimental design matrix with the result of 2⁴ full factorial design. Tensile tests were performed according to standard ASTM 638. Five samples were prepared for each processing parameter. All of the test specimens were conditioned at testing room temperature with cross head speed 5mm/min.

Table 2 Experimental design matrix with the results of 2⁴ full factorial design

| Run | Factors | | | |
|-----|------------------|----------------|----------------|----------------------|
| | Temperature (°C) | Pressure (MPa) | Time (minutes) | Fiber percentage (%) |
| 1 | 210 | 10 | 5 | 50 |
| 2 | 210 | 5 | 15 | 50 |
| 3 | 210 | 5 | 5 | 50 |
| 4 | 190 | 10 | 5 | 30 |
| 5 | 210 | 10 | 15 | 30 |
| 6 | 190 | 5 | 5 | 50 |
| 7 | 210 | 5 | 15 | 30 |
| 8 | 190 | 5 | 15 | 30 |
| 9 | 190 | 5 | 5 | 30 |
| 10 | 210 | 10 | 5 | 30 |
| 11 | 190 | 10 | 5 | 50 |
| 12 | 190 | 5 | 15 | 50 |
| 13 | 200 | 7.5 | 10 | 40 |
| 14 | 190 | 10 | 15 | 50 |
| 15 | 190 | 10 | 15 | 30 |
| 16 | 210 | 5 | 5 | 30 |
| 17 | 210 | 10 | 15 | 50 |

3. RESULTS AND DISCUSSION

From the analysis of ANOVA, it was found that the processing parameter is optimum at temperature 190°C, pressure 5MPa, with 5 minutes pressing time and 50% of kenaf fibers with desirability 0.969. By applying these parameters for hot pressing process, it will give the optimum tensile strength and modulus which are 164.13 MPa and 11947.17 MPa respectively. The confirmation test had been done to ensure the parameter is valid and it was found that the percentage of error is in the range of 10% . This indicates that this model is suitable to be used for the further experiments.

4. CONCLUSIONS

The optimum processing parameter was successfully developed and optimized through DOE, and the data were analyzed using the software Design Expert version 9.0.3.1. From the two-level full factorial design experiments, significant effect of independent factors was analyzed using ANOVA, and the effect was also reported in the form of contour plots. The design of the experiments provides efficient tools for the

optimization of processing factors . The method was further validated and as per the results, the present method is novel, simple, accurate, precise, economic and robust.

ACKNOWLEDGEMENT

Authors acknowledge Ministry of Education Malaysia for sponsoring this work through LRGs/TD/2012/USM-UKM/PT/05 and Ministry of Higher Education Malaysia for granting the scholarship.

5. REFERENCES

- [1] Ahmad, F., Choi, H. S. & Park, M. K., " A Review : Natural Fiber Composites Selection in View of Mechanical, Light Weight, and Economic Properties," *Macromolecular Materials and Engineering*, pp. 1–15, 2015.
- [2] Mohanty, a. K., Misra, M. & Drzal, L. T., "Sustainable Bio-Composites from renewable resources: Opportunities and challenges in the green materials world," *Journal of Polymers and the Environment*, vol. 10, pp. 19–26, 2002.
- [3] John, M. J., Bellmann, C. & Anandjiwala, R. D., "Kenaf-polypropylene composites: Effect of amphiphilic coupling agent on surface properties of fibres and composites," *Carbohydrate Polymers*, vol. 82, no. 3, 549–554, 2010.
- [4] Faruk, O., Bledzki, A. K., Fink, H.-P. & Sain, M., "Biocomposites reinforced with natural fibers: 2000–2010," *Progress in Polymer Science*, vol. 37, no. 11, pp. 1552–1596, 2012.
- [5] Hashim, M., Zaidi, A., Mujahid, A. & Ariffin, S., 2015. Plant fiber reinforced polymer matrix composite: a discussion on composite fabrication and characterization technique. *eprints.uthm.edu.my*,. Retrieved from <http://eprints.uthm.edu.my/2541/>
- [6] Hamdi, L., Boumehdi Toumi, L., Salem, Z. & Allia, K., "Full factorial experimental design applied to methylene blue adsorption onto Alfa stems," *Desalination and Water Treatment*, vol. 3994, pp. 1–8, 2015.
- [7] Sharifi, F., Hadizadeh, F., Sadeghi, F., Hamed Mosavian, M. T. & Zarei, C., "Process Optimization, Physical Properties and Environmental Stability of an α -Tocopherol Nanocapsule Preparation Using Complex Coacervation Method and Full Factorial Design," *Chemical Engineering Communications*, 6445(December), 141217104822009, 2014.

Effects of Drilling Parameter on Hole Surface for Orthopaedic Surgical Bone Drilling

M.s Noorazizi ¹*,², R.Izamshah¹, M.s Kassim¹, Che Hassan Che Haron²

¹)Faculty of Manufacturing Engineering, Universiti Teknikal Malaysia Melaka, Hang Tuah Jaya 76100 Durian Tunggal, Melaka, Malaysia.

²)Department of Mechanical and Material Engineering, Faculty of Engineering and Built Environment, Universiti Kebangsaan Malaysia, 43600 Bangi, Selangor, Malaysia.

*Corresponding e-mail: engr.nms801@gmail.com

Keywords: Medical Drill-Bit; Surface Morphology; Surface Roughness.

ABSTRACT – In orthopaedic surgery, internal fixation of bone fractures using immobilization screws and plate is a common procedure. This surgical procedure involves drilling into bones and fixative components interaction. Many problems are encountered during the bone drilling process such as holes accuracy, drill wander and excessive heat generation which were also directly related with the drilling parameter. This paper investigates the effect of drilling parameter namely spindle speed and feed rate on the cutting force, surface roughness performance and surface morphology of bone debris. Design of Experiment (DOE) historical data of Response Surface Method (RSM) were adopted to evaluate the correlation between the cutting parameter and the holes performance. From the conducted investigation, the most significant parameter that affects the holes performance was spindle speed followed by the feed rate. In addition, the interaction between feed rate and spindle speed also controls the holes performances.

1. INTRODUCTION

Bone is a complex biological tissue which has anisotropic properties. Drilling of bone is normally required in orthopedic operations for allocation of screw process in bone recovery. Close tolerances and surface finish of the drilled bone are critical for the osseointegration ability [1-3]. The surface characteristic affects the bone-screw interface strength as well as the cellular response, which is essential for early and healthy bone growth. Various techniques were employed to enhance bone apposition including bioactive coating and surface texturing of fixative components. Surface roughness is one of the methods to enhanced bone growth during the healing process with promising result [11-12]. There has been ongoing research associated with implant surface topography. Proper mating between two joining surfaces are necessitated for a stable bone-implant interface in minimizing the trauma due to the drilling forces [4]. The drilling conditions in bone drilling process are interrelated by rotational speed and the feed rate which affect the drilling forces and holes qualities. Hence, the understanding on the effects of drilling parameter on the hole performances are necessitate.

Response surface methodology (RSM) is widely used in process optimization and modelling [5]. This method was proved effectively and widely used in the process of industrialization. The optimized response is influenced

by a few of cutting parameters as input variables. In order to convert the independent variable to see the changes of the output response, a series of tests called run was conducted to see the response based on the selecting factors. In order to study the relationship between bone drilling process parameters and the holes performances, a systematically approach DOE and RSM can be used effectively. Kasim et al. [6] demonstrated that RSM is able to predict surface roughness value with less error.

This paper aims to investigate the effects of drilling parameter on holes performance namely surface roughness, surface morphology and drilling force for bone drilling using RSM technique.

2. EXPERIMENTAL

Set of experiments were conducted to investigate the effect of high speed drilling on cutting force and surface roughness. Each test was performed using a HAAS VF-1 CNC Vertical Machine. A Kistler type 9275BA dynamometer was mounted under the work piece fixture to record the thrust force during the process see figure 1. SEM analysis was performed in order to evaluate the physical damage caused by various drilling parameters.



Figure 1 Experimental setup for bone drilling. HAAS VF-1 CNC Vertical Machine, Kistler type 9275BA, Drilling operation.

3. RESULTS AND DISCUSSION

From the conducted investigations, it is evident that drilling parameters (spindle speed and feed rate) are the important criteria that affect the hole performances namely surface roughness, surface morphology and

force magnitude. Experimental result of surface roughness for drilling process is shown in Table 4. From the result, the minimum of surface roughness is 0.736 μm and the maximum is 3.43 μm . The result of cutting force is 7.459 N and the maximum is 19.785 N.

| Standard | Run | Factor A Spindle Speed (rpm) | Factor B Feed Rate (mm/min) | Surface Roughness (μm) | Force (N) |
|----------|-----|------------------------------------|-----------------------------------|---|--------------|
| 7 | 1 | 600 | 25 | 0.753 | 7.459 |
| 8 | 2 | 1500 | 85 | 0.883 | 19.785 |
| 6 | 3 | 1500 | 25 | 1.51 | 12.076 |
| 3 | 4 | 1500 | 85 | 1.25 | 12.853 |
| 4 | 5 | 600 | 85 | 0.736 | 11.236 |
| 1 | 6 | 1500 | 25 | 1.9 | 11.846 |
| 2 | 7 | 600 | 25 | 1.39 | 8.66 |
| 5 | 8 | 600 | 85 | 3.43 | 10.618 |

Figure 2 Interaction factor plot for surface roughness and cutting force.

Drilling quality includes aperture deviation, migration and gradient of the aperture axis and the changes of surface geometry. During the bone drilling, the chips impact the wall of the holes generating small cracks on the chip surface and causing them to break when the critical strain is reached. Thus friction and thermal effects causing a microfracturing are shown in Figure 3.

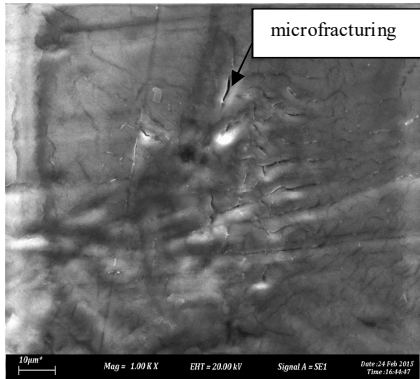


Figure 3 SEM view of drill hole surface for drill parameter D=4.3mm, F=12.076N, n=1500rpm

4. CONCLUSIONS

Investigations of high performances surgical drill-bit bone analysis using Response Surface Method (RSM) historical data were studied. Surface roughness, surface morphology and cutting force were measured for each experimental state. The following conclusion can be drawn as follows:

- This study demonstrated the interaction effect of drilling parameters on surface roughness and cutting force of drilling hole of femur bovine bone using RSM. The interaction between the feed rate and the spindle speed significantly affect the surface roughness and the cutting force.
- From the result, the minimum of surface roughness is 0.736 μm and the maximum is 3.43 μm . The result of cutting force is 7.459N and the maximum is 19.785N. By increasing drill spindle speed (at higher speeds range,

especially), drilling cutting force increases considerably.

- Spindle speed and feed rate had a significant influence on drilling force, bone debris and hole morphology. By increasing spindle speed, the drilling quality was improved and the surface roughness increases gradually up to a specific cutting speed due to the rise in friction between the two surfaces (drill-bit and bone).

To conclude, the results from the conducted experiments can provide reference for force control and selection of rotational speed and feed rate in bone surgeries.

5. REFERENCES

- [1] Richards, R.G., "Surfaces to control implant tissue adhesion for osteosynthesis, Folia Traumatologica Lovaniensia, Reynders, P., Burssens, P.," *Bellemans, J., Broos, P., Ed.; KU Leuven*, pp.15, 2007.
- [2] Hansson, S., Norton, M., "The relation between surface roughness and interfacial shear strength for bone anchored implants. A mathematical model," *Journal of Biomechanics*, vol. 32, pp. 829-836, 1999.
- [3] Abouzia, M. B., AND JAMES, D. F., "Temperature rise during drilling through bone," *International Journal of Oral and Maxillofacial Surgery*, vol. 12, no. 3, pp. 342-353, 1997.
- [4] Vashishth, D.; Tanner, K.E.; Bonfield, W., "Contribution, development and morphology of microcracking in cortical bone during crack propagation," *Journal of Biomechanics*, vol. 33, pp. 1169-1174, 2000.
- [5] M.A. Amran, S.Salmah, N.I.S Hussein, R.Izamshah, M.Hadzley, Kasim, M.S., "Effect on machine parameters on Surface Roughness Using RSM Method in drilling process," *Procedia Engineering*, vol. 68, pp. 24-29, 2013.
- [6] Kasim, M.S., Che Haron, C.H., Ghani, J.A., Sulaiman, M.A., "Prediction Surface Roughness in High-Speed Milling of Inconel 718 under Mql Using RSM Method," *Middle- East Journal of Scientific Research*, pp. 264-272, 2013.
- [7] W.P. Hennessy, M.T. Hillery, "The design and manufacture of a drilling dynamometer for drilling Kevlar-49 reinforced composites," *Proc. IMC-8, Ireland*, pp. 803-816, 1991.

Mechanical Properties of Injection Moulded for Multi-walled Carbon Nanotube/ Kenaf/ Polypropylene Hybrid Composites

Zakaria Razak^{1,2*}, Abu Bakar Sulong¹, Norhamidi Muhamad¹, Mohd Khairul Fadzly Md Radzi¹, Dulina Tholibon¹, Izdihar Tharazi¹, Nur Farhani Ismail¹

¹)Department of Mechanical and Material Engineering,
Faculty of Engineering and Built Environment, Universiti Kebangsaan Malaysia,
43600 Bangi, Selangor, Malaysia.

²) German-Malaysian Institute,
Taman Universiti, 43000 Kajang,
Selangor, Malaysia.

*Corresponding e-mail: zakaria@gmi.edu.my

Keywords: Kenaf fibre, Carbon Nanotube fillers, Injection Moulding, Mechanical properties

ABSTRACT – Carbon nanotubes (CNTs) are encouraging additives for polymer composites due to their excellent special mechanical, electrical, and thermal properties. The compounded samples were organized into test specimens by an injection moulding machine. The composites contained 1, 2, 3 and 4 wt% multi-walled carbon nanotubes (MWCNTs). The impact, tensile, flexural strength, Young's modulus and a flexural modulus of the composites have been examined.

1. INTRODUCTION

Hybrid composite materials have been used as an alternative for metallic materials in the field of Engineering. A combination of "hybrid" and "composite" is called a hybrid composite [1]. This material is simply a hybridization of composite materials, for example, composites reinforced with two or more types of fibres or a laminar composite material containing thin foil metals and fibre-reinforced metals. The meaning of "hybrid" in hybrid composite materials are the hybridization in a macroscopic structure in the metallographic scale.

Composite materials have been utilized in the aircraft industry, automotive, as well as tools for sport. The use of composites in various areas has owned properties such as lightweight, strong, stiff, and resistant to corrosion. The development of composite plastic started to develop since the discovery of composite material that is called reinforced plastic, but the use of composite plastics made from many causes new problems i.e. environmental pollution from waste created as well as depletion of resources will increasingly plastic which of course cannot be updated [2].

Kenaf (*Hibiscus cannabinus* L.) is a herbaceous plant originated from West Africa which has been cultivated since around 4000 B.C. Kenaf is commercially available and economically cheap amongst another natural fibre reinforcing material. Kenaf is comparatively available in the marketplace and economically cheap amongst other natural fibre reinforcing material. Furthermore, kenaf fibre offers the advantages of being biodegradable, low density, non-abrasive during processing and environmentally safe [3].

Carbon nanotubes (CNTs) were found in the soot of an arch discharge by Sumio Iijima in 1991 [4]. Carbon nanotubes are classified as single-walled carbon nanotubes (SWCNTs) and multi-walled carbon nanotubes (MWCNTs) [5]. MWCNTs consist of a variable number of graphene sheets rolled coaxially into a cylinder of nanometric diameter [6]. The typical diameter of MWCNTs are 10–20 nm; their typical length is above 20 μm . Several production methods have been developed aiming at the manufacture of carbon nanotubes in large scale, such as laser vapourisation [7], electric arc discharge [8] and catalytic chemical vapour deposition of hydrocarbons over metal catalysts (CCVD technique) [9]. The first two methods are high-temperature processes and can produce high-quality nanotubes. Nevertheless, the yields are weak and therefore not adaptable for large-scale production. In contrast, the CCVD technique is a suitable method to produce MWCNTs because this method might be a possibility to produce nanotubes at relatively low temperatures on a large scale at a reasonably low cost [10]. CNTs are encouraging additives for polymer composites due to their excellent mechanical, electrical, and thermal properties. The tensile strength of carbon nanotubes is 75-times greater than of steel filaments of the same size, and 15-times higher than of carbon fibres. In the other word, the density of carbon nanotubes is one-sixth of steel. Their densities may be as low as 1.3 g/cm³. Plastics enhanced with carbon nanotubes might be the new family of light and strong composites. [11]

2. METHODOLOGY

The polymer matrix is a PP (pellet form) obtained from Lotte Chemical Titan (M) Sdn. Bhd.. The reinforcement filler, multi-walled carbon nanotubes (MWCNTs), was purchased from Nanocyl SA (Belgium). According to transmission electron microscope (TEM) images, the average diameter of the tubes are 9.5 nm (Fig. 1), the length is 1.5 μm and a purity of 90 %. Kenaf particles of size 20 mesh were used in this study. Kenaf particles were supplied by the National Kenaf and Tobacco Board [12]

For the experiments, feedstock was composed of PP, Kenaf and different MWCNT percentages (Table 1). The materials were mixed using the sigma blade. Processing temperature, time and rotating speed were

190°C, 30 min and 45 rpm, respectively.

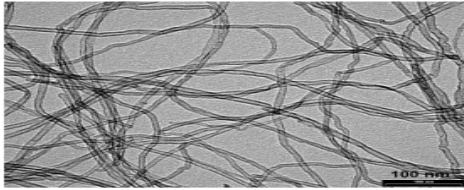


Figure 1. NC7000™ multi-walled carbon nanotubes – scale: 100 nm - TEM. (Source: Technical Data Sheet: NC7000™ | 25th January 2016 | V07)

Table 1. Composition of Materials Used in the Experiment

| Kenaf (wt%) | PP (wt%) | MWCNT (wt%) |
|-------------|----------|-------------|
| 0 | 100 | 0 |
| 30 | 70 | 0 |
| 30 | 69 | 1 |
| 30 | 68 | 2 |
| 30 | 67 | 3 |
| 30 | 66 | 4 |

3. RESULTS AND DISCUSSION

3.1 The results of mechanical properties are shown in Table 2. It was noticed that mixing of MWCNT 3wt% in PP/Kenaf at 190°C with 45 rpm was increased for all tests.

Table 2. Mechanical properties of the PP/Kenaf and its nanocomposites

| Properties | Pure PP | PP/Kenaf | PP/Kenaf | PP/Kenaf | PP/Kenaf | PP/Kenaf |
|--------------------------------------|---------|----------------------------|---|---|---|---|
| | | 30 wt% 30 min 45 rpm | 30 wt%/ MWCNT 1 wt% 30 min 45 rpm | 30 wt%/ MWCNT 2 wt% 30 min 45 rpm | 30 wt%/ MWCNT 3 wt% 30 min 45 rpm | 30 wt%/ MWCNT 4 wt% 30 min 45 rpm |
| Impact Strength (kJ/m ²) | 7.617 | 1.493 | 8.148 | 8.296 | 8.483 | 8.772 |
| Tensile Strength (Mpa) | 18.627 | 15.908 | 16.767 | 20.939 | 23.341 | 20.843 |
| Young Modulus (MPa) | 473.666 | 1804.551 | 1444.562 | 1395.549 | 1865.950 | 1433.184 |
| Flexural Strength (MPa) | 25.258 | 29.420 | 28.017 | 30.937 | 36.728 | 30.604 |
| Flexural Modulus (MPa) | 575.549 | 1548.108 | 1850.122 | 1835.315 | 1826.121 | 1870.890 |

The addition of MWCNT 4 wt% caused all values to decrease except for the impact strength and flexural modulus. This is due to the high contents of MWCNT will cause composite materials to become brittle.

4. CONCLUSIONS

Multi-walled carbon nanotube/ Kenaf/ Polypropylene composites were produced via injection moulding machine. The composites contained 1, 2, 3 and 4 wt% MWCNT. For comparison, composites with kenaf fibre as an additive instead of MWCNT have been made. The izod impact strength, tensile strength, flexural strength and flexural modulus of the composites have been examined. It can be summarized, that the properties of the composites produced with 3 wt% MWCNT contents are the most suitable and better properties. The suitable mechanical value can be achieved with 3 wt% MWCNT contents. According to the measurement results, it can be concluded, that the injection moulding machine is more appropriate for producing of the MWCNT/ Kenaf/ Polypropylene Composites.

ACKNOWLEDGEMENTS

The author wishes to thank the Ministry of Higher Education, Malaysia for their financial support under grant LRGS/TD/2012/USM-UKM/P1/05 and MARA.

5. REFERENCES

- [1] M. Uemura & H. Hukuda, "Hybrid Composites," Ed. CMC Publishing Co., Tokyo, Japan, pp. 1-9, 2002.
- [2] Diharjo K., dkk., "The Effect of Alkali Treatment on Tensile Properties of Random Kenaf Fiber Reinforced Polyester Composites, Part III of Doctorate Dissertation Research Result," *Post Graduate Study, Indonesia*, 2005.
- [3] Nishino T., Hirao K., Kotera M., Nakamae K. and Inagaki H., "Kenaf reinforced biodegradable composite," *Composites Science and Technology*, vol. 63, pp. 1281-1286, 2003.
- [4] S. Iijima, *Nature (London)*, 354, pp. 56, 1991.
- [5] S. Iijima, T. Ichihashi: *Nature*, 360, pp. 603, 1993.
- [6] L.P. Biro, J. Gyulai, Ph. Lambin, J.B. Nagy, S. Lazarescu, G. I. Mark, A. Fonseca, P. R. Surjan, Zs. Szekers, P. A. Thiry, and A. A. Lucas, "Scanning tunneling microscopy (STM) imaging of Carbon nanotubes," *Carbon*, vol. 36, pp. 689-696, 1998.
- [7] Y. Saito, M. Okuda, M. Tomita and T. Hayashi, "Extrusion of Single-wall Carbon Nanotubes Via Formation of Small Particles Condensed Near an Arc Evaporation Source," *Chem, Lett*, vol. 236, no. 4-5, pp. 419-426, 1995.
- [8] T. W. Ebbesen, P. M. Ajayan: *Nature*, vol. 358, pp.220, 1992.
- [9] W. Z. Li, S. S. Xie, L. X. Qian et al., *Science*, vol. 274, pp. 1701, 1996.
- [10] Awang, H., Azree, M., Mydin, O., & Ahmad, M. H., "Mechanical and Durability Properties of Fibre Lightweight Foamed Concrete." *Australian Journal of Basic and Applied Sciences*, 2013.
- [11] J. N. Coleman, U. Khan, W. J. Blau, Y. K. Gun'ko, *Carbon*, vol. 44, pp. 1624, 2006.
- [12] Md Radzi, M. K. F., Sulong, A. B., Muhamad, N., Mohd Latiff, M. A., & Ismail, N. F., "Effect of Filler Loading and NaOH Addition on Mechanical Properties of Moulded Kenaf/ Polypropylene Composite," *Tropical Agricultural Science*, vol. 38, no. 4, pp. 583-590, 2015.

Configuration of wire positioning to minimize parts error in wire electrical discharge turning (WEDT)

M. Akmal^{1,*}, R. Izamshah^{1,2}, M.S. Kasim^{1,2}, M. Hadzley^{1,2}, M. Amran^{1,2}, A. Ramli¹

¹) Faculty of Manufacturing Engineering, Universiti Teknikal Malaysia Melaka, Hang Tuah Jaya, 76100 Durian Tunggal, Melaka, Malaysia.

²) Centre of Excellence for Advanced Manufacturing, Universiti Teknikal Malaysia Melaka, Hang Tuah Jaya, 76100 Durian Tunggal, Melaka, Malaysia.

*Corresponding e-mail: akmalzak@student.utm.edu.my

Keywords: WEDT; WEDM accuracy; Micro cylindrical part.

ABSTRACT – In recent years, advancements in technology such as micro-electromechanical systems (MEMS), electronics productions and medical devices have created an increasing demand for micro size parts and components. Consequently, the development of new machining technique to cater for the precision and complex geometries parts fabrication has steadily increased. One of the newest machining techniques is by incorporating rotational part with the wire electrical discharge turning (WEDT). The main advantage by employing this hybrid process was the reduction in part deflection as compared to other process i.e. micro turning. However, due to the alteration of discharge energy behaviour, a valid estimation on the dimensional accuracy in WEDT limits its application. This paper proposes on the wire compensation configuration that aims to increase the part dimensional accuracy for WEDT process. The configuration model emphasized in the way to control the wire position by taking into account the dynamic and static radial run-out, wire deflection and discharge gap. A set of experimental work has been done to validate the proposed model. Analytical results noticed the desired diameter dimension obtained from the developed model has a close relationship up to 99%, which confirm its validity.

1. INTRODUCTION

The driven in exploration for intricate cylindrical parts for modern applications, especially for hardened material, led the wire electrical discharge turning (WEDT) process in line with the development of microfabrication technology. The alternative method that employed sparking phenomena in fabrication micro-cylindrical part currently is the wire electrical discharge grinding (WEDG). However, WEDG has limitation in volume material removed due the micro-size of electrode wire and the position of a wire guide system that restrict the flexibility in fabricating the parts with the blending of macro-micro geometrical features.

On the contrary, WEDT has high potential in fabricating symmetrical of micro-cylindrical parts, especially for complex macro-micro geometries because the wire guide does not apply in WEDT. Geng et al. [1] proved the WEDT capability by fabricating the bellows core-mould by using micro size electrode wire.

The literature indicates a few of exploration in machining micro-cylindrical parts by using WEDT not to mention evaluation on the dimensional accuracy [2], [3]. Compared to the WEDG, the occurrence of wire

vibration in WEDT is frequently high resulting to poor dimensional accuracy and reduces the capability in achieving large value of machined down diameter.

This paper presents evaluation of dimensional accuracy of micro-cylindrical parts of wire electrical discharge turning (WEDT). The research focuses on material removal configuration in obtaining the accuracy of parts machining in micro-dimensional.

2. METHODOLOGY

2.1 Part Dimensional Configuration Model

The precision of final diameter for cylindrical parts that fabricated by WEDT is determinable by Figure 1 and Equation 1.

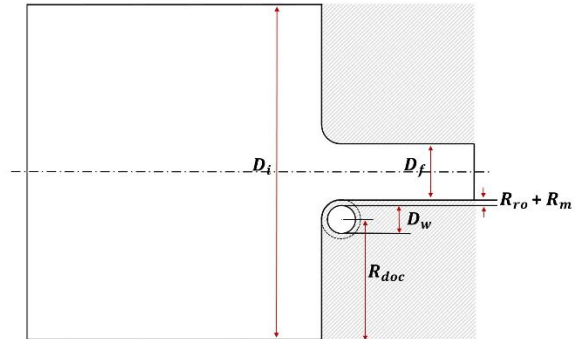


Figure 1: Geometrical model of workpiece dimension

$$D_f = 2 \left[\frac{D_i}{2} - \frac{D_w}{2} - R_{doc} - R_{ro} - R_m \right] \quad (1)$$

Figure 1, D_i is the initial diameter of the workpiece measured at the end of the workpiece by positioning the electrode wire while it rotates. Usually this value is constant and larger than the actual diameter due the off centre error on the spindle shaft.

R_{ro} is the maximum of the radial run-out error possibly by form error of bearing races [4]. D_w is the average diameter of electrode wire that possess variation as stated by Morgan et al.[5]. Therefore, this variation is categorized as error and be included in radial miscellaneos (R_m). R_m is the error that was inherent during the fabrication process. Among the error that included in this R_m are wire deflection, wire diameter variation and discharge gap.

Based on the upon configuration model, the desired final diameter (D_f) may only be specified by controlling the value of radial depth of cut (R_{doc}) which serves as input value for positioned electrode wire by machine system. Equation 2, indicates the determination

of part final diameter (D_f) and removal volume, according to radial depth of cut (R_{doc}).

$$R_{doc} = \frac{D_i}{2} - \frac{D_f}{2} - \frac{D_w}{2} - R_{ro} - R_m \quad (2)$$

2.2 Experimental Work

The model of dimensional configuration is verified by a series of experimental works on Ti6Al4V as a material with diameter 9.49 mm and single pass cutting condition on straight turning path. 500 rev/min rotational spindle speed is used which possess maximum of the radial run-out error as much as 7 μm and 0.25 mm of brass electrode wire is selected. In this experiment, 22 μm as value for R_m was acquired by several preliminary experiments with the same input parameters for obtaining the sum value of discharge gap and others variation of errors.

3. RESULTS AND DISCUSSION

A typical Ti6Al4V micro-cylindrical part produced by WEDT is illustrated by Scanning Electron Microscopy (SEM) micrograph in Figure 2. The actual diameter of the parts was machined down from 9.49 mm to 306.32 μm with single pass cutting condition.

The measurement of each the design dimension of micro-cylindrical parts are tabulated in Table 1. It is noticed that the error deviated by using the configuration model is less than 13 μm approximately 5%, the error appeared as much as 17% from the design dimension without employing the configuration model. Comparing the results between employed and unemploy configuration model, the differences as much as 10 to 15% of overcut phenomena on part dimension is due to the uncontrolled electrode wire compensation.

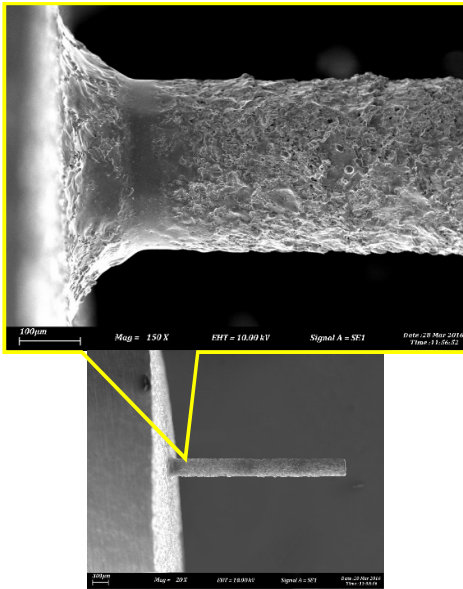


Figure 2: SEM micrograph of Ti6Al4V micro-cylindrical part produced by WEDT

Table 1: Error deviation between design and measured dimensional diameter

| Design | Dimensional Accuracy |
|--------|----------------------|
|--------|----------------------|

| Configuration Model | Without | Dimension (μm) | Measured Dimension (μm) | Error (μm) |
|---------------------|---------|-----------------------------|--------------------------------------|-------------------------|
| | | 250 | 208.35 | 41.65 |
| With | 300 | 259.20 | 40.80 | |
| | 250 | 253.72 | 3.72 | |
| With | 250 | 250.39 | 0.39 | |
| | 300 | 312.26 | 12.26 | |
| | 300 | 306.32 | 6.32 | |

4. CONCLUSIONS

This paper has introduced configuration on dimensional accuracy focused on WEDT for evaluation of the fabrication parts dimensional diameter. The corresponding radial depth of cut is indispensable to arrange and is controlled for producing desired parts accuracy. Experimental results verified the proposed configuration model with deviated error less than 5% from the desired dimension.

5. ACKNOWLEDGMENT

The study was funded by the Ministry of Higher Education Malaysia under grant: [FRGS/2/2014/TK01/UTEM/03/2].

6. REFERENCES

- [1] Geng, X., Chi, G., Wang, Y., and Wang, Z., "Study on Microrotating Structure Using Microwire Electrical Discharge Machining," *Materials and Manufacturing Processes*, vol. 29, no. 3, pp. 274–280, 2013.
- [2] Hsue, A. W. J., Wang, J. J., Chang, C. H., and Chuan, Y., "Removal Analysis for Multi-Axial WEDM and Ultrasonic Assisted WEDG Processes with Augmented Rotational Axes," *Advanced Materials Research*, vol. 579, pp. 201–210, 2012.
- [3] Gjeldum, N., Bilic, B., and Veza, I., "Investigation and modelling of process parameters and workpiece dimensions influence on material removal rate in CWEDT process," *International Journal of Computer Integrated Manufacturing*, vol. 28, no. 7, pp. 715–728, 2014.
- [4] Qu, J., Shih, A. J., and Scattergood, R. O., "Development of the cylindrical wire electrical discharge machining process, part 1: Concept, design, and material removal rate," *Journal of Manufacturing Science and Engineering, Transactions of the ASME*, vol. 124, no. 3, pp. 702–707, 2002.
- [5] Morgan, C., Shreve, S., and Vallance, R. R., "Precision of micro shafts machined with wire electro-discharge grinding," in *Proceedings of the Winter Topical Meeting on Machines Processes for Micro-Meso-Scale Fabrication, Metrology, Assembly. American Society for Precision Engineering (ASPE)*, pp. 26–31, 2003.

Part surface compensation method for springback-free automotive stamped structural part design

Ahmad Zakaria* , Muhamad Safaadzudin Adzman

UniKL Institute of Product Design and Manufacturing ,
Taman Shamelin Perkasa, Cheras , Kuala Lumpur, Malaysia

*Corresponding e-mail: dzakaria@unikl.edu.my

Keywords: Springback compensation, High Strength Steel, Springback-free design .

ABSTRACT – This paper proposes a new approach to the springback compensation method for sheet metal stamping. Unlike the conventional practice where the die face is modified in order to compensate for the springback error, the new approach on the other hand, modifies the part surface. This is achieved by adding a series of bead patterns on the part surface. Location of these bead patterns are generated by topography optimization. The part having this kind of modified surface is said to have a characteristic of springback-free property since die face modification is completely eliminated. The concept was numerically validated by using three NUMISHEET benchmark geometries namely straight rail , S-Rail rail and U-bend. The results of springback error before and after compensation for two different materials cold rolled steel and high strength steel were than compared. The depth of the bead pattern appears to have a significant effect on the springback values. The addition of bead pattern of depth 0.5 mm to the original part surface reduces the springback error within the tolerance of $\pm 0.5\text{mm}$ acceptable by automotive industry. More importantly this method of springback reduction can be achieved in a single iteration.

1. INTRODUCTION

The quest for a fuel efficient car is a subject of an on-going active research since the last two decades or so. Various technologies have been developed to overcome this critical issue since then. These include electric or hybrid vehicle. As the main contributor to the weight of a vehicle is the steel structure or body in white(BIW), the other focus research area is on the use of high strength light weight material. High strength steel or HSS has been the popular choice to meet this criteria. Unfortunately forming or stamping of HSS parts poses another problem. This is springback that causes serious dimensional inaccuracy of the part and costly repair of the tools.

In general, the springback management can be done in three ways: traditional techniques, process control, and die face compensation. The traditional techniques include activities such as over-bending or re-striking. The later process requires additional process or die. On the shop floor, the springback errors can also be minimized by modifying the process control. These can be done by adding stiffener beads, draw beads, optimizing die gaps or even modifying die addendum. Yoshida et al.[1] suggested the introduction of partial bead on die and width reduction of part geometry. Springback can also be reduced by adding beads to the

part sidewall and by chamfering the punch radii . Fekete et al [2] reported the addition of swages, beads or dart on the side wall and bend radii has remarkably reduced the magnitude of springback for more than 50%.

The most widely used method for predicting springback is by the finite element method. This method produces excellent result in predicting formability but seems to having difficulty in predicting springback. Many factors such as process parameters influencing its accuracy cited in the literature[3,4]. However, choosing the correct material model which incorporated the Bauschinger effect [5] is critically important. Mixed isotropic and kinematic hardening models are proven to perform exceedingly well [6]. Such models include Lemaitre-Chaboche(L-C) ,Yoshida-Uemori (Y-U)[7] and Hill48 coupled with isotropic and kinematic hardening rule [8]. Other factors influencing accuracy of springback prediction are associated with the finite element method codes such as element type and size, integration scheme and integration points and the time step [9].

Current tasks of springback reduction are performed by the tool designer via several techniques described above. This research is focused on a new method by which springback issue can be resolved by the part designer via part surface compensation

2. PART SURFACE COMPENSATION METHOD

The conventional method of springback compensation is illustrated in Fig. 1.

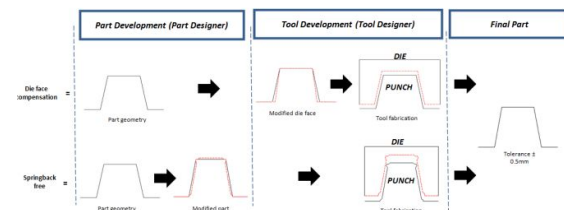


Figure 1. Die face compensation versus springback free approach

For a given part geometry, the die face is iteratively modified such that when the blank is formed, the final part geometry will be within the desired tolerance of $\pm 0.5\text{mm}$. In this case, the die size is smaller than the part size. On the contrary the part surface compensation approach[10] incorporates similar compensation but on

the part geometry by adding a series of beads at appropriate locations. The increase of part stiffness in effect reduces the resulted springback error. Hence similar desired tolerance is obtained. The figure also clearly shows that the die face is an exact replica of the part surface. The next question is what and/or where to locate those beads. This is why topography optimization is employed

3. METHODOLOGY

Initially the concept of springback-free design was developed by numerically analysing the effects of manually created bead patterns on selected NUMISHEET part geometry on springback errors using commercial CAE software. Similar procedure was repeated by using beads created by topography optimization. The springback errors were measured by the gap between the reference geometry and the springback geometry. The concept was then verified and validated by using other NUMISHEET part geometries.

4. RESULTS AND DISCUSSION

The results of springback for U bend made of HSS are shown in Fig.2 . As expected maximum springback value for U bend without bead is observed at point 1 and 2 as shown in Fig.3. However, the presence of beads on the same geometry has resulted in a significant reduction in springback value to within the tolerance of $\pm 0.5\text{mm}$.

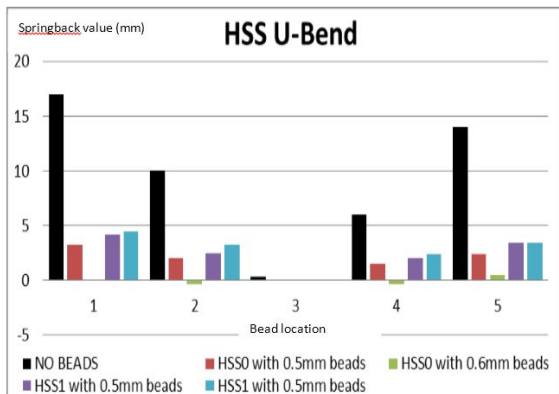


Figure 2. Springback results for U bend

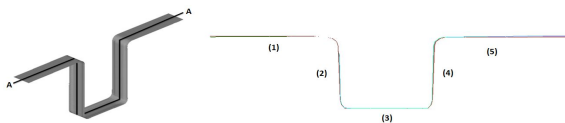


Figure 3. Measurement points at U bend

The reduction in the springback is due the smaller magnitude of stress generated after bending compared to non-beaded geometry as discussed by Kronauer et al.[11]. The springback errors as predicted by this study is within the range obtained by the NUMISHEET benchmark of similar geometry[12].

5. CONCLUSIONS

The bead depth of between 0.5~0.6mm generated on the part surface by topography optimization has the ability to produce springback-free stamped part of

thickness between 0.7 to 1.2mm. The concept can be extended to a thicker material by selecting suitable material model.

6. REFERENCES

- [1] Yoshida, T., Uenishi, A, Isogai, E., Sato, K.,Yonemura, "Material Modelling for Accuracy Improvement of the Springback Prediction of High Strength Steel Sheets," *Nippon Steel Technical Report*, no. 103, pp. 63-69. 2013.
- [2] Fekete, J.R., Hall, J.N., Meuleman, D.J, Rupp, M., "Progress in Implementation of Advanced High Strength Steels into Vehicle Structures," *International Conference on New Developments in Advanced High-Strength Sheet Steels*.
- [3] Burchitz, A.L., "Improvement of Springback Prediction in Sheet Metal Forming," *Thesis*, University of Twente, Netherland, 2008.
- [4] Nagur Aziz, K.B.,Norhamidi M., Baba M.D., Zakaria A., Ashari S.,Mobin A.,Safuan M. and Abdul M., "Multi-regression Modelling for Springback effect on Automotive Body of white Stamped Parts," *Material and Design*, vol .46, pp. 175-190, 2013.
- [5] Uemori, T., Sumikawas, S., Yoshida, F., "Modeling of Bauschinger Effect During Stress Reversal," *Steel Research International*, vol. 84, no. 12, 2013.
- [6] Chongthairungruang B, Uthaisangsk V., Suranuntchai S., Jirathearant S., "Experimental and Numerical Investigation of Springback Effect for Advanced High Strength Dual Phase Steel," *Materials and Design*, vol. 39, pp. 318-328, 2008.
- [7] Zhang, X.K., Zheng, G.J., Hu, J.N, Li, C.G., Hu, P., "Compensation Factor Method for Modeling Springback of Auto Part Constructed from High Strength Steels," *Int. J. Automotive Technology*, vol. 11, no. 5, pp. 721-727, 2010.
- [8] Adamus, J., Lacki, P.,Lyzniak, J., Zawadzki, M., "Analysis of Springback During Forming of the Element Made of AMS 5604 Steel," *Archives of Metallurgy and Materials*, vol. 56, pp. 423-430, 2011.
- [9] Banabic, B., *Sheet Metal Forming Processes "Constitutive Modelling and Simulation,"* Springer-Verlag Berlin Heidelberg, 2010.
- [10] Zakaria A and Adzman M.S., "Design of Springback-free part Structural Stamped Part," *Journal of Applied Environmental and Biological Sciences*, vol. 4, no. 10, pp. 94-98, 2015.
- [11] Krönauer, B. et al., "Automated Bead Design Considering Production Constraints," *NUMIFORM 2010: Proceedings of the 10th International Conference on Numerical Methods in Industrial Forming Processes*, 2010.
- [12] Huh,H. Chung K, Han S.S. and Chung, W.J. (eds). "NUMISHEET 2011 Part C Benchmarks Problems and Results," *The NUMISHEET Benchmark Study of the 8th International Conference and Workshop on Numerical Simulation of 3D Sheet Metal Processes*, 2011.

Influence of Tool Path Strategies and Pocket Geometry on Surface Roughness in Pocket Milling

Muhammad Munzir bin Razak^{1*}, MZA Yazid¹

¹ Manufacturing System Engineering,
 Universiti Kuala Lumpur, Institute of Product Design and Manufacturing,
 119 Jalan 1/91, Taman Shamelin Perkasa, 3.5 Miles Cheras,
 56100 Kuala Lumpur, Malaysia.

*Corresponding e-mail: mmunzir.razak@s.unikl.edu.my

Keywords: Tool Path Strategy, Pocket Geometry, Surface Roughness.

ABSTRACT – This paper discusses the the effect of tool path strategy and pocket geometry on surface roughness in pocket milling process. The machining processes have been performed on mould steel DF2 using carbide insert end mill as the cutting tool. The experiments were designed using three-level factorial design. The cutting parameters were kept constant while the variables are tool path strategies (one direction path, back and forth path, and spiral cutter path) pocket geometry (3 different pocket shapes). The effectiveness of different tool path strategy and different pocket geometry is evaluated in terms of measured surface roughness. The lowest surface roughness measurement was produced by the parallel spiral strategy and pocket geometry.

1. INTRODUCTION

Tool path is the path that leads cutting tool through the machined region. It is used to remove all the material inside some arbitrary closed boundary on a flat surface of a workpiece to a fixed depth. Such a shape is frequently called a generalized pocket, or (more simply) a pocket, and the process is called pocketing. Mainly, there are two types of tool path namely, contour-parallel or spiral (normal and smooth spiral) and direction-parallel or zigzag (normal and smooth zigzag). Milling of pocket feature in machining parts may be accomplished by employing different cutter path strategies. In general, three of them, which are one direction, back and forth (Zigzag), and spiral cutter path strategies, are often utilized in CAM software. One direction is a cutter path strategy where the cutter moves in parallel lines across the surface to be machined. At the end of line, the cutter moves up and comes back, it then scans the area with a fixed step over values. In back and forth milling, the cutter draws a zigzag cutter path by moving back and forth across the workpiece in the X – Y plane. Spiral milling is a strategy where the cutter may start at the centre of the pocket and then proceeds spirally outwards.

In the past, studies have focused on the influence of tool path strategy and pocket geometry in parameters such as machining time, cutting forces generated and surface roughness. The aim of this research work is to investigate the influence of tool path strategies and pocket geometry on the surface roughness in pocket milling of mould steel DF2 material, which is one of the most commonly used plastic mould steel (Gokler & Ozanozgu 2000), using carbide end mills. The variable in

this study are the three level of tool path strategies (one direction path, back and forth path, and spiral cutter path) and three level of pocket geometry (A, B and C).

The effectiveness of different tool path strategy and pocket geometry is evaluated in terms of the generated surface roughness. This project was conducted by using design of experiment (DOE), with three (3) levels – full factorial design.

2. METHODOLOGY

Machining tests are conducted under dry conditions at a feed rate of 300 mm/min, spindle speed of 10,000 rpm and depth of cut of 0.3 mm. After the machining, longitudinal and transversal surface roughness is measured using the Mitutoyo’s Surftest SV-3100.

Table 1 shows the order of experimental runs which was developed using Minitab software.

Table 1 Data generates by Minitab software.

| Std Order | Run Order | Pt Type | Blocks | Toolpath Strategy | Pocket Geometry |
|-----------|-----------|---------|--------|-------------------|-----------------|
| 9 | 1 | 1 | 1 | Parallel Spiral | C |
| 15 | 2 | 1 | 1 | One Direction | C |
| 13 | 3 | 1 | 1 | One Direction | A |
| 10 | 4 | 1 | 1 | Zigzag | A |
| 11 | 5 | 1 | 1 | Zigzag | B |
| 7 | 6 | 1 | 1 | Parallel Spiral | A |
| 2 | 7 | 1 | 1 | Zigzag | B |
| 6 | 8 | 1 | 1 | One Direction | C |
| 1 | 9 | 1 | 1 | Zigzag | A |
| 5 | 10 | 1 | 1 | One Direction | B |
| 3 | 11 | 1 | 1 | Zigzag | C |
| 18 | 12 | 1 | 1 | Parallel Spiral | C |
| 17 | 13 | 1 | 1 | Parallel Spiral | B |
| 12 | 14 | 1 | 1 | Zigzag | C |
| 4 | 15 | 1 | 1 | One Direction | A |
| 8 | 16 | 1 | 1 | Parallel Spiral | B |
| 14 | 17 | 1 | 1 | One Direction | B |
| 16 | 18 | 1 | 1 | Parallel Spiral | A |

Figure 1 shows the different path strategies that were investigated. They are One direction, back and forth and Spiral strategies. The different pocket geometries are shown in Figure 2 namely, Pocket A, Pocket B and Pocket C. Pocket A is the simplest pocket and Pocket B is the most complex, whilst Pocket C is the intermediate.

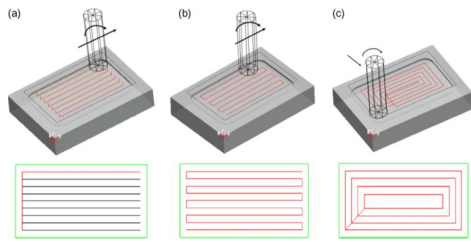


Figure 1 Cutter path strategies in pocket milling: (a) One direction; (b) Back and forth; and (c) Spiral

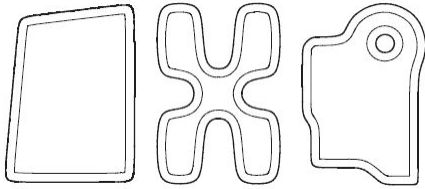


Figure 2 Geometries performed during the tests: pocket A; pocket B; pocket C

3. RESULTS AND DISCUSSION

The lowest surface roughness was obtained with Parallel Spiral followed by Zigzag and Spiral for Pocket A. In terms of tool path strategy, the surface roughness recorded with Parallel Spiral strategy was $0.72 \mu\text{m}$, and in terms of pocket geometry factors, pocket geometry B recorded $0.75\mu\text{m}$.

4. CONCLUSIONS

The Parallel Spiral strategy produced the lowest Ra measurements which is between $0.3 \mu\text{m}$ to $1.2 \mu\text{m}$ in the various types of pocket geometry. It can be concluded that pocket geometry and tool path strategy affect surface roughness (Ra).

5. REFERENCES

- [1] Benardos, P.G., Vosniakos, G.C., "Predicting surface roughness in machining: a review," *Int. J. Mach. Tools Manuf.*, vol. 43, pp. 833–844, 2003.
- [2] Elkeran, A., El-Midany, T. T., & Tawfik, H., "Toolpath Pattern Comparison: Contour-Parallel with Direction-Parallel," *Geometric Modeling and Imaging--New Trends*, vol. 6, pp. 77 – 82, 2006.
- [3] Gokler, M.I., Ozanozgu, A.M., "Experimental investigation of effects of cutting parameters on surface roughness in the WEDM process," *Int. J. Mach. Tools Manuf.*, vol. 40, no. 13, pp. 1831–1848, 2000.
- [4] Gologlu, C., & Sakarya, N., "The effects of cutter path strategies on surface roughness of pocket milling of 1.2738 steel based on Taguchi method," *Journal of Materials Processing Technology*, vol. 206, no. 1–3, pp. 7-15, 2008.
- [5] Groover, M. P., *Fundamentals of modern manufacturing: materials, processes, and systems* (4th ed.). Hoboken, N.J., Wiley, 2010.
- [6] Groover [a], M., "Chapter 1; Introduction and Overview of Manufacturing," In *Principles of modern manufacturing* Hoboken, N.J.: J. Wiley & Sons, 4th ed., pp. 10-11, 2011.
- [7] Groover [b], M., "Chapter 19; Theory of Metal Cutting," In *Principles of modern manufacturing*

Hoboken, N.J.: J. Wiley & Sons, 4th ed., pp. 476-479, 2011.

- [8] Montgomery, D. C., "Other Topics on Factorial and Fractional Factorial Designs. Design and analysis of experiments," 7th International student version. 7th ed., 111 River Street, Hoboken, NJ, Wiley-Blackwell, 07030, (201) 748-6011, pp. 360-363, 2009.
- [9] Romero, P., Dorado, R., Díaz, F., & Rubio, E., "Influence of Pocket Geometry and Tool Path Strategy in Pocket Milling of UNS A96063 Alloy," *Procedia Engineering*, vol. 63, pp. 523-531, 2013.
- [10] Toh, C.K., "A study of the effects of cutter path strategies and orientations in milling," *J. Mater. Process Technology*, vol. 152, pp. 346–356, 2004.
- [11] Wang, M.Y., Chang, H.Y., "Experimental study of surface roughness in slot end milling AL2014-T6," *Int. J. Mach. Tools Manuf.*, vol. 44, 51–57, 2004.

resultant cutting force, presumed to be due to the compliance of the specimen used - Ø50 mm - in the experiment. Conceivably, in the case of a specimen of Ø20 mm, the elastic deflection would be relatively greater causing a larger degree of variance in the dimensions.

| X's | Y's | Y's | Correlation Value (-1 ~ +1) | Significance (P) |
|-------------------------|-------------------------|--------------------|-----------------------------|---------------------|
| Analysis Group A | | | | |
| Depth of Cut | Notch Wear | - | 0.80 (→ +1) | 0.000 Significant |
| Depth of Cut | Cutting Force | | 0.54 (→ +1) | 0.004 Significant |
| - | Cutting Force | Notch Wear | 0.51 (→ +1) | 0.007 Significant |
| - | Cutting Force | Flank wear | 0.64 (→ +1) | 0.000 Significant |
| Analysis Group B | | | | |
| - | Notch Wear | Avg. Dim. Variance | -0.10 (→ 0) | 0.602 Insignificant |
| - | Flank Wear | Avg. Dim. Variance | 0.16 (0 ←) | 0.43 Insignificant |
| Analysis C | | | | |
| - | Resultant Cutting Force | Avg. Dim. Variance | 0.12 (0 ←) | 0.567 Insignificant |

Table 2: Correlation & significance statistics

Further analysis show that regardless of the magnitude of depth of cut, cutting speed and tool wear, the surface roughness is observed to vary positively with regards to variance in the feed rate

4. CONCLUSIONS & RECOMMENDATIONS

The influence of its low elastic modulus which is further aggravated by the depth of cut and the generated cutting force contributes to between 25 - 40 % of residual stock on the diameter of a turned Ti6Al4V cylinder. An experimental comparison of the above results with specimens of Ø20 and Ø30 would provide more stable justification on this effect. a balanced design of tool tip radius & relief angles has to be optimized in order to reduce or eliminate the effects of Elastic modulus on the dimensional instability in machining of Ti6Al4V and also to produce better surface finish on the machined workpiece

5. REFERENCES

[1] Yang, X., & Richard Liu, C., "Machining Titanium and its Alloys", *Machining Science and Technology*, vol. 3, no. 1, pp.107-139, 1999.
 [2] Suresh, S., Jamil, M. A., Sulaiman, S., & Shokor, M. R. M., "Optimization of Electrode material for EDM Die-sinking of Titanium Alloy Grade 5-Ti6Al4V", *International Journal on Advanced Science, Engineering and Information Technology*, vol. 6, no. 4, 2016.
 [3] Carlos Oldani and Alejandro Dominguez, "Titanium as a Biomaterial for Implants, Recent Advances in Arthroplasty," Dr. Samo Fokter (Ed.), ISBN: 978-953-307-990-5, InTech, DOI: 10.5772/27413, 2012.
 [4] Titanium Machining Guide, Kennametals
 [5] Kahles, J. F., Field, M., Eylon, D., & Froes, F. H.,

"Machining of Titanium Alloys," *JOM*, vol. 37, no. 4, pp. 27-35, 1985, doi: 10.1007/BF03259441.
 [6] Veiga, C., Davim, J. P., & Loureiro, A. J. R., "Review on machinability of titanium alloys: the process perspective," *Reviews On Advanced Materials Science*, vol. 34, no. 2, pp. 148-164, 2013.
 [7] Su, H., Liu, P., Fu, Y., & Xu, J., "Tool Life and Surface Integrity in High-speed Milling of Titanium Alloy TA15 with PCD/PCBN Tools," *Chinese Journal of Aeronautics*, vol. 25, no. 5, pp. 784-790, 2012.
 [8] Dr R. R. Malagi, Rajesh. B. C., "Factors Influencing Cutting Forces in Turning and Development of Software to Estimate Cutting Forces in Turning," *International Journal of Engineering and Innovative Technology (IJEIT)*, vol. 2, pp. 37-43, 2012.
 [9] Ribeiro, M. V., Moreira, M. R. V., & Ferreira, J. R., "Optimization of titanium alloy (6Al-4V) machining," *Journal of Materials Processing Technology*, vol. 143-144, pp. 458-463, 2003.
 [10] Chauhan, D. K., & Chauhan, K. K., "Optimization of Machining Parameters of Titanium Alloy for Tool Life," *Journal of Engineering Computers & Applied Sciences*, vol. 2, no. 6, pp. 57-65, 2013.
 [11] Abdulkareem, S., Rumah, U. J., & Adaokoma, A., "Optimizing Machining Parameters during Turning Process," *International Journal of Integrated Engineering*, vol. 3, no. 1, pp. 23-27, 2011.
 [12] Dandekar, C. R., Shin, Y. C., & Barnes, J., "Machinability improvement of titanium alloy (Ti-6Al-4V) via LAM and hybrid machining," *International Journal of Machine Tools and Manufacture*, vol 50, no 2, pp. 174-182, 2010.
 [13] Ibrahim, G. A., Haron, C. C., & Ghani, J. A., "The effect of dry machining on surface integrity of titanium alloy Ti-6Al-4V ELI", *Journal of Applied Sciences*, vol. 9, no. 1, pp. 121-127, 2009.
 [14] Suresh, S., Moe, A. L., Ahmad, N. B., & Sulaiman, S. B., "Experimental Study on the Determinants of Surface Finish in Automated Polishing of Moulds," In *Applied Mechanics and Materials*, vol. 664, pp. 122-127, 2014.
 [15] Suresh, S., Moe, A. L., & Abu, A., "Defects Reduction in Manufacturing of Automobile Piston Ring Using Six Sigma." *Journal of Industrial and Intelligent Information*, Vol 3, no. 1, 2015.
 [16] Izelu, C. O., Eze, S. C., Oreko, B. U., Edward, B. A., & Garba, D. K., "Response surface methodology in the study of induced machining vibration and work surface roughness in the turning of 41Cr4 alloy steel," *Int J Emerg Technol Adv Eng*, vol. 3, pp. 13-17, 2013.
 [17] <http://www.aerospacemetals.com/titanium-ti-6al-4v-ams-4911.html>
 [18] Rafai, N. H., Lajis, M. A., & Hosni, N., "Performance of TiAlN-PVD coated carbide tools in milling AISI D2 hardened steels", 2013.
 [19] Dobrzanski, L., Staszuk, M., Golombek, K., Sliwa, A., & Pancielejko, M., "Structure and properties PVD and CVD coatings deposited onto edges of sintered cutting tools," *Archives of Metallurgy and Materials*, vol. 55(1), pp. 187-193, 2010.
 [20] FUCHS. (n.d.). *Product Information* [Brochure]. Mannheim: Author. PI 1-0180e, Page 1/ Freiler/ 07.07
 [21] Donachie, M. J. *Titanium: a technical guide*. ASM international, 2000.
 [22] Jadhav, J. S., & Jadhav, B. R., "Experimental study of Effect of Cutting Parameters on Cutting Force in Turning Process", 2014.
 [23] Armendia, M., Garay, A., Iriarte, L. M., & Arrazola, P. J., "Comparison of the machinabilities of Ti6Al4V and TIMETAL® 54M using uncoated WC-Co tools." *Journal of Materials Processing Technology*, vol. 210, no. 2, pp. 197-203, 2010.

Experimental investigation and analysis in drilling woven kenaf fiber reinforced composites

Suhaily Mokhtar^{1,2}, Che Hassan Che Haron^{2*}, Jaharah A.Ghani^{2*}, Azmi Harun²

¹Department of Materials and Manufacturing Engineering,
Faculty of Engineering, International Islamic University of Malaysia,
Gombak, Selangor, Malaysia

²Department of Mechanical and Material Engineering,
Faculty of Engineering and Built Environment, Universiti Kebangsaan Malaysia,
43600 Bangi, Selangor, Malaysia.

*Corresponding e-mail: chase@eng.ukm.my

Keywords: RSM; woven kenaf; drilling; surface roughness.

ABSTRACT – The objective of this research was to investigate the influence of machining parameters (spindle speeds, feed rate and drill size) on surface roughness during the drilling of kenaf fibre-reinforced composites. In the present study, Response Surface Method design of experiments were carried out in order to observe the formulation on surface roughness of drilled kenaf fibre-reinforced composites with non-coated HSS and non-coated carbide drill bits. The drilling parameters of spindle speed, feed rates, drill sizes were taken as model variables, whereby, the Analysis of Variance (ANOVA) was employed with the intention of studying the influence of machining parameters on the surface roughness quality of drilled holes. In the previous study, it was observed that the surface roughness values in drilling of woven kenaf/epoxy composites are higher when using the non-coated HSS drills in comparison to lower surface roughness values using the non-coated carbide drills. The influence of different parameters and their interactions were examined and presented in this study.

1. INTRODUCTION

Natural fibres are environmentally friendly and sustainable materials which can be used to replace synthetic fibres in the composite industry. The source of the fibres are from plants or animals and are categorized into few parts for example bast fibres (jute, flax, hemp, ramie and kenaf), leaf fibres (banana, sisal, agave, and pineapple), seed fibres (coir, cotton and kapok), core fibres (kenaf, hemp and jute), grass and reed (wheat, corn and rice) and other types of fibres. The machining of composites varies significantly from the machining of metal in a few respects. Composites are known for its unique properties than metals owing to its anisotropy, non-homogeneous behavior and abrasive reinforcing fibers. Machining parameters which are not properly and carefully chosen for the task of machining composites may prompt genuine damage of machine tools. Ever since the acceptance of composite material in manufacturing and design industry, the machining process of composites, particularly the drilling operation is extensively utilized for producing bolted joint and riveting for the design of structural assembly. In drilling operation of composite materials, any imperfection emerging and formed on the structure demands for

rework, or renders it as scrap and eventually put a tremendous economic impact in the industry. Therefore, machining of composites demands for a high performance and high precision process in the entire machining process. Machined surface finish is the measurement of the finer surface inconsistencies that occurred on the surface texture, depending upon the cutting speed, feed rate and mechanical properties of the machined work material [1]. A fine surface roughness influences the practicality attributes of the machined component, as an instance its fatigue, friction, wearing, light reflection, heat transmission and lubrication, of the component quality that is needed to be at top level of performance [2]. According to Naveen et al [3], the quality of the drilled hole resembling waviness or roughness of its wall surface, axial straightness and roundness of the crossed section hole, could cause high stresses on the rivet later leads to its failure as expressed by Santhanam and Chandrasekaran [4], that the implications of fibre pull out from the matrix throughout the cutting process by the drill tool could lead to excessive roughness on the facet walls that eventually affects the hole quality.

In the present work, statistical analysis software Design Expert 6.0 is used to perform the Box Behnken Design and ANOVA analysis. The response variable chosen is surface roughness of the drilled woven kenaf/epoxy composites.

2. METHODOLOGY

The Box Behnken design was used with 17 tests to run for data acquisition and modelling response surface designs is shown as in Table 1.

Table 1 Three levels cutting parameters

| Level | Cutting Speed | Feed Rate | Drill size |
|------------|---------------|-----------|------------|
| | (m/min) | (mm/rev) | (mm) |
| | A | B | C |
| Low (-1) | 20 | 0.1 | 6 |
| Middle (0) | 45 | 0.2 | 9 |
| High (+1) | 70 | 0.3 | 12 |

3. RESULTS AND DISCUSSION

From the experimental result shown in Figure 1, the surface roughness values of non-coated HSS are

found to be higher than surface roughness using the non-coated carbide drills in the drilling of the investigated work material. Such observation occurred could be probably due to high temperature generated during the machining process using the non-coated HSS drills. Even though the heat generated at the cutting zone may softens the work material and facilitate an easier cutting process, due to low thermal conductivity of non-coated HSS drill, the heat generated during the drilling process not easily dissipated from cut zone. Henceforth, a huge amount of heat is found trapped on or over the cutting zone that intensifies the temperature. Moreover, as according by Khashaba [5], in drilling polymeric matrix composites, the high accumulated heat around the tool destroys the stability and thus produces thermal images (delamination) and rough cuts.

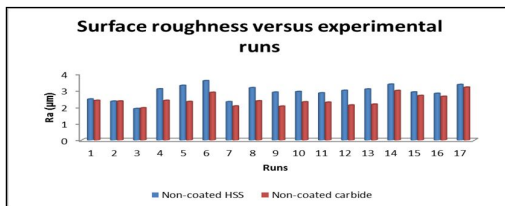


Figure 1 Influence of machining parameters on surface roughness between non-coated HS and non-coated carbide drill

Figure 2 shows the SEM micrographs of drilling woven kenaf/epoxy composites by non-coated carbide drills. The figure shows a minimal material damages formed and exhibit better surface finish as the respective cutting parameters, in comparison to the SEM micrographs shown in Figure 3 of drilled holes using the non-coated HSS drills.

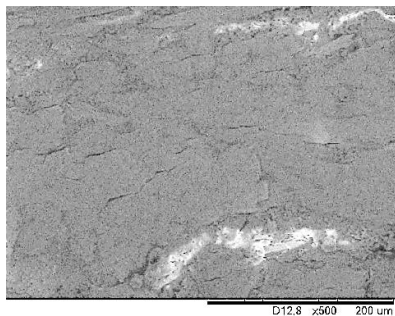


Figure 2 SEM images of the drilled hole when drilling of woven kenaf/epoxy composite laminates using non-coated carbide drills at v_c : 70 m/min; f : 0.1 mm/rev; d : 9 mm

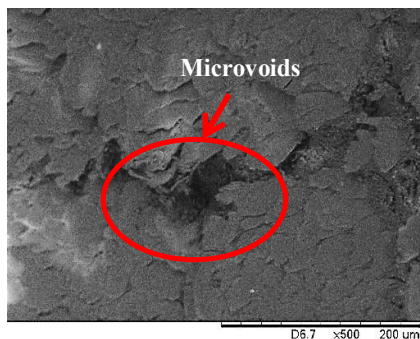


Figure 3 SEM images of the drilled hole when drilling

of woven kenaf/epoxy composite laminates using non-coated HSS drills at at v_c : 45 m/min; f : 0.1 mm/rev; d : 12 mm

4. CONCLUSIONS

The non-coated carbide drill bits were observed to perform better in producing lower surface roughness values and smooth surface texture under SEM during drilling of woven kenaf/epoxy composites.

5. REFERENCES

- [1] D. Saran and P. B. J, "Experimental Analysis of the Effect of Process Parameters on Surface Finish in Radial Drilling Process," *Int. J. Eng. Innov. Technol.*, vol. 4, no. 4, pp. 49–56, 2014.
- [2] T. Rajmohan and K. Palanikumar, "Optimization of Machining Parameters for Surface Roughness and Burr Height in Drilling Hybrid Composites," *Mater. Manuf. Process.*, vol. 27, no. 3, pp. 320–328, 2012.
- [3] P. N. E. Naveen, M. Yaraswi, and R. V Prasad, "Experimental Investigation of Drilling Parameters on Composite Materials," *J. Mech. Civ. Eng.*, vol. 2, no. 3, pp. 30–37, 2012.
- [4] V. Santhanam and M. Chandrasekaran, "A Study on Drilling Behavior of Banana-Glass Fibre Reinforced Epoxy Composite," no. November, pp. 194–199, 2014.
- [5] U. Khashaba, "Drilling of polymer matrix composites: A review," *J. Compos. Mater.*, no. July 2012, 2012.

Thrust force in drilling of woven kenaf fiber reinforced epoxy composite laminates

Suhaily Mokhtar^{1,2}, Che Hassan Che Haron^{2*}, Jaharah A.Ghani^{2*}, Azmi Harun²

¹Department of Materials and Manufacturing Engineering,
Faculty of Engineering, International Islamic University of Malaysia,
Gombak, Selangor, Malaysia

²Department of Mechanical and Material Engineering,
Faculty of Engineering and Built Environment, Universiti Kebangsaan Malaysia,
43600 Bangi, Selangor, Malaysia.

*Corresponding e-mail: chase@eng.ukm.my

Keywords: RSM; woven kenaf; drilling; delamination

ABSTRACT – Drilling or the creating of holes in composite parts is a necessary and sensible task, preponderantly for facilitating the assembly of joints. Within the present investigation, the drilling operation on natural fibre-reinforced thermosetting (epoxy) composite laminates was assessed in terms of the drilling force. This study conjointly incorporated the employment of a Box-Behnken design (RSM) with 17 test runs within which machining parameters corresponding to the cutting speed, feed rate and drill size were taken under consideration because the input variables. The consequences of two differing kinds of tool materials (non-coated HSS and carbide) were conjointly evaluated within the study. The Response Surface Methodology (RSM) was accustomed analyse and establish the empirical relationships among the method parameters. The results demonstrated that all three factors (cutting speed, feed rate and drill size) had a major impact on the cutting force that was produced. The thrust force that was developed when utilizing the non-coated HSS drill was found to be higher than that of the non-coated carbide drill throughout the drilling of the woven kenaf/epoxy composite laminates.

1. INTRODUCTION

Natural fibres are chosen as reinforcement material as they are able to reduce tool wear throughout the machining operation also as respiratory irritation, and provide possibility option for artificial fibre composites due to public concern over energy security and environmental preservation [1]. The kenaf plant, that is additionally known as the *Hibiscus cannabinus* L. (belonging to the Malvacea family), is usually used as a reinforcement in compound of polymer matrix composites [2]. In the past few years, varied studies are performed on kenaf fibre-reinforced composites, and their application as a replacement composite material substitute is incredibly conceivable due to their low density, renewability, high specific strength and low cost value [3]. Despite the fact that the tools used for the machining of metals can presently be used for the machining of composites, care should be taken to retain the most effective level of feed rate, thrust force and other influences [4]. In an exceedingly study conducted by Vinayagamoorthy and Rajeswari [5] on the machining (end milling) of commercially woven jute

fibres reinforced with polyester, it absolutely was shown that the thrust force and torque were affected by the speed, feed rate and depth of cut throughout the milling of the materials under investigation. In the drilling of composite materials, the drill geometry, feed rate and cutting speed influence the developed thrust force and torque throughout the machining operation [6]. Khashaba et al. [7] expressed that the thrust force is incredibly concerning to the delamination damage that happens within drilling of polymeric composite laminates. They ascertained that through the suitable selection of drilling parameters (feed and speed), drill geometry, drill type and drill material, it would be possible to regulate the delamination size throughout the drilling of polymeric composite materials. In drilling operations, the drilling forces ought to be decreased so as to obtain a low induced-delamination damage through the selection of suitable machining parameters, for instance, the feed rate, cutting speed and drill point geometry [8]. Therefore, the current work investigated the consequences of machining parameters (cutting speed, feed rate, and drill size) and also the influence of tool materials on the thrust force within the drilling of woven kenaf fibre-reinforced epoxy composites. The correlations between the thrust force and also the investigated parameters were examined.

2. METHODOLOGY

Woven kenaf fibre-reinforced epoxy laminated composites were developed using the hand lay-up technique with a fibre weight fraction of 60% in the epoxy matrix. The drilling of the laminated composites was carried out on a Computer Numerical Control machining centre (SPINNER VC 450). Two types of standard two-flute straight shanks, namely non-coated high-speed steel (HSS) and non-coated carbide drill bits with diameters of 6, 9 and 12 mm and a point angle of 118°, were used. The drilling process was carried out at three different levels of cutting speeds (20, 45 and 70 m/min), feed rates (0.1, 0.2 and 0.3 mm/rev) and drill bit sizes (6, 9 and 12 mm). During the drilling operation, the thrust force signals were recorded by a Neo-MoMac cutting force measuring system, which uses a strain gauge-based dynamometer. The dynamometer was placed under the workpiece, while the backing plate was placed over the machining table.

All the test runs were performed under dry machining conditions.

Table 1 Three levels cutting parameters

| Parameters | Values |
|-----------------------|------------------|
| Cutting speed (m/min) | 20, 45 and 70 |
| Drill diameter (mm) | 6, 9 and 12 |
| Feed rate (mm/min) | 0.1, 0.2 and 0.3 |

3. RESULTS AND DISCUSSION

The experimental results of the thrust force in the drilling of woven kenaf/epoxy composite laminates using non-coated HSS and non-coated carbide drills are shown in Figure 1. It could be observed from the figure that there was a drastic reduction in the thrust force in the non-coated carbide drill compared to the non-coated HSS drill.

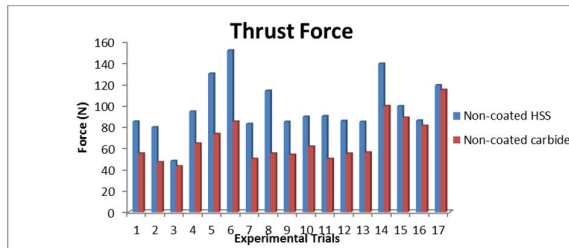


Figure 1 Comparison of experimental results of thrust force between non-coated HSS and non-coated carbide drills

Several researchers corroborated that the developed thrust force when using a non-coated HSS drill was expected to be higher than that produced by the utilization of a non-coated carbide drill during the machining of composite materials [9,10]. The significant difference in the thrust forces when using a non-coated HSS drill and a non-coated carbide drill could be attributed to the higher hot hardness of the non-coated carbide drill, which is superior to that of the non-coated HSS drill. The hot hardness and hardness of the carbide tool are known to be greater than that of high-speed steels, cast alloys and carbon tool steels, as shown in Figure 2. The high hardness property in carbide tool ensures that the tool does not encounter any plastic deformation and thus retains its shape and sharpness. The heat generated between the tip of the tool and the workpiece is less in carbide drills thus results in less stick-slip friction at the interface of the tool and the workpiece. Therefore, lower thrust force was produced with non-coated carbide drills.

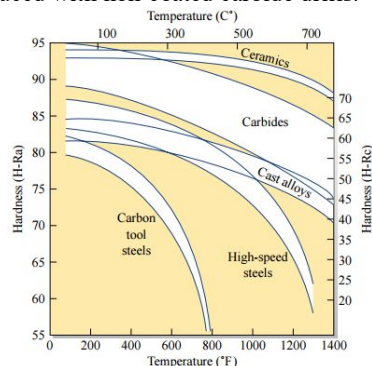


Figure 2 Hot hardness variations for different cutting tool materials as a function of temperature [11]

4. CONCLUSIONS

It was found that the thrust force values increased as feed rate and drill bit diameter values increased in the utilization of non-coated HSS and carbide drills. The developed thrust force was higher when the drilling of woven kenaf/epoxy composite laminates was carried out using a non-coated HSS drill in comparison to the thrust force developed using a non-coated carbide drill.

5. REFERENCES

- [1] H. Cheung, M. Ho, K. Lau, F. Cardona, and D. Hui, "Natural fibre-reinforced composites for bioengineering and environmental engineering applications," *Compos. Part B Part B*, vol. 40, no. 7, pp. 655–663, 2009.
- [2] H. . Akil, M. . Omar, A. A. . Mazuki, S. Safiee, Z. A. . Ishak, and A. A. Bakar, "Kenaf fiber reinforced composites: A review," *2Journal Mater. Des.*, vol. 32, pp. 4107–4121, 2011.
- [3] S. Ochi, "Mechanical properties of kenaf fibers and kenaf/PLA composites," *Mech. Mater.*, vol. 40, no. 4–5, pp. 446–452, 2008.
- [4] D. Chandramohan and S. Rajesh, "Study of machining parameters on natural fiber particle reinforced polymer composite material," *Acad. J. Manuf. Eng.*, vol. 12, no. 3, pp. 72–77, 2014.
- [5] R. Vinayagamoorthy and N. Rajeswari, "Analysis of cutting forces during milling of natural fibered composites using fuzzy logic," *Int. J. Compos. Mater. Manuf.*, vol. 2, no. 3, pp. 15–21, 2012.
- [6] C. C. Tsao and H. Hocheng, "Taguchi analysis of delamination associated with various drill bits in drilling of composite material," *Int. J. Mach. Tools Manuf.*, vol. 44, no. 10, pp. 1085–1090, 2004.
- [7] U. a. Khashaba, I. a. El-Sonbaty, a. I. Selmy, and a. a. Megahed, "Machinability analysis in drilling woven GFR/epoxy composites: Part II - Effect of drill wear," *Compos. Part A Appl. Sci. Manuf.*, vol. 41, no. 9, pp. 1130–1137, 2010.
- [8] P. K. Bajpai and I. Singh, "Drilling behavior of sisal fiber-reinforced polypropylene composite laminates," *J. Reinf. Plast. Compos.*, vol. 32, no. 20, pp. 1569–1576, 2013.
- [9] Wang, X., Wang, L. J. & Tao, J. P. 2004. Investigation on thrust in vibration drilling of fiber-reinforced plastics. *Journal of Materials Processing Technology*, doi:10.1016/j.jmatprotec.2003.12.019
- [10] Taskesen, A. & Kütükde, K. 2013. Optimization of the drilling parameters for the cutting forces in B4C-reinforced Al-7XXX-series alloys based on the Taguchi method. *Materials and Technology*, 47(2), 169–176.
- [11] S. J. George, *Cutting Tools Application*. George Schneider Jr, 2002, 2002.

Fabricating (Manufacturing) Spiral Bevel Gear With Using Cad/Cam And 5-Axis Cnc Machine

Wan Nur Izzati Wan Badiuzaman¹, Mohd Sayuti Ab Karim^{1*}, Aly Diaa Mohammed Sarhan¹, Mehdi Hourmand¹

¹Department of Mechanical Engineering,
Faculty of Engineering, University of Malaya,
50603 Kuala Lumpur, Malaysia.

*Corresponding e-mail: mdsayuti@um.edu.my

Keywords: spiral bevel gear; CNC milling; CAD/CAM technology.

ABSTRACT –The main application of spiral bevel gear (SBG) is in a vehicle differential where the drive direction from the drive shaft must be turned 90 degrees to drive the wheels. The production of SBG in the industries nowadays is mostly using the conventional 3-axis CNC machine. 3-axis CNC machine have limited angle of rotation that makes the fabricated SBG less precise and lower quality. The best solution to this problem is by using 5-axis CNC milling machine to produce the spiral bevel gear. CAD/CAM technology can help to produce it by using CNC machine. This research study involves to design the spiral bevel gear with 40 number of teeth and 3 module size. Moreover, the 3D model is created by using Solidworks software based on mathematical calculation. The G-code programming was generated by using MTS Topmill software for 5-axis CNC machine and spiral bevel gear cutter. Finally, aluminum spiral bevel gear was successfully fabricated.

1. INTRODUCTION

Bevel gears are a pair of gears where the axes of the two shafts coincide and the tooth-bearing appearances are conically shaped [1, 2]. The purpose of the design of bevel gear is for transmitting power and movement. Most transmissions happen at right angle, yet the shaft angle can be at any quality. Spiral bevel gears, compared to straight or zerol bevel gears, have additional overlapping tooth action which makes a smoother gear mesh [3, 4]. The production of bevel gear can be done by several methods, and one of the methods is by using CAD/Cam and 5-axis CNC machine.

The first process in order to fabricate the gear is by the application of face milling process. Face milling is utilized to remove flat surfaces or appearances into the workpiece, or to remove flat-bottomed cavities[5]. It is the most well-known processing operation and can be performed utilizing an extensive variety of distinctive instruments. The spiral teeth is then fabricated by using 5-axis CNC machine. 5-axis CNC machine is a CNC machine that able to perform movement about five different axis simultaneously[6]. By using this machine, the fabrication of the spiral bevel gear tooth surfaces is much more precise and efficient.

This research study involves to design the spiral bevel gear and pinion with 40 and 20 teeth respectively and 3 module size. Moreover, the 3D model is created by using Solidworks software based on mathematical calculation[7]. Finally, the developed G-code programming was generated by using MTS Topmill

software for 5-axis CNC machine with face mill tool.

2. METHODOLOGY

In this experiment, SPINNER U-620 5-axis CNC machine and spiral bevel gear cutter was utilized to manufacture a spiral bevel gear because of its complex shape as shown in Fig. 1. Aluminum was selected as a spiral bevel gear material [2]. At first, the dimensional geometry of a spiral bevel gear material with 40 number of teeth and 3 module size was calculated by following equations[8] :

$$1. m = \frac{D_2}{Z_2} \quad (1)$$

$$2. A_{oG} = \frac{0.5 D_2}{\sin \Gamma} \quad (2)$$

$$3. A_{mG} = A_{oG} - 0.5F \quad (3)$$

$$4. \Gamma = 90^\circ - \gamma \quad (4)$$

$$5. P_{mG} = (\pi)(m) \left[\frac{A_{mp}}{A_{op}} \right] \quad (5)$$

$$6. m_{90} = \sqrt{\frac{Z_2 \cos \gamma}{Z_1 \cos \Gamma}} \quad (6)$$

$$7. C_1 = 0.210 + \left[\frac{0.290}{(m_{90})^2} \right] \quad (7)$$

$$8. h_{wG} = (k_1) (m) \left[\frac{A_{mG}}{A_{oG}} \right] \cos \psi \quad (8)$$

$$9. a_G = (C_1)(h_{wG}) \quad (9)$$

$$10. b_G = h_{wG} - a_G \quad (10)$$

$$11. c = (k_2)(h_{wG}) \quad (11)$$

$$12. h_{mG} = h_{wG} - c \quad (12)$$

$$13. \delta_{dG} = \arctan \left(\frac{b_G}{A_{mG}} \right) \quad (13)$$

$$14. \delta_{aG} = \delta_{dp} \text{ pinion gear} \quad (14)$$

$$15. \theta_{fG} = \Gamma + \delta_{aG} \quad (15)$$

$$16. \theta_{rG} = \Gamma - \delta_{dG} \quad (16)$$

$$17. a_{oG} = a_G + 0.5F \tan \delta_{dp} \quad (17)$$

$$18. b_{og} = b_G + 0.5F \tan \delta_{dG} \quad (18)$$

$$19. h_k = a_{op} + a_{oG} \quad (19)$$

$$20. h_t = a_{op} + b_{op} \quad (20)$$

$$21. \alpha_n = \frac{\alpha_{np} + \alpha_{nG}}{2} \quad (21)$$

$$22. D_{oG} = D_2 + 2a_{oG} \cos \Gamma \quad (22)$$

$$23. X_G = A_o \cos \Gamma - a_{op} \sin \Gamma \quad (23)$$

where m is module, D2 is diameter of the gear, Z2 is

number of teeth, h is the workpiece thickness, AOG is outer cone distance, Γ is pitch angle, AmG is mean cone distance, γ is pinion pitch angle, PmG is mean circular pitch, m_{90} is equivalent 90° ratio, C_1 is mean addendum factor, hw_G is mean working depth, a_G is mean addendum, b_G is mean dedendum, c is clearance, hm_G is mean whole depth, δd_G is dedendum angle, δa_G is addendum angle, θf_G is face angle, θr_G is root angle, ao_G is outer addendum, bo_g is outer dedendum, hk is outer working depth, ht is outer whole depth, α_n is mean normal pressure angle, Do_G is outer diameter, and X_G is pitch cone apex to crown.

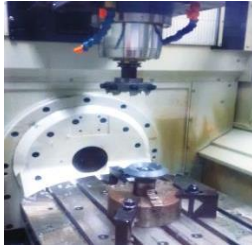


Fig. 1 Experimental setup for manufacturing spiral bevel gear

After that, Solidworks software was utilized to draw the 3D model of spiral bevel gear according to mathematical calculation. Next, this 3D model was transfer to MTS Topmill software for generating G-code programming and G-code programming was generated for 5-axis CNC machine and spiral bevel gear cutter. Finally, these G-code programming was send to 5-axis CNC machine for manufacturing the gear.

3. RESULTS AND DISCUSSION

The dimensional geometries of spiral bevel gear were calculated by using Equations 1-23. Its dimensional geometries are as follows:

$$A_{oG} = 67.08204^\circ, A_{mG} = 59.58204 \text{ mm}, \Gamma = 63.43495^\circ, P_{mG} = 8.37106 \text{ mm}, m_{90} = 2.00000, C_1 = 0.2825, h_{wG} = 4.36541 \text{ mm}, a_G = 1.23329 \text{ mm}, b_G = 3.67778 \text{ mm}, c = 0.54566 \text{ mm}, h_{mG} = 4.91107 \text{ mm}, \delta_{dG} = 3.53218^\circ, \delta_{aG} = 1.68136^\circ, \theta_{fG} = 65.11631^\circ, \theta_{rG} = 59.90277^\circ, a_{oG} = 1.45344 \text{ mm}, b_{og} = 4.14073 \text{ mm}, h_k = 5.07851 \text{ mm}, h_t = 5.59417 \text{ mm}, \alpha_n = 20^\circ, D_{oG} = 121.30000 \text{ mm}, X_G = 28.70000 \text{ mm}, t_G = 2.56927 \text{ mm}.$$

Fig.2 shows the isometric view of spiral bevel gear which was created using Solidworks software based on Solidworks software. After that, MTS Topmill was used to generate G-code programming of 3D model of Fig. 2 for Siemens 840D-SL controller of 5-axis CNC machine and spiral bevel gear cutter. The manufacturing of gear was performed based on experimental setup in Fig.1. The initial testing of G-code programming was performed on PVC material [9]. Finally, aluminum spiral bevel gear was successfully produced as shown in Fig. 3.

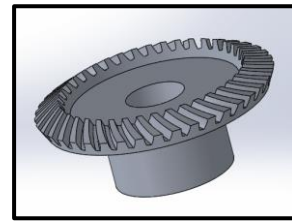


Fig. 2 Isometric view of spiral bevel gear

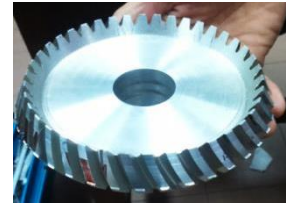


Fig. 3 Aluminum spiral bevel gear

4. CONCLUSIONS

In this research, spiral bevel gear with 40 number of teeth and 3 module size was designed. CAD/CAM technology was utilized to draw its 3D model using Solidworks software and generate G-code programming MTS Topmill software for 5-axis CNC machine and spiral bevel gear cutter. Finally, aluminum spiral bevel gear was successfully manufactured.

5. REFERENCES

- [1] Argyris, J., A. Fuentes, and F.L. Litvin, "Computerized integrated approach for design and stress analysis of spiral bevel gears," *Computer methods in applied mechanics and engineering*, vol. 191, no. 11, pp. 1057-1095, 2002.
- [2] Handschuh, R.F., "Thermal behavior of spiral bevel gears," Case Western Reserve University, 1993.
- [3] Brown, M.D., "Design and Analysis of a Spiral Bevel Gear," Rensselaer Polytechnic Institute, 2009.
- [4] Mao, K., "Gear tooth contact analysis and its application in the reduction of fatigue wear," *Wear*, vol. 262, no. 11, pp. 1281-1288, 2007.
- [5] Litvin, F.L., et al., "Computerized design, simulation of meshing, and contact and stress analysis of face-milled formate generated spiral bevel gears," *Mechanism and Machine Theory*, vol. 37, no. 5, pp. 441-459, 2002.
- [6] Deng, X.-z., et al., "Face-milling spiral bevel gear tooth surfaces by application of 5-axis CNC machine tool." *The International Journal of Advanced Manufacturing Technology*, vol. 71, no. 5-8, pp. 1049-1057, 2014.
- [7] Wang, J., et al., "The mathematical model of spiral bevel gears-A review," *Journal of Mechanical Engineering*, vol. 60, no. 2, pp. 93-105, 2014.
- [8] Lei, B., et al., "Remanufacturing the pinion: an application of a new design method for spiral bevel gears." *Advances in Mechanical Engineering*, vol. 6, pp. 257581, 2014.
- [9] Kurokawa, M., et al., "Performance of plastic gear made of carbon fiber reinforced polyamide 12," *Wear*, vol. 254, no. 5, pp. 468-473, 2003.

Effects of Steam Explosion Pretreatment (SEP) On Natural Fibers: A Review

Siti Atiqah Al Zahra Binti Mat Darus¹, Mariyam Jameelah Ghazali^{1*}, Che Husna Che Azhari¹, Rozli Zulkifli¹, Mohd Tamizi Mustafa², Hanifi Sarac³

¹) Department of Mechanical and Material Engineering,
Faculty of Engineering and Built Environment, Universiti Kebangsaan Malaysia,
43600 Bangi, Selangor, Malaysia.

²) Forest Research Institute of Malaysia,
Jalan Frim, Kepong, 52109 Kuala Lumpur, Selangor, Malaysia

³) Faculty of Chemical and Metallurgical Engineering,
Yildiz Technical University, 34210 Istanbul, Turkey.

*Corresponding e-mail: mariyam@ukm.edu.my

Keywords: Natural Fiber; Steam Explosion; morphology,

ABSTRACT – Surface treatment on natural fibers is normally performed to enhance the workability and compatibility between the matrix-fibers in composites. This paper presents a review of a steam explosion pretreatment (SEP) on natural fibers for natural composites. The review emphasized on the optimum parameters of the SE (steam explosion) method, chemical composition, morphology and the produced fiber size along with the mechanical properties of the produced composites. In short, the SEP is an effective method in obtaining 10⁻⁶ to 10⁻⁹ m (meso-scaled) sized BF (bamboo fibers) for high quality natural fiber composites.

1. INTRODUCTION

In striving for sustainable ecosystem and cost, natural fibers are very much preferable compared to the synthetic fibers. However, when dealing with natural fibers, it may have to consider many factors as they are incompatible with the hydrophobic polymer matrix due its hydrophilic in nature. Within the natural fibers, the hemicellulose is the most hydrophilic and thermally unstable, and the lignin may migrated to the fiber surface if heated above the glass transition. The incompatibility may affect the composites by forming aggregates during extrusion, making them heterogeneous with poor adhesion between the matrix-fiber, thus limiting stresses which triggered fiber pull-outs in fracture surfaces. Natural fibers are also poor in resisting moisture (high water absorption), thus resulting poor mechanical properties in the composites. An increase in the hydrophobicity characteristic may lead to an increase in the mechanical properties of the composites.

There are various types of surface modifications in order to increase the adhesion between matrix and fiber such as silane coupling agent, alkali, acetylation, benzoylation, permanganate and peroxide with various levels of success. It was noted that bamboo fibre composites via SEP exhibited higher tensile strength compared to the same composites via mechanical extraction and alkali treatment [1]. Table 1 shows the effect of surface treatments on tensile strength for several natural fiber composites. Tensile strengths between reinforced fibers were also found varied with the size of the fibres. The treatment by

SEP followed by other treatments (either acidic or alkaline) [2] also showed a successful removal of unwanted hemicellulose and lignin, resulting in a decrease in the fiber size at the same time. In addition, smaller particles exhibited good mechanical properties because of better dispersion in the matrix. Moreover, the chemical composition, thermal properties and morphological properties of the fibers are greatly affected by the SEP in which the separation of nanofibres from the natural fibers can be made with ease.

Thus this review mainly focuses on the optimisation of the SEP method and its effectiveness in removing unwanted contents like hemicellulose and lignin. The researcher see that the utilization of bamboo fiber is one of the best alternative natural fiber as reinforcement in composites due to the short maturity, good material properties and high yield resources.

2. OPTIMISATION OF STEAM EXPLOSION TECHNIQUE

A steam explosion pretreatment (SEP) was first introduced and patented by Mason et al. in 1926 for a biomass pretreatment. Originally, it was used for fermentation, hydrolysis or densification process. The SEP was then utilised as a pretreatment method in producing fibers for composites as it involved hot steam ranging from 180 to 240 °C, with pressure between 1 to 3.5 MPa, followed by an explosive decompression. The sudden release of the pressure may defibrillated the cellulose bundles which open-up the fibers for subsequent processes with ease. Table 2 shows the effect of SEP parameter on the lignocellulosic content for various types of natural fibers.

It was noted that the pressure, temperature and retention time are vital in optimizing high quality of fibers. The processing of natural fiber by SEP with high pressure of 138 kPa could increased the weight percentage of the cellulose up to 98.63 % [3]. Han and co-workers [4] had observed that by using high temperature and a long retention time in the SEP, the fiber size can also be reduced between 5 nm to 60 nm [3,5-6].

Table 1: Composites of natural fiber: Effect of surface treatment on tensile strength

| Types of treatment | Tensile strength (MPa) | | Increased by (%) |
|---------------------------|------------------------|---------|------------------|
| | Untreated | Treated | |
| SEP [7] | 16.25 | 23.75 | 46 |
| NaOH [8] | 14 | 18.76 | 34 |
| Silane Coupling Agent [9] | 56 | 67 | 20 |

Table 2: The effect of SEP parameters on lignocellulosic contents for various type of natural fibers

| Fiber | | Cellulose | Hemi-cellulose | Lignin | Pressure (kPa), Temperature (°C), (hour) |
|--------------------|------------|-----------|----------------|--------|--|
| | | (wt%) | (wt%) | (wt%) | |
| Coir [14] | Before SEP | 39.3 | 2 | 49.2 | - |
| | After SEP | 93.7 | - | - | 0.137 kPa, 100-150°C, 1h |
| Wheat straw [15] | Before SEP | 45.7 | 37.12 | 17.43 | - |
| | After SEP | 86.38 | 8.13 | 6.34 | 103 kPa, 4h |
| Banana fiber [2] | Before SEP | 64 | 19 | 5 | - |
| | After SEP | 95.9 | 0.4 | 1.9 | 138 kPa, 110-120°C, 1 h |
| Pineapple leaf [3] | Before SEP | 81.27 | 12.31 | 3.46 | - |
| | After SEP | 98.63 | 0.53 | 0.77 | 138kPa, 1h |

Figure 1 shows the defibrillation of the fibers (removal of hemi-cellulose and lignin) by using the SEP. The size of the fibers was observed to reduce up to 90 % after the pretreatment [2-3,5-6], resulting in an improved mechanical properties of the composite with better dispersion in the matrix.

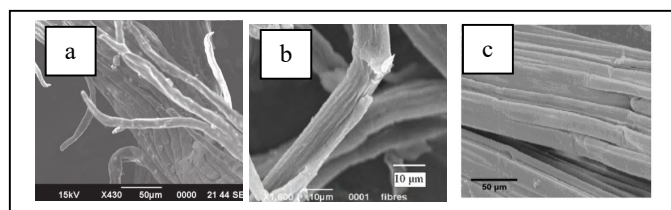


Figure 1 : SEM images of a) coir, b) wheat straw and c) pineapple fibers using SEP [2-3,5-6]

3. CONCLUSIONS

Natural fibers were chosen as an alternative for synthetic fibers due to their advantages like biodegradability, low cost, high specific strength and renewable. Interfacial adhesion between natural fiber and matrix has always been the main reason of low performance in the mechanical properties. A high potential of fibers treatment like SEP is proven to give good results after the defibrillation of the fibers with an increase in the cellulose weight percent up to 99 %,

eliminating the hemicellulose and lignin as well as decreasing the fiber size up to 90%. Further process such as alkali or acid treatments, however, is needed after the SEP for producing nano-scale fibers with hemicellulose and lignin free. The key parameters in the SEP such as pressure, temperature and retention time varied for different types of fibers and requirements. In short, the optimum parameters in producing high quality fibers were at 138 kPa of pressure and temperature at 150°C.

4. REFERENCES

- [1] R. Tokoro, D. M. Vu, K. Okubo, T. Tanaka, T. Fujii, and T. Fujiura, "How to improve mechanical properties of polylactic acid with bamboo fibers," *J. Mater. Sci.*, vol. 43, no. 2, pp. 775-787, 2008.
- [2] B. Deepa, E. Abraham, B. M. Cherian, A. Bismarck, J. J. Blaker, L. a. Pothan, A. L. Leao, S. F. de Souza, and M. Kottaisamy, "Structure, morphology and thermal characteristics of banana nano fibers obtained by steam explosion," *Bioresour. Technol.*, vol. 102, no. 2, pp. 1988-1997, 2011.
- [3] B. M. Cherian, A. L. Le??o, S. F. de Souza, S. Thomas, L. A. Pothan, and M. Kottaisamy, "Isolation of nanocellulose from pineapple leaf fibres by steam explosion," *Carbohydr. Polym.*, vol. 81, no. 3, pp. 720-725, 2010.
- [4] G. Han, J. Deng, S. Zhang, P. Bicho, and Q. Wu, "Effect of steam explosion treatment on characteristics of wheat straw," *Ind. Crops Prod.*, vol. 31, no. 1, pp. 28-33, 2010.
- [5] E. Abraham, B. Deepa, L. A. Pothan, J. Cintil, S. Thomas, M. J. John, R. Anandjiwala, and S. S. Narine, "Environmental friendly method for the extraction of coir fibre and isolation of nanofibre," *Carbohydr. Polym.*, vol. 92, no. 2, pp. 1477-1483, 2013.
- [6] A. Kaushik, M. Singh, and G. Verma, "Green nanocomposites based on thermoplastic starch and steam exploded cellulose nanofibrils from wheat straw," *Carbohydr. Polym.*, vol. 82, no. 2, pp. 337-345, 2010.
- [7] J. Qu, B. Tan, Y. Feng, and S. Hu, "Mechanical Properties of Poly(Butylene Succinate) Reinforced with Continuously Steam-Exploded Cotton Stalk Bast," *Polym. Plast. Technol. Eng.*, vol. 50, no. 14, pp. 1405-1411, 2011.
- [8] T. Lu, M. Jiang, Z. Jiang, D. Hui, Z. Wang, and Z. Zhou, "Effect of surface modification of bamboo cellulose fibers on mechanical properties of cellulose/epoxy composites," *Compos. Part B Eng.*, vol. 51, pp. 28-34, Aug. 2013.
- [9] T. Lu, S. Liu, M. Jiang, X. Xu, Y. Wang, Z. Wang, J. Gou, D. Hui, and Z. Zhou, "Effects of modifications of bamboo cellulose fibers on the improved mechanical properties of cellulose reinforced poly(lactic acid) composites," *Compos. Part B Eng.*, vol. 62, pp. 191-197, 2014.

Optimization study on delamination factor (F_d) in milling kenaf fibre reinforced plastic composite materials

Azmi bin Harun^{1,2}, Che Hassan Che Haron^{2*}, Jaharah A. Ghani², Suhaily bin Mokhtar², Sia Ting Ting¹

¹Pusat Pengajian Kejuruteraan Pembuatan, Universiti Malaysia Perlis,
Kampus Tetap Pauh Putra, Jalan Arau-Changlun,
02600 Arau, Perlis, Malaysia.

²Jabatan Kejuruteraan Mekanikal dan Bahan,
Fakulti Kejuruteraan dan Alam Bina, Universiti Kebangsaan Malaysia,
43600 Bangi, Selangor, Malaysia.

*Corresponding e-mail: chehase@gmail.com

Keywords: Kenaf Fibre; Taguchi Method; Delamination; Optimization.

ABSTRACT – Kenaf is known by its scientific name, *Hibiscus cannabinus*, which is similar to jute and cotton and is also a warm season yearly fibre crop. In the past, sackcloth and twine to manufacture rope, and kenaf is also used as a cordage crop. A machine surface's quality normally depends on its reliability for the service application. The machining process changes in the mechanical and chemical properties of individual constituents used in the composite. The objectives of this research are to study the effects of milling parameters and determining optimum conditions for a range of milling parameters under investigation to minimize delamination factor (F_d) in milling kenaf fibre reinforced plastic composite using the Taguchi Method. The Taguchi Method L_8 (2^3) design is used to conduct a non-sequential experiment. The experimental results were analyzed using Minitab 16 software. A study was carried out to investigate the relationship between the milling parameters and their effects on kenaf reinforced plastic. The composite panels were fabricated using the vacuum assisted resin transfer molding (VARTM) method. This study found that the optimum parameters for the minimum delamination factor were a cutting speed of 500 rpm, a feed rate of 200 mm/min, and depth of cut of 2.0 mm. The feed rate and cutting speed make the biggest contribution to the delamination factor (F_d). The use of high spindle speeds and low feed rates leads to minimized delamination factor (F_d) during the milling kenaf reinforced plastic composite materials.

1. INTRODUCTION

Natural fibre is sustainable as well as eco-efficient therefore it has been used to replace glass fibre as well as other synthetic polymer fibres that have various kind of a caption in engineering [1].

Kenaf is known by its scientific name, *Hibiscus cannabinus*, which is similar to jute and cotton and is also a warm season yearly fibre crop. In the past, sackcloth and twine to manufacture rope, and kenaf is also used as a cordage crop [2]. Recently, kenaf is widely used in various industries due to an increasing demand for green and clean industrial products. Additionally, kenaf plant fibre can be processed to produce paper pulp, building materials, construction materials, automotive materials, and biofuels because of the following properties of a low weight, high specific properties, and renewability. This indicates that kenaf acts as a good potential natural fibre to be used in the automotive and construction industries.

The Taguchi Method uses a signal-to-noise (S/N) ratio as a statistical measure of performance. The S/N ratio considers both variability and mean. The ratio of the mean (Signal) to the standard deviation (Noise) is the S/N ratio. The ratio depends on the quality characteristics of the process or product to be optimized. The standard S/N ratios used were as follows: higher is better (HB), lower is better (LB), and nominal is best (NB) [3]. Hence, S/N ratio is expressed as the mean (signal) to the noise, which is the deviation from the target maximizing S/N ratio would give a minimum deviation and, therefore, the S/N ratio is to be maximized [4].

The machine surface quality normally depends on the machine component reliability in the service application. The performance of a composite material is minimally dependent on the surface condition produced from machining. This research is focused on the parameter settings such as spindle speed, feed rate, and depth of cut effect the delamination factor (F_d). Kenaf fibre composite can be machined through the computer numerical control (CNC) milling operation.

2. METHODOLOGY

For this research study, orthogonal arrays (OA) are used to complete the design of the experiment. The OA L_8 have been selected for the experiment due to its composition of three factors and two levels; and also can be written in the form of L_8 (2^3). Table 1 shows the experimental form of OA L_8 (2^3).

Table 1 Orthogonal array L_8 (2^3) in Experiment form.

| L_8 (2^3) Test | A – Spindle Speed, rpm | B – Feed rate, mm/min | C – Depth of cut, mm |
|-------------------------|---------------------------|--------------------------|-------------------------|
| 1 | 500 | 200 | 1.0 |
| 2 | 500 | 200 | 2.0 |
| 3 | 500 | 1200 | 1.0 |
| 4 | 500 | 1200 | 2.0 |
| 5 | 1000 | 200 | 1.0 |
| 6 | 1000 | 200 | 2.0 |
| 7 | 1000 | 1200 | 1.0 |
| 8 | 1000 | 1200 | 2.0 |

3. RESULTS AND DISCUSSION

From experiment analysis and simulation using Minitab, Figure 1(a) and Figure 1(b) indicate that the main effect plot for S/N ratios for the factor of delamination at F_d 1 (delamination factor of specimen A) and F_d 2 (delamination factor of specimen B). The main effect plot shows the trend of the factor influenced by observing the slope of a line in the graph. The highest slope contributed to a significant impact for the delamination factors. In the graph, the x-axis indicates the value of each process parameter at two levels and the y-axis as the response value. The horizontal line indicates the mean value of the response [5]. The main effects plot are used to determine the optimal design conditions to obtain optimal factors of delamination. According to this main effect plot, the optimal condition for F_d 1 is: spindle speed at level 1 (500 rpm), feed rate at level 1 (200 mm/min), and depth of cut at level 1 (1.0 mm). For F_d 2 the optimal condition is spindle speed and feed rate at level 1 with 500 rpm and 200 mm/min, respectively; as well as depth of cut at level 2 (2.0 mm).

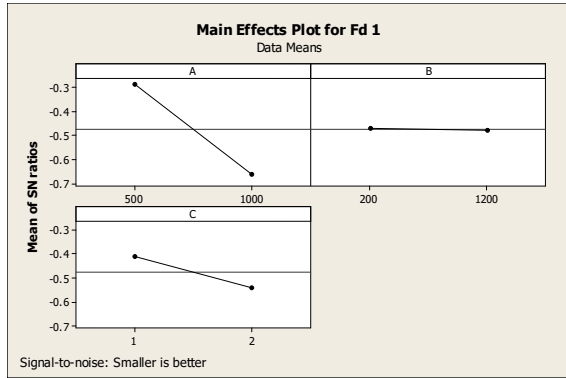


Figure 1 (a) Graph of main effects plot for F_d 1.

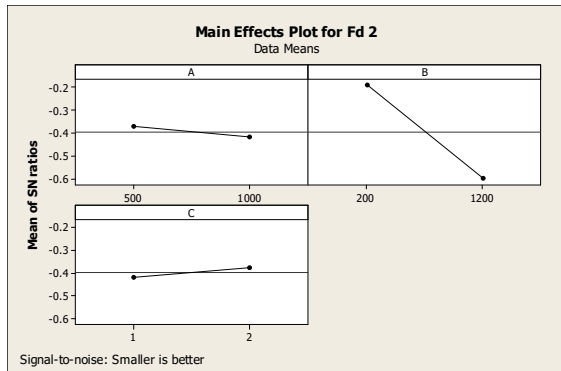


Figure 1 (b) Graph of main effects plot for F_d 2.

B. Uma Mahes Gowd showed that the use of a high cutting speed and low feed rate will favor minimum delamination and lead to better quality of slots. The results obtained for F_d 1 and F_d 2 do not correspond as indicated by B. Uma Mahes Gowd. Other than that, the results from this research study differ from R. Jeyapaul, which stated that the delamination factor (F_d) steadily increases with the increase in feed rate and a decrease in spindle speed. Yamini Kasu indicated the feed rate and

cutting speeds were the largest contributors to delamination with a high cutting speed and low feed rate, which favors minimum delamination of fibre reinforced composites. Further, their results differ from corresponding research because the mixture used for this study is not the same. For example, B. Uma Mahes Gowd indicated that resin polyester is used to prepare the specimen; however, for this study an unsaturated polyester was used to prepare the specimen. Furthermore, these dissimilar results were likely due to the bonding between the polymers or the mixtures do not mix uniformly with some parts of the binder or bond with kenaf fibre.

4. CONCLUSIONS

Based on the results obtained, the feed rate and spindle speed make the greatest contribution to the effects of delamination factor (F_d). Therefore, the use of high spindle speed and low feed rate will lead to minimum delamination factors in milling kenaf fibre reinforced plastic composites. The optimum parameters for delamination factor were spindle speed is 500 rpm, feed rate of 200 mm/min, and depth of cut of 2.0 mm.

5. REFERENCES

- [1] M. Ho, J.-H. Lee, C. Ho, K. Lau, J. Leng, D. Hui, and H. Wang, "Critical factors on manufacturing processes of natural fiber composite," *Compos. Part B*, pp. 3549–3562, 2012.
- [2] A. M. M. Edeerozey, Hazizan M. Akil, A. B. Azhar, and M. I. Z. Ariffin, "Chemical modification of kenaf fiber," *Mater. Lett.*, pp. 2023–2025, 2007.
- [3] S. R. Meshram and N. S. Pohokar, "Optimization of Process Parameters of Gas Metal Arc Welding to Improve Quality of Weld Bead Geometry," *Int. J. Eng. , Bus. Enterp. Appl. (IJEBA)*, pp. 46–52, 2013.
- [4] K. S. Narayana, K. N. S. Suman, and K. A. Vikram, "Optimization of Surface Roughness of Fiber Reinforced Composite Material in Milling Operation using Taguchi Design Method," *Int. J. Mech. Struct.*, vol. 2, no. 1, pp. 31–42, 2011.
- [5] S. R. Das, D. Dhupal, and A. Kumar, "Effect of machining parameters on surface roughness in machining of hardened AISI 4340 steel using coated carbide inserts," vol. 2, no. 4, pp. 445–453, 2013.

Chemical and Physical Properties of Commercial and Bionovolac Phenolic Resin for Electrospinning Process

Siti Noorul Aina Ab Rahim¹, Sarani Zakaria¹, Sharifah Nabihah Syed Jaafar¹, Chin Hua Chia¹ and Rasidi Roslan²

¹) Bioresources and Biorefinery Laboratory, Faculty Science and Technology,
Universiti Kebangsaan Malaysia, 43600 Bangi, Selangor

²) Material Technology, Faculty of Industrial Science & Technology,
Universiti Malaysia Pahang, Lebuhraya Tun Razak, 26300 Gambang, Kuantan, Pahang

*Corresponding author: szakaria@ukm.edu.my

Keywords: Molecular weight, empty fruit bunch, electrospun, viscosity, phenolic, polymer

ABSTRACT – Oil palm empty fruit bunch (EFB) was liquefied with Phenol to EFB ratio of 1:3 to produce Liquefied EFB (LEFB). Then, the LEFB was resinified with formaldehyde at the molar ratio 1:0.5 to form novolac type phenolic resin. The bionovolac resin (BN) and commercial novolac resin (CN) being electrospun at 30 kV high voltage and 15 cm distance between tip and collector and the flow rate was 0.5 mL/hour. The viscosity, solid content and molecular weight of the resin were recorded. The formation of bionovolac phenolic fibre was observed under Scanning Electron Microscope (SEM).

1. INTRODUCTION

Liquefaction is a process where biomass in solid form is converted into a liquid. Nowadays, liquefaction of oil palm empty fruit bunch (EFB) has been done widely. Phenol is used as the liquefaction reagent in the presence of an acid catalyst to degrade the biomass components into a smaller fraction. The liquefied biomass can be used as raw materials for the phenolic resins synthesis. The formation of phenolic resins can be in two types that are resol and novolac; where the ratio of phenol:formaldehyde more than 1 and less than 1 respectively. Both resins have their own advantages depending on the usage.

Fibres made from the liquefied biomass by electrospinning method has been reported elsewhere [1]. Electrospinning is a process that used electrostatic forces to form continuous thin fibres up to nanoscaled fibres [2]. It is a one-step forming of two- or three-dimensional nanofibre network structure. As phenolic resin has a three-dimensional network structure, this electrospinning method is applicable to be used [3]. However, the spinnability of the phenolic resin is difficult to be done because of the low molecular weight. For electrospinning, fiber diameter relies on polymeric solution properties such as solution viscosity, concentration, conductivity and surface tension. Other than that, it also depends on the spinning parameter which are applied voltage, the distance between needle tip and the collector, also the flow rate. The objective of this study is to investigate the different physico-properties of the bionovolac and commercial resin affecting the formation of electrospun fibre.

obtain continuous fibre from bionovolac resin. The fibre morphology is highlighted.

2. METHODOLOGY

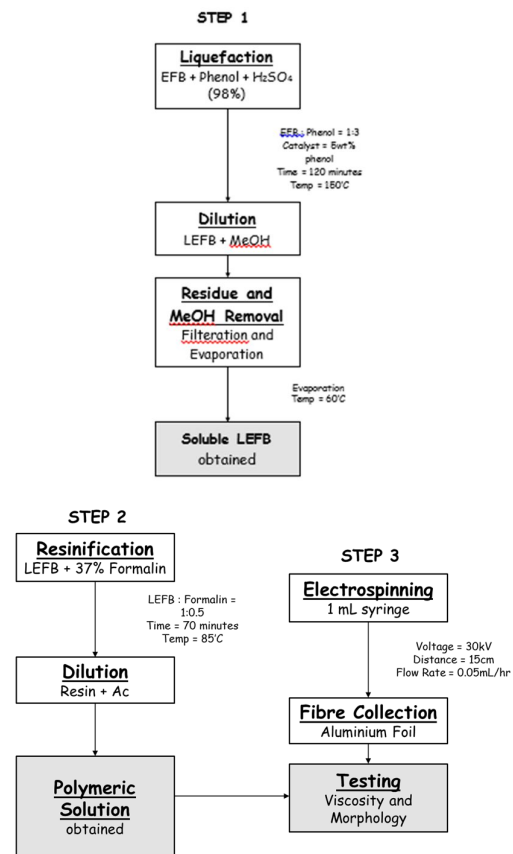


Figure 1: Methodology flow chart

3. RESULTS AND DISCUSSION

Table 1 shows the physical properties of both samples; molecular weight, solid content, and viscosity. Figure 2 shows the functional group present in both commercial and bionovolac resin. The peak at 3340cm⁻¹ was assigned for Commercial Novolac (CN) and 3283cm⁻¹ for Bionovolac (BN). The OH-group presents but with the smaller amount. The area under the graph for these peaks were 19.5 and 101.2 respectively. The C=C stretching at 1609cm⁻¹ (CN) and 1594cm⁻¹ (BN) and C-C-OH asymmetric stretch of

phenolic at 1209cm^{-1} (CN) and 1222cm^{-1} (BN) were detected [4].

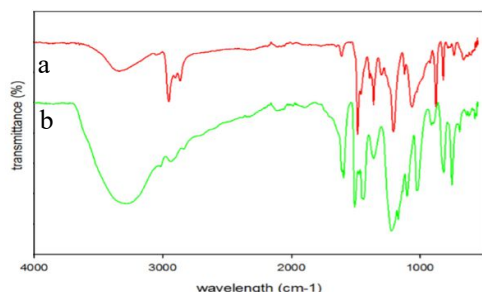


Figure 2: FT-IR spectra a) commercial phenolic resin
b) bionovolac resin

Table 1: Physical properties of commercial and bionovolac resin

| Samples | Molecular Weight (Mw) | Solid Content (%) | Viscosity (Cp) |
|---------|-----------------------|-------------------|----------------|
| CN | 6095 | 54.1 | 2.4 |
| BN | 5483 | 73.4 | 4.8 |

Figure 3 (a) and (b) show the fibre formed were discontinuous for both commercial and bioresin. This is due to the inadequate voltage supplied [5]. In addition, it was also because of low molecular weight of those resins. Normally, the molecular weight of electrospun polymer solution is 13,000 onwards [6]. The electrospun bionovolac resin formed are in beads and beads-on string fibres as shown in Figure 3 (b). This is due to high surface tension and also low viscosity indicating there was resistance for the polymer solution to flow [6,7]. A polymer with low viscosity tends to be electrospay instead of electrospun thus resulting in beads formation. High molecular weight and viscosity will be able to eliminate the beads and form a smooth fibre.

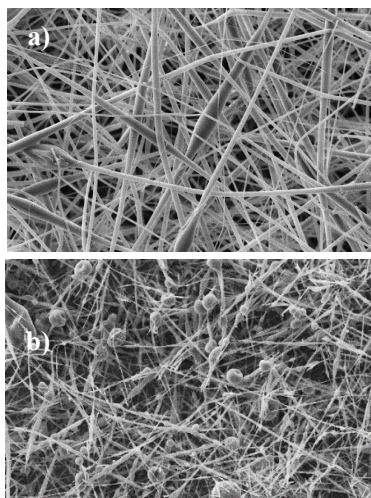


Figure 3: Morphology of a) commercial phenolic resin
b) bionovolac resin

4. CONCLUSION

The study showed that although the chemical structure of both BN and CN were different, their physical properties were almost similar. Thus, modification of the resin itself needs to be done in order to obtain continuous and thin fibre.

5. ACKNOWLEDGEMENTS

The authors thank Universiti Kebangsaan Malaysia for the financial support via the research project grants PRGS/1/2015/SG06/UKM/01/1. The authors are also thankful to the Cell Fuel Institute at UKM and FSTUKM Chemistry Department for providing the testing services.

6. REFERENCES

- [1] Ahn, Y., Lee, S. H., Kim, H. J., Yang, Y., Hong, J. H., Kim, Y. & Kim, H., "Electrospinning of Lignocellulosic Biomass Using Ion in Liquid," *Journal of Carbohydrate Polymers*, vol. 88, pp. 395-398, 2012.
- [2] Imaizumi, S., Matsumoto, H., Suzuki, K., Minagawa, M., Kimura, M. & Tanioka, A., "Phenolic Resin-Based Carbon Thin Fibers Prepared by Electrospinning: Additive Effects of Poly(vinyl butyral) and Electrolytes," *Polymer Journal*, vol. 40, no. 12, pp. 1124-1128, 2009.
- [3] Suzuki, K., Matsumoto, H., Minagawa, M., Kimura, M. & Tanioka, A., "Preparation of Carbon Fibre Fabrics from Phenolic Resin by Electro Spray Deposition," *Polymer Journal*, vol. 39, no. 11, pp. 1128-1134, 2007.
- [4] Poljansek, I. & Krajnc, M., "Characterization of Phenol-Formaldehyde Prepolymer Resins by In Line FT-IR Spectroscopy," *Acta Chim. Slov.*, vol. 52, no. 238-244, 2005.
- [5] Agarwal, S., Burgard, M., Greiner, A. & Wendorff, J., *Electrospinning: A Practical Guide to Nanofibres*, Book of Technology & Engineering, 2016.
- [6] Koski, A., Yim, K. & Shivkumar, S., "Effect of Molecular Weight on Fibrous PVA Produced by Electrospinning," *Materials Letters*, vol. 58, no. 493-497, 2004.
- [7] Fong, H., Chun, I. & Reneker, D. H., "Beaded Nanofibers Formed during Electrospinning," *Polymer*, vol. 40, no. 4585, 1999.

Optimization Processing Parameters on Mechanical Properties of Thermoplastic Natural Rubber (TPNR) blend with Polyaniline (PANI)

Farrah Diyana Zailan¹, Sahrim Ahmad¹, Ruey Shan Chen¹, Dalila Shahdan¹

¹School of Applied Physics,
Faculty of Science and Technology, Universiti Kebangsaan Malaysia
43600 Bangi, Selangor, Malaysia.

*Corresponding e-mail: fadiyana_zailan@yahoo.com

Keywords: Polymer Blend; Liquid Natural Rubber; Natural Rubber; Polyaniline.

ABSTRACT –The fabrication blend of TPNR/PANI was carried out to determine the optimization of processing parameter by the mechanical (tensile, flexural and Izod impact) testing. The TPNR matrix made up of linear low-density polyethylene (LLDPE), natural rubber (NR), and liquid natural rubber (LNR) as a compatibilizer with the composition ratio at 40:50:10. TPNR/PANI (90 wt % /10 wt %) blend was prepared via melt blending method using an internal mixer with various mixing parameter condition. The influence of processing parameters including mixing temperature (°C), mixing speed of rotation (rpm) and mixing processing time (min) on the mechanical properties of the blend was investigated. The results showed that the optimum processing parameter for preparing the TPNR/PANI blend obtained at 130°C, 30 rpm, and 13 min. The morphological test has been done on TPNR and TPNR/PANI blend using SEM characterization. The SEM micrograph confirmed the dispersion of PANI within TPNR matrix.

1. INTRODUCTION

Polymer blends functionally produce the new polymeric materials which have better properties compare to neat polymer materials. In recent years, the thermoplastic natural rubber (TPNR) which is a blending of natural rubber and polyolefin has been developed by some researchers [1-2]. For examples, NR/LLDPE/LNR and NR/polypropylene (PP)/LNR in the ratio 50:40:10 [4] were fabricated in order to study the compatibility of the blends with the addition of LNR as compatibilizer into blend systems. Commonly, TPNR prepared via melt blending method. In addition, TPNR was used as a matrix in various composites systems, such as the addition of nickel zinc ferrite nanoparticles in TPNR (PP/NR/LNR in the ratio of 70:20:10) [3].

PANI is one of infusible conductive polymer in a blend of the composite system which indicates to have better dispersion in a thermoplastic matrix polymer. It also contributed to the decrease of the particles surface tension, form aggregates and cause it easy to mix in the thermoplastic polymer. The utilization of PANI as a matrix in a blend of NR/PANI-dodecylbenzene sulfonic acid (DBSA) [5], LLDPE/nanorod-PANI [6] showed that PANI improved the mechanical and electrical conductivity properties of blends. However, a homogenous mixture of a blend containing PANI is one of critical factor to determine the enhancement of blend performance [5]. In order to produce well-dispersed

PANI in TPNR, the aim of this research was to investigate the influence of processing parameter on mechanical properties of TPNR/PANI blend and to determine the optimum processing parameter for the fabrication of TPNR/PANI blend.

2. METHODOLOGY

Indirect mixing technique (IDT) was applied in order to prepare composites which involved a pre-mixing of PANI particles with LNR by manually stirred using glass rod, before it was melt blended with LLDPE and NR. The TPNR of NR/LLDPE/LNR (50:40:10) with 10 wt% PANI particle were prepared by using an internal mixer (Haake Rheomix 600P) with the various condition of processing parameters such as mixing temperature (120-150°C), rotor speed (20-50 rpm) and mixing time (13-15min) of mixing. Note that for mixing temperature investigation, speed of rotation (50 rpm) and mixing time (13 min) are kept constant; for rotor speed investigation, mixing temperature (130°C) and mixing time (13 min) are kept constant and lastly for mixing time investigation, mixing temperature (130°C) and speed of rotation (30 rpm) are kept constant. NR was first placed into the mixer and allowed to melt for about 3 min, the pre-mixture of LNR and PANI was added then LLDPE resins were added after 5 min. The whole mixing process was completed at 13 min. After blending process, the samples were prepared by compression moulding via hot press under pressure 6.9 MPa at 130°C.

3. RESULT AND DISCUSSION

Figure 1 shows the influence of processing parameters on tensile strength, which the highest tensile strength TPNR/PANI achieved at mixing temperature of 130°C at 1.68 MPa. The tensile properties dropped gradually when the applied mixing temperature higher than 130°C, due to the oxidation of NR and the aging of the blend during mixing at a higher temperature which led to degradation of the blend's strength [7]. While 30 rpm showed the highest tensile strength is at 1.62 MPa. In which, the rotor speed of the blended mixture can be related to the rubbery properties of TPNR and PANI particles (nanosize) which influence the dissolution rate. This showed the rotation speed also affected the matrix dispersion with the presence of PANI and LNR lead to better interaction between amorphous NR and LLDPE [8]. For the mixing time parameter, blend mixed at 13 min possessed the highest

tensile strength at 1.64 MPa. The longer time of mixing (more than 13 min), is not suitable because the longer the time of mixing the more mixture exposed to the heat, thus may lead to the oxidation NR which will cut off the polymer chain [9].

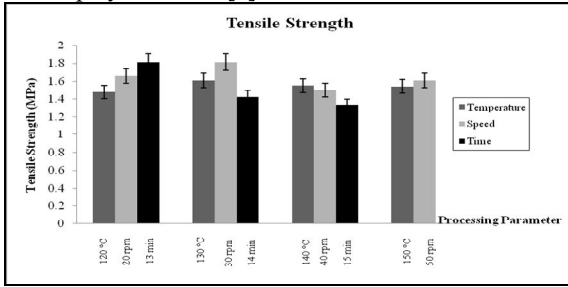


Figure 1 Effect of processing parameter on tensile properties

Figure 2 and 3 show the effect of processing parameter on impact and bending strength respectively. Both results exhibited the similar trend as tensile strength in Figure 1. From the mechanical results, it can be concluded that the optimum parameter of TPNR/PANI is at 130°C, 30 rpm, 13 min that was tensile strength of 1.81 MPa, impact strength of 5.93 kJm⁻² and bending strength of 1.65 MPa. Generally, the interfacial interaction of more than two polymer components in blend is one of the important factors to determine the optimum mechanical properties of blends.

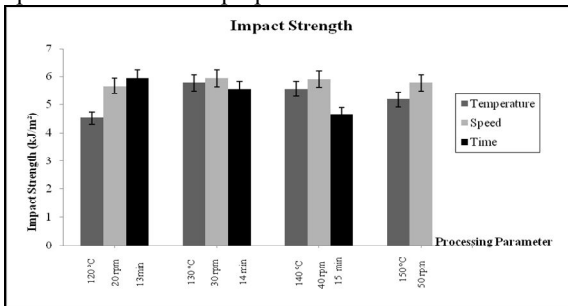


Figure 2 Effect of processing parameter on impact properties

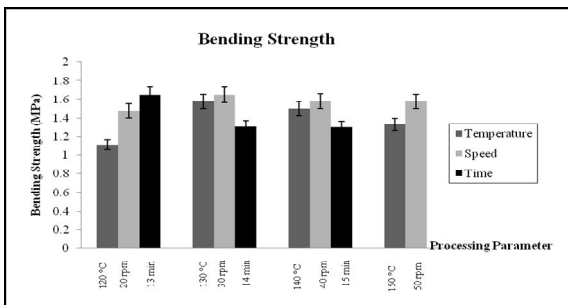


Figure 3 Effect of processing parameter on flexural properties

The SEM micrographs in Figure 4(a) and (b) show the surface of the fractured sample after tensile testing. Figure 4(a) shows a clear, with holes and homogenous surface which indicated a good dispersion of rubber particles in LLDPE matrix [7]. While Figure 4(b) shows the micrograph of TPNR/PANI had no holes which filled by PANI particle that contributed to good dispersion in the matrix phase as supported in better

mechanical properties [1-2].

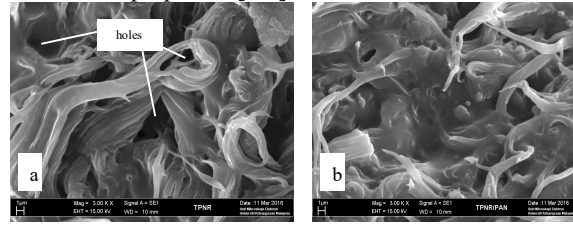


Figure 4 SEM micrograph of (a) TPNR blend (b) TPNR/PANI blend.

4. CONCLUSIONS

The mechanical results showed that the optimum processing parameter for fabrication of TPNR/PANI was found at 130°C, 30 rpm and 13 min. Besides, the optimum processing parameter also showed good mechanical properties in tensile strength, flexibility and toughness of composites, while it was proven that by SEM micrograph which showed a good dispersion of PANI within TPNR matrix, and thus led to good mechanical properties.

5. REFERENCES

- [1] Dahlan H.M., Khairul Zaman M.D., Ibrahim A., "The Morphology and Thermal Properties (LNR)-Compatibilized 60/40 NR/LLDPE blends," *Polymer Testing*, vol. 21, pp. 905-911, 2002.
- [2] Azlina H.N., Norita H., Ahmad S., Rashid R., Anuar H., Bonnia N.N., Surip S.N., "Physical and Mechanical Properties of TPNR Nanocomposites," *Advanced Materials Research*, vol. 576, pp. 394-397, 2012.
- [3] Tarawneh M.A., Ahmad S., S.Y. Yahya, Rashid R., Eh Noum S.Y. "Thermal Behavior of MWNT-reinforced TPNR," *Journal of Reinforced Plastic and Composites*, pp. 1-6, 2011.
- [4] Ibrahim A., Sahrim A., Che Som S., "Blending of Natural Rubber with Linear Low-Density Polyethylene," *Journal of Applied Polymer Science*, vol. 58, pp. 1125-1133, 1995.
- [5] Jonas da Silva M., Sanches A.O., Malmonge L.F. Malmonge J.A., "Electrical, Mechanical and Thermal Analysis of NR-PANI-DBSA composite," *Materials Research*, vol. 17, no. 1, 59-63, 2014.
- [6] Ashveen V.N., Sudip R., J. Trivas-Sejdic, Paul A.K., "Characterization of Antioxidant LDPE/PANI blends via Extrusion" *Materials Chemistry and Physics*, vol. 135, pp. 903-911, 2012.
- [7] Mohd Bijarimi, Sahrim A., Rozaidi R., "Mechanical, Thermal and Morphological Properties of PLA/PP Melt Blends," *International Conference of Agriculture, Chemical and Environmental Sciences*, pp. 115-117, 2012.
- [8] Ibrahim A. & Dahlan M., "Thermoplastic Natural Rubber Blends," *Polymer Science*, vol. 23, pp. 665-706, 1998.
- [9] Kazimi M.R., Tahir S., Shima J., Faizal C.K.M., "Characterization of Fuctionalized LDPE/PANI Nanofiber Composite," *Journal of Medical and Bioengineering*, vol. 3, pp. 307-310, 2014.

Application of Rapid Prototyping in redesigning the roller clamp intravenous tubing in medical application

W A Y Yusoff¹, M H Shazwan², A H Mohamed³, Saufi Awang⁴

^{1,2,3}Faculty of Engineering, International Islamic University Malaysia (IIUM)

⁴Faculty of Medicine, International Islamic University Malaysia (IIUM)

*Corresponding e-mail: yusmawiza@iium.edu.my

Keywords: Roller clamp, intravenous tubing, rapid prototyping, medical engineering

ABSTRACT –The purpose of this research is to improve and to enhance a medical instrument by applying Fused Deposition Modeling (FDM). A medical instrument selected for this project is roller clamp which is one of the parts attached to Intravenous (I.V) Tubing used in Intravenous therapy. A machine that works under FDM principle will be used to produce the final prototype. Before proceeding with the process to manufacture the final product, the critical path that must be considered is the improvement of the final product compared to existing product as well as the reference concept. Some survey has been done in order to collect required information to improve existing design of roller clamp. The data collected then is analyzed using graphical representation such as a graph. Besides, to ensure the final product of roller clamp is completely fulfill the criteria demanded by users, the data collected from the survey will be analyzed using PDS (Product Design Specifications) tool.

1. INTRODUCTION

The medical sector is one of the best platforms for rapid prototyping to develop. One of the popular treatments in the medical sector is intravenous (I.V.) therapy. The word ‘intravenous’ simply means ‘within a vein’. I.V. therapy is the infusion of liquid substances into vein [1]. The term vein is taken from Latin phrase which is ‘vena’ which means blood vessels. Blood vessels are considered as the route for I.V. therapy. Indications for I.V. therapy include achieving or maintaining fluid and electrolyte balance, replacing or supplementing needed blood components, providing nutrients, and administering medications [2]. Some of the purposes of I.V. therapy are to transfuse blood products and to administer fluids and medications with the ability to rapidly/accurately change blood concentration levels by either continuous, intermittent or IV pushes method [3].

The possibilities for medication errors to occur still are very high. Back to intravenous therapy, the device used is called Intravenous (I.V) Tubing. Intravenous (I.V) Tubing is a device with a combination of several parts such as cannula, butterfly, stopper, needle, tube, roller clamp and so on [4]. Among these parts, roller clamp is one of the parts that have led to many problems as well as medication errors. Roller clamp has an important and critical function for the intravenous therapy which is to control the flow rate of the medication supplied [5]. The existing roller clamp still has some weaknesses at the design and need to be improved to avoid medication errors and increase the effectiveness of the treatment. This research is to re-design the roller clamp in the Intravenous (I.V) Tubing to the optimum design by considering several

factors such are material, dimension, cost, and mechanism.

2. METHODOLOGY

The manual survey form was distributed at the Hospital Kuala Lumpur and Tengku Ampuan Afzan Hospital, Kuantan, while online survey form was distributed using the email and social network. The questionnaire contains 13 questions as well as criteria and has been rated by respondents taken among doctors, nurses and medical students. The data from the questionnaire is very important and will be used to construct Product Design Specification (PDS) on the next step. Concept selection is the process of evaluating concepts with respect to the customer needs and other criteria, comparing the relative strengths and weaknesses of the concepts, and selecting one or more concepts for further investigation. Several design concepts are generated using CATIA V5 software to be evaluated by the users for concept selection. Selection of design concept was done in two phases which are concept screening and concept scoring. In the selection of the design concept for further development, a prototype of roller clamp was fabricated using Fused Deposition Modeling (FDM).

3. RESULTS AND DISCUSSION

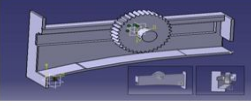
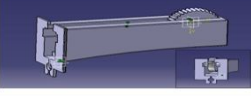
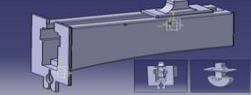
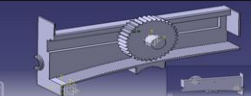
As shown in table 1 is a table for the result of the questionnaire. The result of selection of criteria is from the total 53 respondents, among medical students, doctors, and nurses. There are 13 criteria in the table and each of the criteria is given a score between 1 (very poor) to 5 (very good) by each respondent. To analyze the data in the table, a graphical method is used which involving the creation of graph. As shown in table 2, from the previous analysis on the data gathered from questionnaire and PDS, the research procedure is preceded and 5 concept designs have been successfully created. Basically, the design of roller clamp consists of two parts, a roller and a body. These parts will be combined to form roller clamp and below is the table of 5 concept designs that have been successfully produced. Each of the design has its own special features and differences. These designs produced using CATIA V5 software and the differences between the designs can be observed in term of the shape of a roller. From the net score for design concept A and B are same, these two designs will be combined. So design concepts C, E, and AB (combination of A and B) will be taken to the Concept Scoring Phase for further comparison. Design D is rejected because of the least score and the lowest rank. After implementing 2 stages of selection concept which are concept screening and concept scoring,

design E has the highest final score compare to design AB and C and ranked in the first place. Both of concept screening and concept scoring are rated by medical officers and surgeons of Hospital Kuala Lumpur (HKL). As the result from the procedure, concept design E has been successfully chosen as the best design and will be developed.

Table 1 Selection of Criteria of Roller Clamp

| Criteria | Number of respondents for each score per criteria | | | | |
|--------------------------------------|---|----|----|----|----|
| | 1 | 2 | 3 | 4 | 5 |
| 1 Light in weight | 1 | 3 | 10 | 33 | 6 |
| 2 Accurate Liquid Flow | 0 | 1 | 4 | 5 | 43 |
| 3 Compatibility with tube | 0 | 0 | 6 | 14 | 33 |
| 4 Easy to push/handle | 0 | 1 | 2 | 21 | 29 |
| 5 Low cost material used | 1 | 1 | 21 | 18 | 12 |
| 6 High degree of complexity of parts | 4 | 11 | 14 | 18 | 6 |
| 7 Large number of assemblies | 5 | 10 | 15 | 19 | 4 |
| 8 Smooth Surface | 1 | 4 | 19 | 22 | 7 |
| 9 Rough Surface | 6 | 10 | 27 | 7 | 3 |
| 10 Flexible | 0 | 3 | 10 | 25 | 15 |
| 11 Small Size | 0 | 2 | 25 | 17 | 9 |
| 12 Large Size | 3 | 16 | 27 | 3 | 4 |
| 13 Attractive in appearance | 7 | 9 | 28 | 2 | 7 |

Table 2 Five concept designs of roller clamps

| No. | Design | Remarks |
|-----|---|--|
| A |  | Non-linear slope of bottom part of roller clamp. Different from current design which use linear slope of the bottom part. More intuitive to use. Flow rate can be control easier. |
| B |  | New improved part to be used as tube holder. |
| C |  | Small hole designed at the left side that functioning as tube holder. The upper surface of bottom part is made rougher. More grip to the tube. |
| D |  | The roller of previous design is replaced with a new design as shown in the image. |
| E |  | The hole at the left side is made embossed to increase the rigidity of tube. At the bottom part: Finger rest part is designed at the bottom to increase gripping force while pushing the roller. |

The results of the survey suggested that to increase the accuracy of flow rate, the bottom part as shown in the first row of the table above need to be modified. The reference concept uses the linear shape of the bottom part. As shown in figure 1, after several steps, the result of the process has been successfully achieved and design E has been chosen as the best design. Design E is then fabricated using FDM machine through the application of rapid prototyping technology.

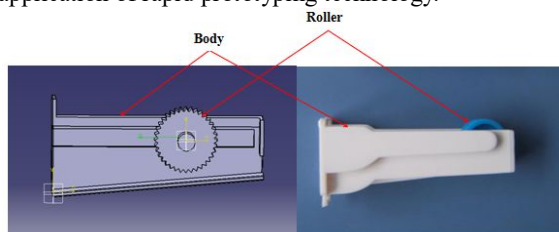


Figure 1 the best roller clamp design selected (Design E)

4. CONCLUSIONS

The research has successfully done and enough information regarding the existing product is collected. The information has been used in the process to select the best design and as the result, concept design E has been selected among five generated designs. The prototype of the design has been successfully fabricated and proven to have better function, quality and criteria compared to the reference concept as well as the existing roller clamp. Overall, the research has successfully achieved the objectives.

5 ACKNOWLEDGEMENT

We would like to thank the medical staff of the Tuanku Afzan Hospital, Kuantan and General Hospital, Kuala Lumpur for their cooperation as research partners and at the same time for guiding and assisting us in doing this project. This research project is sponsored by Research Acculturation Grant Scheme No: RAGS 12-050-0050.

6 REFERENCES

- [1] Zimmerman JJ, Strauss RH, "History and current application of intravenous therapy in children," *Pediatr Emerg Care.*, vol. 5, no. 2, pp.120-127, 1989.
- [2] Jelena Milovanovi and Miroslav Trajanović, "Medical Application of Rapid Prototyping," *Mechanical Engineering*, vol. 5, no.1, pp. 79 – 85, 2007.
- [3] L.C. Hieu, N. Zlatov, J. Vander Sloten, E. Bohez, L. Khanh, P.H. Binh, P. Oris, Y. Toshev, Medical rapid prototyping applications and methods, *Assembly Automation*, vol. 25, no. 4, 2005.
- [4] Rich Nass, "Medical Device Prototyping for Clinical Trials," *Medical Device and Diagnostic Industry Journal*, vol. 33, no. 2, 2011.
- [5] Chung P, Heller JA, Etemadi M, Ottoson PE, Liu JA, Rand L, Roy S., "Rapid and low-cost prototyping of medical devices using 3D printer," *Journal of Visualized Experiments*, vol. 88, 2015.

Moldability of Natural Filler Reinforced Polymer Composite For Automotive Components Through Numerical Simulation

Zaliha Wahid ^{1*}, Abu Bakar Sulong¹, Baharuddin Mohd Zanggi²

¹⁾ Department of Mechanical and Material Engineering,
 Faculty of Engineering and Built Environment, Universiti Kebangsaan Malaysia,
 43600 Bangi, Selangor, Malaysia.

²⁾ Politeknik Port Dickson,
 KM 14, Jalan Pantai,
 71050, Si Rusa, Negeri Sembilan, Malaysia

*Corresponding e-mail: zaliha@eng.ukm.my

Keywords: Moldability; Taguchi method; simulation.

ABSTRACT – Nowadays, as we move to green technology, the use of natural ingredients as materials in automotive parts became very demanding. Unfortunately, composite making involving new ingredient always have some moldability issues. Therefore, this study aims to determine optimized parameters for injection molding process and to determine the significant parameters influencing some qualities of injection molding process by using Taguchi method. The process was simulated using MPI software first for studying the feedstocks flow in the mold. Analysis by ANOVA and Taguchi method found that the significant parameters influencing the process are the flow rate and temperature of the mold. The study is important as it may save the time and cost as trial and errors attempt to determine suitable parameters are no longer needed.

1. INTRODUCTION

Proton Waja CamPro engine cover is fabricated through injection molding process and comprises of 60% Wood Plastic Composite (WPC) as filler and 40% of polypropylene (PP) binder. The Polymer Matrix Composites is designed so that the mechanical loads to which the structure is subjected in service are supported by the reinforcement which provides high strength and stiffness. Despite weaknesses in the mechanical properties, studies have been done on natural fibers as reinforcement to maximize its full potential as an alternative to synthetic fibers [1]. This has led to the prediction that in the near future plastics and polymer composites will comprise about 15% of the total weight of the car [2].

To save cost and time, modeling and simulation would be desirable in process optimization as there is no necessity to conduct the real process in order to predict the behavior of the process. Moldflow Plastics Insight (MPI) has been developed by Moldflow Corporation to assist designers in the plastics industry to reduce product development time and rework, and anticipate any problems associated with products processability and provide options for a variety of processing parameters and materials for plastic and composite products [3].

Taguchi techniques were widely used in engineering analysis in the system, parameter and tolerance design [4]. The most important stage in Taguchi Method is the selection of control factors so

that it would be possible to identify non-significant variables at the earliest opportunity [5].

2. METHODOLOGY

The orthogonal array L₉ in Taguchi method which can accommodate three levels setting parameters was used as shown in Table 1. Analysis of variance (ANOVA) is used to find out significant parameters acting on specific desired quality effects. The flow chart is shown in Figure 1 for the simulation methodology.

Table 1 Three levels cutting parameters

| Level | Injection Temperature (°C) | Mold Temperature (°C) | Flow Rate (cm ³ /s) | Injection Pressure (MPa) |
|-------|----------------------------|-----------------------|--------------------------------|--------------------------|
| | A | B | C | D |
| 0 | 250 | 40 | 50 | 300 |
| 1 | 260 | 50 | 60 | 325 |
| 2 | 270 | 60 | 70 | 350 |

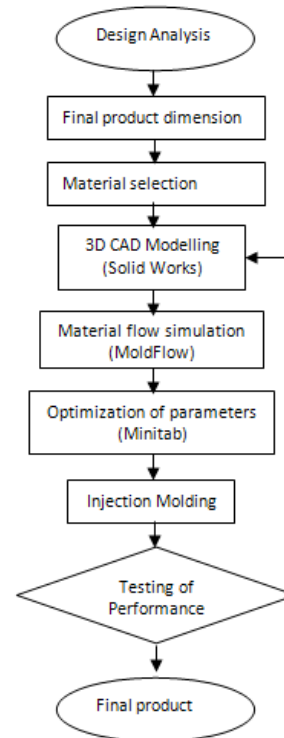


Figure 1 Study flow chart

3. RESULTS AND DISCUSSION

The simulation results for each parameter are analyzed and then taken for analysis using Taguchi method and ANOVA. In this study, the chosen desired characteristics are filling time, average speed, sink marks, shear rate and shear rate. Figure 2 shows a MoldFlow simulation result for filling time. The flow can be represented by color-coded contours from blue to red which red contours show the beginning of the injection, while the blue shows the last place to be filled. From the figure, we know that the filling time is 22.84s. If the material has not entered any part of the product (short shots), then the affected parts must be present with transparent color [3]. ANOVA analysis results are simplified in Table 2. For example, to achieve the lowest filling time, the optimized parameters to be used is the combination of mold temperature at 40°C, injection temperature at 250°C, 70 cm³/s and injection pressure of 300MPa.

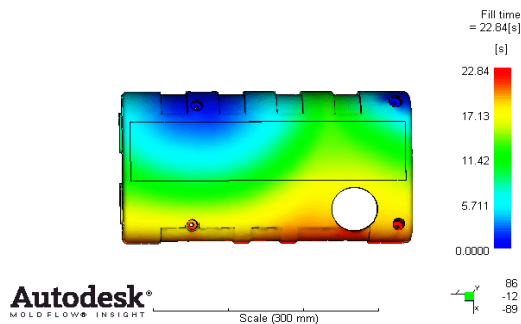


Figure 2 Filling time in MoldFlow

| Desired Quality | Optimized parameters |
|-----------------------|---|
| Filling Time | A 250°C, B 40°C, C 70cm ³ /s, D 300MPa |
| Average Velocity | A 250°C, B 40°C, C 70cm ³ /s, D 325MPa |
| Volumetric Shrinkage | A 250°C, B 60°C, C 70cm ³ /s, D 325MPa |
| Sink Marks Percentage | A 250°C, B 60°C, C 70cm ³ /s, D 300MPa |
| Shear Stress | A 270°C, B 60°C, C 50cm ³ /s, D 300MPa |

Table 3 ANOVA analysis for each desired set quality

4. CONCLUSIONS

Through Taguchi method and ANOVA analysis, it was found that significant parameters influencing the injection molding of the CamPro Proton Waja engine cover are flow rate and temperature of the mold then followed by injection temperature and injection pressure. Therefore, the optimization of the process through experimental design methods have been successfully identified.

5. REFERENCES

- [1] Zampaloni, M., Pourboghraat F., Yankovich S.A., Rodgers B.N., Moore J. Drzal L.T., Mohanty A.K. and Misra M., “Kenaf natural fiber reinforced polypropylene composites: A discussion on manufacturing problems and solutions,” *Composites Part A*, vol. 38, no. 6, pp. 1569–1580. 2007.
- [2] Bismarck, A., Mishra, S., Lampke, T., “Plantfibers as reinforcement for green composites. In: Mohanty,” *Natural fibers, biopolymers, and biocomposites*, Boca Raton, Crc Press-Taylor & Francis Group, 2005.
- [3] Imihezri, S.S.S., Sapuan, S.M., Sulaiman, S., Hamdan, M.M., Zainuddin, E.S., Osman, M.R., “Mouldflow and component design analysis of polymeric based composite automotive clutch pedals,” *J Mater Proc Technol*, vol. 71, pp. 358–65, 2006.
- [4] Pease, G. S., “Taguchi Methods: A Hands-on Approach to Quality Engineering,” Addison Wesley, New York, 1993.
- [5] Ghani, J. A., Choudhury, I. A. and Hassan, H. H., “Application of Taguchi Method in the Optimization of End Milling Parameters,” *Journal of Materials Processing Technology*, vol. 145, pp. 84–92, 2004.

FINITE ELEMENT MODELLING OF ROTARY DRYER MACHINE WITH MOISTURE FIBER CONTENT

SRI YULIS BT M. AMIN^{1a}, MUHAMMAD AMIR HAKIM BIN ABD WAHAB^{1b} & MOHD HALIM IRWAN IBRAHIM^{1c}

Faculty of Mechanical & Manufacturing Engineering
Universiti Tun Hussein Onn Malaysia
86400 Parit Raja, Batu Pahat Johore

Corresponding e-mail: yulis@uthm.edu.my^a

Keywords: Rotary Dryer Machine, Finite element analysis, stress-strain analysis, thermal analysis

ABSTRACT - Finite element method (FEM) analysis was conducted to the rotary dryer machine for the SMD BIOMASS Sdn. Bhd. The use of this rotary dryer machine is to dry the moisture fiber content. This study was carried out to determine the stress and strain analysis and thermal stress analysis of rotary dryer machine. In this paper, the 18m length and 2m diameter of the machine is designed by using SOLIDWORK 2015 software. Then, the model is analyzed by using ANSYS WORKBENCH 16.0 to study the stress-strain behavior of rotary dryer machine due to the maximum load of 2.8 tonnes per hour. The maximum temperature is 120°C of hot gasses. Then, the results are analyzed according to the standard of ASME rules (Asme Boiler and Pressure Vessel Code VIII- Alternative Rules. The American Society of Mechanical Engineers, 2004). It can be concluded that the behavior of the material is in the elastic region as the stress is lower than the tensile yield strength. The fatigue life of the rotary dryer machine is 870 000 number of cycle.

1.0 INTRODUCTION

Rotary dryers are used in chemical, food, and tobacco industrial process as an important equipment, which affects the quality of materials under different operation conditions and it also used to perform heating, moisture removing and mixing [1]. It becomes the common machine in Malaysia to produce agriculture products. However, rotary drying is a very complicated process that implies not only thermal drying but also the movement of particles within the dryer [2].

In the previous study, the finite element method (FEM) is applied to the nonlinear analysis of a cement rotary kiln for the Rais Hamidou factory in Algeria. The nonlinear analysis that included stress and ovalization analysis and dynamic analysis that included of fatigue test have been conducted by finite element method (FEM). The FEM analysis of the rotary kiln with the maximum length of 67.5 meters and a maximum diameter of 5.2 meters is performed for the different operating and live loads at different positions of the rotary kiln. Then, the stress and displacement components are evaluated according to the standard of ASME rules (Asme Boiler and Pressure Vessel Code VIII- Alternative Rules. The American Society of Mechanical Engineers, 2004) [3].

In this research, FEM modeling is applied to the rotary dryer in order to study the stress-strain behavior, and estimating the fatigue life due to thermal stress.

2.0 METHODOLOGY

2.1 Model Development of Rotary Dryer Machine

The structure of the cylinder of the rotary dryer is divided into 9 sections. The inclination of this machine is about 10.6% and the total weight of 36.11 tonnes. The cylinder structure model from SOLIDWORK is shown in Figure 1.

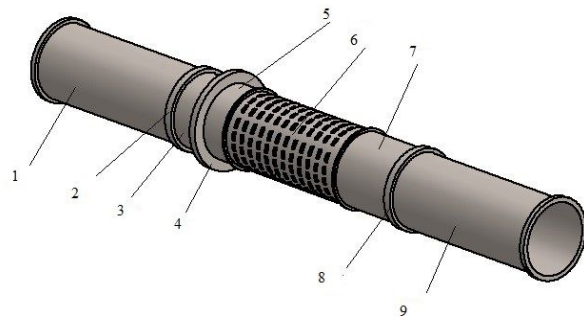


Figure 1: Full model of rotary dryer machine.

The rotary dryer machine is meshed by using tetrahedral element shapes. The cylinder has 6 Degree of Freedom (DOF) that along the X, Y, Z direction, and X, Y, Z axis of rotation. The total numbers of nodes are 120016 and the elements are 48073. Then, all the constraints were added into the drawing after the meshing. For the cylindrical support, it has to be fixed in radial and free in axial and tangential as to be in frictional support [7]. Figure 2 shows the meshed model of the rotary dryer.

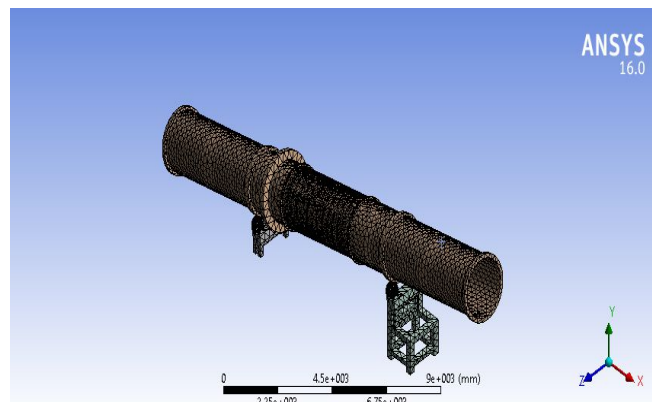


Figure 2: Meshed model of rotary dryer machine

2.2 Properties Evaluation According to ASME Standard

Based on the result of the stress-strain analysis, it will be evaluated based on the ASME rules (Asme Boiler and Pressure Vessel Code VIII. Division 2- Alternative Rules). The greatest main stresses that corresponding to the maximum of foregoing S_{ij} [4]

$$S_{ij} < 3S_m \quad (3.5)$$

where S_m is the stress limit of the rotary dryer machine.

After that, it is possible to find the cycle as shown in Figure 3. Thus, the fatigue life can be found by applying the cycle with the rotary dryer velocity and the time of operation in a year.

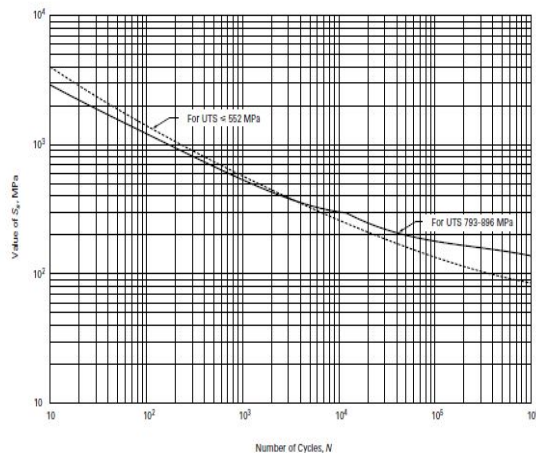


Figure 3: Design fatigue curve for carbon low alloy [4]

3.0 RESULT AND DISCUSSION

3.1 FEM Stress Strain Analysis Result

From the stress and strain result from the simulation of the full body of rotary dryer, the graph of stress against strain is plotted to get the characteristic of the material of rotary dryer machine.

The value of stress increase as the strain increase and the maximum value of the stress is 112.29 MPa and the maximum value of the equivalent strain is 5.8865E-04. The maximum value of stress shows that it does not exceed the property's value tensile yield strength of the material that is 460 MPa. Thus, it can be concluded that the characteristic of the material is in elastic behavior.

3.2 Fatigue Test Result

From the ASME standard, it shows that the number of cycle gain from the stress amplitude is 870 000 cycles. The rotary dryer machine has a velocity of 2 cycles per minute and it is assumed that the factory operation is 300 day per year. The number of cycle of the rotary dryer machine is 1 year after calculated from fatigue life.

3.3 Thermal Stress Analysis Result

According to the result of the simulation, it shows that the effect of thermal stress on the maximum stress happened

at the y-axis that the value is 554.62 MPa. The maximum deformation also located at the y-axis of the rotary dryer machine that value is 1.9181mm.

4.0 CONCLUSION

It shows that the maximum value of equivalent stress is on the 2nd and 8th section which at the rotary dryer tyre section that the value is 112.29 MPa. Then, the maximum total strain is on the 2nd and 8th section which at the rotary dryer tyre section that the value is 5.886E-04. It can be concluded that the behavior of the material is in elastic region as the stress is lower than the tensile yield strength. that is 112.29 MPa does not exceed 460 MPa of tensile yield strength. The value of allowable stress, S_m obtained 195 MPa according to the stress limit in ASME Section II. The fatigue life of the rotary dryer machine is 870 000 number of cycle.

Based on the thermal stress analysis, maximum stress detected at the y-axis that the value is 554.62 MPa. The maximum deformation also located at the y-axis of the rotary dryer machine that the value is 1.9181mm. The value of stress is lower than then stress limit that gains from stress analysis 554.62 MPa. $< 3(112.29)$.

REFERENCES

- [1] Gu, C., Zhang, X., Li, B., & Yuan, Z., "Study on heat and mass transfer of flexible filamentous particles in a rotary dryer," *Powder Technology*, vol. 267, pp. 234-239, 2014.
- [2] Iguaz, a., Esnoz, a., Martínez, G., López, a., & Virseda, P., "Mathematical modelling and simulation for the drying process of vegetable wholesale by products in a rotary dryer," *Journal of Food Engineering*, vol. 59, no. 23, pp. 151-160, 2003.
- [3] Coz, J. J., & Mazã, F. R., "Design and finite element analysis of a wet cycle cement rotary kiln," *Finite Elements in Analysis and Design*, vol. 39, pp. 17-42, 2002.
- [4] Moaveni, S., "Finite element analysis—theory and application with ANSYS." *Minerals Engineering*, 1991, doi:10.1016/S0892-6875(99)90030-4.
- [5] Ansys Help and Documentation, SAS, IP, Inc., 1992 2000. Agreement Number #104834
- [6] Asme Boiler and Pressure Vessel Code VIII, Division 2—Alternative Rules, Appendix 5, "Design based on fatigue analysis", 2004.
- [7] Capitaine, S. Le, & Makos, G., "Co-Current Vs .Counter Current Drying. Retrieved" on 22 November 2015, from <http://feeco.com/co-current-vs-counter-current-drying/>

Morphology, Chemical and Mechanical Properties of Kenaf and Oil Palm Empty Fruit Bunch Cellulose

Khairunnisa Waznah Binti Baharin¹, Sarani Zakaria¹, Noraini Talib²

¹Bioresources and Biorefinery, School of Applied Physics, Universiti Kebangsaan Malaysia, 43600 Bangi, Selangor, Malaysia.

²Plant Anatomy, Faculty of Science & Technology, Universiti Kebangsaan Malaysia, 43600 Bangi, Selangor, Malaysia.

*Corresponding e-mail: szakaria@edu.ukm.my

Keywords: Microscopic image; Lumen size; Fiber structure; Bleaching; Zero span.

ABSTRACT – Fiber and pulp from Kenaf and empty fruit bunch (EFB) of oil palm plant were studied and compared. High value-added product made from a renewable material such as lignocellulose has been quite popular and highly on demand recently. The structure of both fibers was viewed and studied under high power microscope. The surface topology and the cross section of the fibers then were further studied by using Field Emission Electron Scanning Microscope (FESEM). The zero span tensile strength of the fibers was also calculated. The chemical constituents of the fiber were estimated according to TAPPI method and compared with previous studies. From the FESEM and microscopic analysis, the structure of OPEFB pulp shows more rigid lumen structure compared to Kenaf pulp. However, the zero spans tensile strength of Kenaf pulp is higher than OPEFB pulp.

1. INTRODUCTION

The biomass wastes from industry such as palm oil plantation as well as Kenaf plantation has the potential to be turned from lignocellulose material to a high value added a product such as phenol [1]. This is a way to reduce the dependence or to substitute petroleum-based chemicals as oil price keep fluctuating and less available.

Palm oil plant (*Elaeis guineensis sp.*) originated from West Africa and is a type of tropical plant. The fruit can be classified into three different types referring to its shell's thickness which is *dura* (thick shell), *tenera* (thin shell) and *pisifera* (without shell). They grow on fertile soil with high humidity and suitable to be planted in tropical climate countries such as Malaysia and Indonesia [2]. Empty fruit bunch (EFB) is obtained after the fresh fruit bunch is pressed in order to extract the crude palm oil (CPO). Generally, palm oil plant waste is used as natural fertilizer or boiler fuel. Kenaf (*Hibiscus cannabinus sp.*) is an annual non-wood plant of Malvaceae family which originated in central Africa. They grow best in warm and wet condition. Based on previous work, fiber morphology of kenaf bast fibers was long and slender, while the core fibers were much shorter and wider [3].

The conducting cells in the xylem which is tracheids and vessel elements enable xylem to transport large quantities of water with great efficiency. Tracheids are elongate and hollow dead cell which contain

numerous pits in the region where the secondary wall is absent but primary wall remains. The shape and pattern of wall pitting vary with species and organ type. Tracheids are present in all vascular plant.

Bleaching was done on the OPEFB AND Kenaf fiber in order to yield cellulose. The chemical used in the bleaching process such as 1.7% sodium chlorite and 4% to 6% sodium hydroxide in certain temperature and reaction time could help remove hemicellulose and lignin in plant fiber [3].

2. METHODOLOGY

Raw Kenaf core fiber was obtained from Malaysian Agricultural Research and Development Institute (MARDI) whereas the oil palm empty fruit bunch fiber were obtained from Eko Pulp & Paper Sdn. Bhd. 35 g of the oven dried disintegrated pulp was bleached through D-E-E-D treatment series where D and E involved chemical treatment of as 1.7% sodium chlorite and 4% to 6% sodium hydroxide respectively [3]. The work flow of this study is shown in Figure 1.

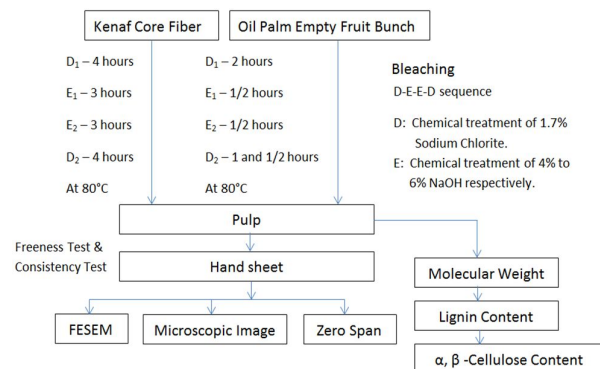


Figure 1 Study flow chart

3. RESULTS AND DISCUSSION

The range of lumen size and diameter is measured using ImageJ software of fibers from FESEM and microscopic image. The sample was prepared in pulp form for microscopic analysis and in handsheet form for FESEM analysis.

It is reported that vast amount of silica bodies can be found on OPEFB strand [4]. However, it is quite difficult to find the silica bodies on the OPEFB fiber in this study as the OPEFB had been treated previously

with the pulping and bleaching process.

It is also suggested that the formation of silica might be inside out, which means that the silica went through a pathway called siliceous pathways and form a perforated structure on the OPEFB strands [4]. Another suggestion which can be taken into consideration is the naturally existing bordered pits on the OPEFB fiber.

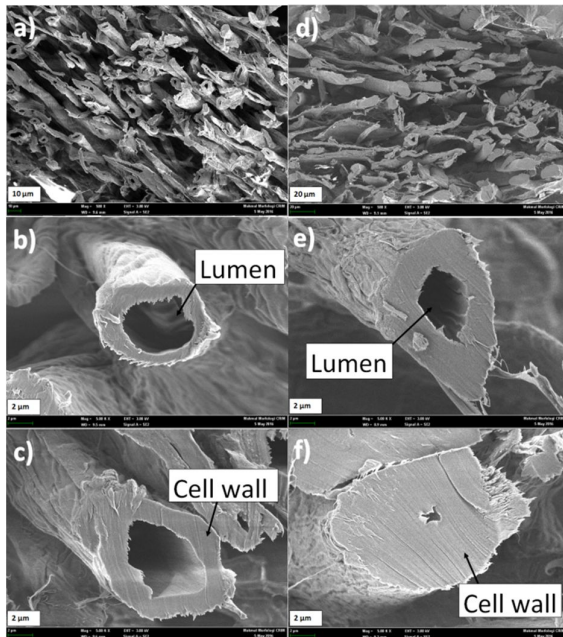


Figure 2 Cross section of Oil palm empty fruit bunch pulp (a,b,c) and Kenaf pulp (d,e,f) under FESEM

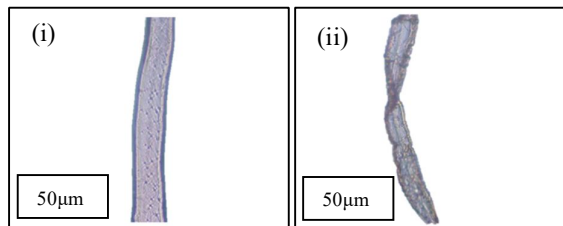


Figure 3 Microscopic view of Oil palm empty fruit bunch pulp (i) and Kenaf pulp (ii)

Table 1 Average lumen size and cell wall of OPEFB and Kenaf pulp

| Pulp | Scanning Electron Micrograph (FESEM) Image | | Microscopic Image |
|-------|--|------------------------|-----------------------|
| | Average Lumen perimeter (µm) | Average cell wall (µm) | Average diameter (µm) |
| OPEFB | 15.32-16.89 | 1.56-2.57 | 18.56 |
| Kenaf | 15.12-15.83 | 2.56-3.45 | 23.06 |

Table 2 Zero Span tensile strength results

| Pulp | Readings | | | | | | | Average |
|-------|----------|-----|-----|-----|-----|-----|-----|---------|
| | 1 | 2 | 3 | 4 | 5 | 6 | 7 | |
| OPEFB | 1.6 | 1.9 | 1.7 | 1.5 | 1.7 | 1.4 | 1.9 | 1.7 |
| Kenaf | 4.7 | 4.6 | 4.3 | 4.9 | 4.6 | 4.1 | 5.0 | 4.6 |

4. CONCLUSIONS

Structure and properties of OPEFB and Kenaf fiber were analyzed. Chemical properties of the fibers were also determined. Morphological studies

revealed that cross section of OPEFB fiber showed structured round shape lumen or is called lacuna compared to Kenaf. It is quite difficult to find Kenaf fiber with nice round shaped lumen. However, the zero spans tensile strength shows Kenaf fiber is stronger than OPEFB fiber. Finally, it is important to mention that the properties of oil palm fiber and kenaf fiber are comparable to other natural fibers and study on it are still developing nowadays.

5. REFERENCES

- [1] Zakaria, S., Roslan, R., Amran, U. A., Chia, C. H., Bakaruddin, S. B., "Characterization of residue from EFB and Kenaf core fibres in the liquefaction process," *Sains Malaysiana*, vol. 43, pp. 429-435, 2014.
- [2] Ibrahim, M.N.M., Salleh, N. M., "Keistimewaan lignin daripada kelapa sawit," Penerbit Universiti Sains Malaysia, pp. 10-15, 2010.
- [3] Kaco, H., Zakaria, S., Razali, N. F., Chia, C. H., Zhang, L., Jani, S. M., "Properties of cellulose hydrogel from kenaf core prepared via pre-cooled dissolving method," *Sains Malaysiana*, vol. 43, pp. 1221-1229, 2014.
- [4] Law, K. N., Wan Daud, W. R., Ghazali, A., "Morphological and chemical nature of fiber strands of oil palm empty-fruit-bunch (OPEFB)," *BioResources*, vol. 2, pp. 351-362, 2007.
- [5] Sreekala, M. S., Kumaran, M. G., Thomas, S., "Oil palm fibers: morphology, chemical composition, surface modification, and mechanical properties," *Journal of Applied Polymer Science*, vol. 66, pp. 821-835, 1997.
- [6] Sreekala, M. S., George, J., Kumaran, M. G., Thomas, S., "Water-sorption kinetics in oil palm fibers," *Journal of Applied Polymer Science*, vol. 39, pp. 1215-1223, 2001.
- [7] Sreekala, M. S., Thomas, S., "Effect of fibre surface modification on water-sorption characteristics of oil palm fibres," *Composites Science and Technology*, vol. 63, pp. 861-869, 2003.
- [8] Tran, L. Q. N., Minh, T. N., Fuentes, C. A., Chi, T. T., Vuure, A. V., Verpoest, I., "Investigation of microstructure and tensile properties of porous natural coir fibre for use in composite materials," *Industrial Crops and Products*, pp. 1-30, 2014.
- [9] Ying, T. Y., Teong, L. K., Wan Abdullah, W. N., Peng, L. C., "The effect of various pretreatment methods on oil palm empty fruit bunch (EFB) and kenaf core fibers for sugar production," *Procedia Environmental Sciences*, vol. 20, pp. 328-335, 2014.
- [10] Caplow M., "Kinetics of carbamate formation and breakdown," *Journal of the American Chemical Society*, vol. 90, no. 24, pp. 6795-6802, 1998.
- [11] Mohd Saidi, A. S., Zakaria, S., Chia, C. H., Syed Jaafar, S. N., Mohammad Padzil, F. N., "The effect of acid hydrolysis pretreatment on crystallinity and solubility of kenaf cellulose membrane," *AIP Publishing*, vol. 1678, pp. 1-6, 2015.